ERDC TR-24-12

U.S. ARMY

US Army Corps of Engineers®

ERDC

Post-wildfire Curve Number Estimates for the Southern Rocky Mountains in Colorado, USA

Jeremy Giovando, Wyatt Reis, Rose Shillito, Elizabeth Shaloka, Christina Chow, Michael S. Kohn, and Natalie Memarsadeghi

June 2024

Engineer Research and Development Center

Cover photo credit: Jeremy Giovando, US Army Corps of Engineers–Cold Regions Research and Engineering Laboratory

The US Army Engineer Research and Development Center (ERDC) solves the nation's toughest engineering and environmental challenges. ERDC develops innovative solutions in civil and military engineering, geospatial sciences, water resources, and environmental sciences for the Army, the Department of Defense, civilian agencies, and our nation's public good. Find out more at www.erdc.usace.army.mil. To search for other technical reports published by ERDC, visit the ERDC online library at https://erdclibrary.on.worldcat.org/discovery.

ERDC TR-24-12
June 2024

Post-wildfire Curve Number Estimates for the Southern Rocky Mountains in Colorado, USA

Jeremy Giovando, Wyatt Reis, and Christina Chow

US Army Engineer Research and Development Center (ERDC)
Cold Regions Research and Engineering Laboratory (CRREL)
72 Lyme Road
Hanover, NH 03755-1290

Rose Shillito and Natalie Memarsadeghi

US Army Engineer Research and Development Center (ERDC)
Coastal and Hydraulics Laboratory (CHL)
3909 Halls Ferry Road
Vicksburg, MS 39180-6199

Elizabeth Shaloka

US Army Corps of Engineers
Philadelphia District
1650 Arch Street
Philadelphia, PA 19103

Michael S. Kohn

US Geological Survey
Colorado Water Science Center
Denver Federal Center, MS-415 Building 53
Denver, CO 80225

Final Report

Prepared for US Army Corps of Engineers (USACE)
Washington, DC 20314-1000

Under AMSCO 504507

Abstract

The curve number method first developed by the US Department of Agriculture Soil Conservation Service (now the Natural Resources Conservation Service) is often used for post-wildfire runoff assessments. These assessments are critical for land and emergency managers making decisions on life and property risks following a wildfire event. Three approaches (i.e., historical event observations, linear regression model, and regression tree model) were used to help estimate a post-wildfire curve number from watershed and wildfire parameters. For the first method, we used runoff events from 102 burned watersheds in Colorado, southern Wyoming, northern New Mexico, and eastern Utah to quantify changes in curve number values from pre- to post-wildfire conditions. The curve number changes from the measured runoff events vary substantially between positive and negative values. The measured curve number changes were then associated with watershed characteristics (e.g., slope, elevation, northness, and eastness) and land cover type to develop prediction models that provide estimates of post-wildfire curve number changes. Finally, we used a regression tree method to demonstrate that accurate predications can be developed using the measured curve number changes from our study domain. These models can be used for future post-wildfire assessments within the region.

Contents

Figures and Tables

Figures

Tables

Preface

This study was conducted for the US Army Corps of Engineers (USACE) under Floodplain Management Services (FPMS) per Sec. 206 of the 1960 Flood Control Act, AMSCO 504507. The technical monitor was Mr. Bradley Hoefer, USACE Omaha District.

The work was performed by the Terrain and Ice Engineering Group of the Remote Sensing/GIS Center of Expertise, US Army Engineer Research and Development Center–Cold Regions Research and Engineering Laboratory (ERDC-CRREL). At the time of publication, Dr. Meghan C. L. Quinn was group lead; and Mr. David Finnegan was center director. The acting deputy director of ERDC-CRREL was Ms. M. Kelly Swiderski, and the acting director was Dr. Ivan P. Beckman.

The work was also performed by the River and Estuarine Engineering Branch of the Flood and Storm Protection Division, ERDC-Coastal Hydraulics Laboratory (CHL). At the time of publication, Mr. Casey M. Mayne was acting branch chief; and Mr. David P. May was division chief. The deputy director of ERDC-CHL was Mr. Keith Flowers, and the director was Dr. Ty V. Wamsley.

The authors would like to credit the US Geological Survey (USGS)–Water Mission Area Integrated Water Prediction Program, National Hydrologic Geospatial Fabric project, and the Water Availability Impact of Extreme Events Program for providing a script that was used to identify wildfire affected streamgages. The authors appreciate all the reviewers; their comments were constructive and helped to improve this document. In addition the authors would like to acknowledge the USGS Groundwater and Streamflow Information Program and the Colorado Department of Transportation Applied Research and Innovation Branch for providing funds for Michael S. Kohn to contribute streamgage information and publish the R script in the corresponding USGS data release.

COL Christian Patterson was commander of ERDC, and Dr. David W. Pittman was the director.

This page intentionally left blank.

1 Introduction

1.1 Background

Worldwide, wildfire and hazards associated with wildfire place communities and infrastructure at risk. Researchers expect the frequency of wildfire occurrence and magnitude of wildfire effects to increase in the future (Brown et al. 2021). Jolly et al. (2015) found wildfire season has lengthened for over one-quarter of the Earth's vegetated surface and the burnable area has doubled during the period of 1979–2013 because of the lengthened fire season. The risk will continue to increase in the future because of climate change, especially as areas of moisture-limited fire regimes become drier (Ellis et al. 2022). Wildfire activity has already increased in the western United States (US), with substantial increases in large-wildfire frequency in the mid-1980s especially in midelevation, Northern Rocky Mountain forests (Dennison et al. 2014; Westerling et al. 2006). A more recent analysis indicates that other regions of the western US have also showed increased wildfire activity in response to warming and early spring snowmelt (Westerling 2016). The 2003–2012 increase in wildfire occurrence ranged from approximately 250% (Southern Rockies) to 1,000% (Northwest) relative to the 1973–1982 average (Westerling 2016). Increases in wildfire activity in the western US are also linked to changes in summer seasonal precipitation. Holden et al. (2018) reported that May–September total precipitation and the number of wetting rain days had negative trends (–5 mm per decade or 1 day per decade, respectively) for 82%–94% of forested areas in the western US. These trends were calculated using multiple gridded data sets from 1984–2015.

Increased streamflow from a watershed immediately following a fire event is well documented (Ebel et al. 2012; Moody and Martin 2001; Neary et al. 2003; Stoof et al. 2012). As the revegetation process begins, the changes to overall water supply and mean annual streamflow are more site specific. Following fires in the Gila River watershed in Arizona, the mean annual streamflow increased (controlling for climate and snowpack variability) although there was no evidence of a streamflow increase in the Jemez River watershed in New Mexico (Wine and Cadol 2016). However, Wine et al. (2018) found that mean streamflow values increase by 2%–14% for watersheds that have very large wildfires. This indicates that both flood risk modeling immediately after the wildfire and long-term water supply estimates should be considered when assessing wildfire effects to the water

balance and streamflow regime. In the Cache La Poudre River watershed in Colorado, following the 2012 High Park Fire, a 75% increase in runoff was observed for certain high-burn severity subwatersheds, whereas the hydrologic response at the watershed scale was minimally affected (Havel et al. 2018). For detectable changes at larger catchment scales, at least 20% of the watershed must be affected by wildfire (Wine and Cadol 2016).

In recent years, the importance of developing models to evaluate post-wildfire shifts in streamflow metrics has been highlighted and a variety of hydrologic models were used to estimate post-wildfire streamflow. These models range from process based representations that include vegetation recovery (Bart et al. 2020) to relatively simple models used by land managers (Robichaud and Ashmun 2013) to assess potential changes in streamflow. The process based models include the Limburg Soil Erosion Model (LISEM) (De Roo et al. 1996) which was applied by Van Eck et al. (2016) to burned eucalypt and pine plantations in central Portugal. Another study using the Integrated Hydrology Model (VanderKwaak 1999) by Ebel et al. (2016) simulated changes in streamflow caused by wildfire along the Colorado Front Range. Wang et al. (2020) created a post-wildfire hydrology modeling tool (PFHydro) by integrating soil water repellency into an existing hydrology model (UFORE-Hydro; Wang et al. 2005). The model KINEROS2 (Smith et al. 1995; Smith and Quinton 2000), is another process based hydrology model that was used to model burned conifer watersheds in the southwestern US (Canfield et al. 2005) and chaparral areas of California (Chen et al. 2013). Another model that is used is the Hydrologic Engineering Center–Hydrologic Modeling System (HEC-HMS) from the US Army Corps of Engineers (USACE). This model was used by Cydzik and Hogue (2009) to estimate post-wildfire streamflow in the San Bernardino Mountains in California. Chen et al. (2013) also used HEC-HMS for comparison to KINEROS2 results in the Arroyo Secco watershed in California.

Ebel et al. (2023) provides a summary of post-wildfire hydrologic studies for locations in North America, Europe, and Australia. Within the US, many studies were conducted on watersheds in California and Southern Rockies. The accuracy of post-wildfire modeling simulations varies by modeling tool. The model performance summarized by Ebel et al. (2023) shows both process based and simple hydrology models have substantial variation in model accuracy. A cross-comparison of models can be useful but controlling for available calibration data and skill by the modeler can

be challenging. The range of post-wildfire hydrology models that were used in recent years is substantial and is likely going to continue to increase as other hydrology modeling tools are developed or adapted to estimate both short and long-term post-wildfire watershed conditions. Although process based models may be needed to understand the complex interactions at the land surface following wildfires, there could still be applications for relatively simple models by land and emergency managers performing rapid risk assessments. The curve number method (NRCS 2004a) is one of the simplest methods for estimating runoff from a watershed and important for post-wildfire hydrology modeling (NRCS 2016). Details of this method are discussed in Section 2 of this report.

1.2 Study Area

This study is focused within the forested areas of the southern Rocky Mountains, including the majority of central and western Colorado, southern Wyoming, eastern Utah, and northern New Mexico (Figure 1). The High Plains and Tableland Ecoregions of eastern Colorado were excluded from this study due to the documented erosion and vegetation recovery periods from wildfire in grassland and shrubland environments are different compared to forested mountainous regions (Stavi 2019).

Figure 1. Digital elevation map (DEM) of the study area with watershed boundaries (*black*) for each of the 102 streamgages used in the analysis (Appendix A). The burned area perimeters from Welty and Jeffries (2021) are shown in *red*. The base map is elevation from the North American Datum of 1983 (NAD 83) horizontal datum and North American Vertical Datum of 1988 (NAVD 88) vertical datum.

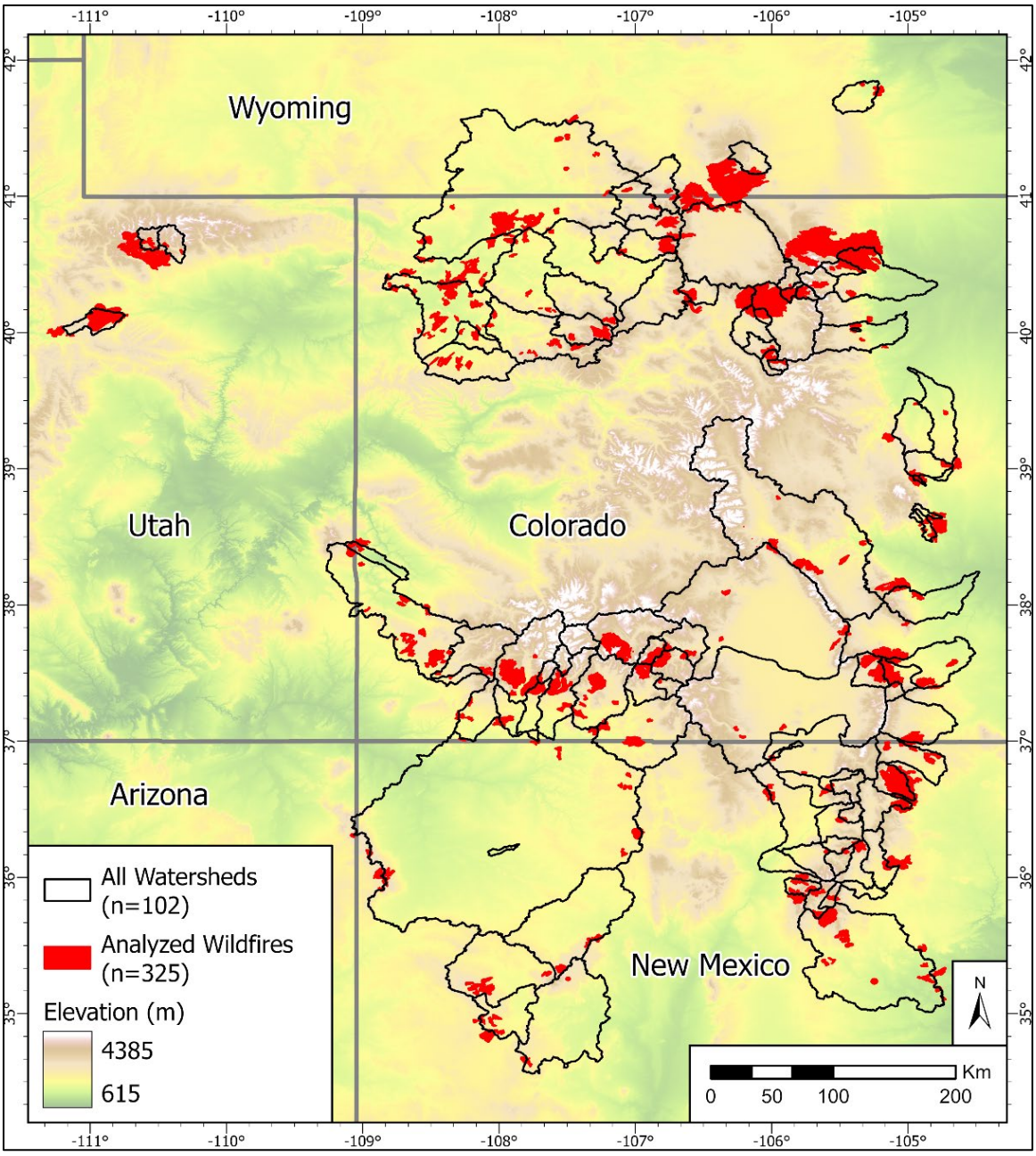

1.3 Regional Climate

The majority of the study area falls within the Southern Rocky Mountain Ecoregion (Omernik and Griffith 2014). The Southern Rocky Mountain Ecoregion is characterized by varied topography and high mountainous elevations, which directly influence the temperature and precipitation patterns across the region. The central portion of the study area has the highest elevations leading to cooler temperatures throughout the year compared to areas at lower elevations. Like the elevation-driven temperature gradients, precipitation is also highly variable in the region with high mountains receiving substantial snowfall while lower elevation areas to the east and west of the Continental Divide have semiarid and high-desert climates. For example, in Colorado, the state-wide average annual precipitation is 18 in., yet there is high variability with some areas receiving approximately 7 in. whereas others receive more than 60 in. a year.[1] For the high elevation areas of the region, most precipitation falls as snow during the winter, whereas monsoonal thunderstorm patterns are a primary source of precipitation at low elevations. The southern Rocky Mountains experience four distinct seasons which directly affect temperature and precipitation patterns in the region. This high variability can lead to frequent drought, which can increase the likelihood of wildfires.

1.4 Objective

The overall objective of our study is to identify the potential changes in rainfall-driven runoff events in burned areas of Colorado and associate those changes in runoff to differences in curve number (CN) estimates that can be used in post-wildfire hydrologic studies. To accomplish this objective, the research team has been assembled to include engineers and scientists with specialized experience in hydrology, watershed modeling, and post-fire runoff analysis. To achieve the study objectives, the project scope included the following:

1. For a full list of the spelled-out forms of the units of measure used in this document and their conversions, please refer to *US Government Publishing Office Style Manual*, 31st ed. (Washington, DC: US Government Publishing Office, 2016), 248–52 and 345–47, https://www.govinfo.gov/content/pkg/GPO-STYLEMANUAL-2016/pdf/GPO-STYLEMANUAL-2016.pdf.

- Provide a summary of methods used to adjust CN values following a wildfire.
- Develop empirical estimates of CN value adjustments based on streamgage information.
- Provide CN value adjustment guidelines for modelers performing post-wildfire risk assessments.

1.5 Approach

In this study, our approach used streamflow data from streamgages located in or downstream of wildfire affected watersheds to estimate CNs for each runoff event. Using the population of estimated CN values for hundreds of individual storm events, we determined the change in median pre- and post-wildfire CNs. From this assessment, we developed models to predict the post-wildfire CN change based on watershed characteristics (i.e., slope, elevation, northness, eastness, land cover type, and percent burned) and the years since the wildfire occurred.

1.6 Scope

The scope of our study was limited to areas of the Southern Rocky Mountains including southern Wyoming, Colorado, northern New Mexico, and eastern Utah. The methodology can be applied to other regions of the US provided streamflow, precipitation, and historical wildfire information are available.

2 Summary of Curve Number (CN) Method

2.1 CN Background

The CN method is a simple method that relates precipitation and watershed characteristics to runoff magnitude. The CN method is widely used for estimating surface runoff from watersheds (Hawkins et al. 2005; Ponce and Hawkins 1996; Soulis 2018). This method was developed in the 1950s by the USDA Soil Conservation Service (SCS) (Rallison 1980; Plummer and Woodward 1998). The agency would later be renamed the Natural Resources Conservation Service (NRCS) and the method is still published in the NRCS National Engineering Handbook (NRCS 2004a). The CN method assumes that precipitation is divided into water that is stored in the soil column and water that produces surface runoff. The ratio of storage to runoff amounts is dependent on watershed characteristics (e.g., vegetation and soil type).

The derivation of the generalized CN equations we present in this report follows the process described in Ponce and Hawkins (1996). The equations describing the CN method match those found in the NRCS National Engineering Handbook (NRCS 2004a). The CN method assumes a proportionality between water retention and surface runoff,

$$\frac{F}{S} = \frac{Q}{P}, \tag{1}$$

where

F = actual water retention,
S = the potential water retention,
P = total precipitation, and
Q = actual runoff.

The actual water retention (F) is equal to the difference between total precipitation (P) and actual runoff (Q). The method also assumes that at the beginning of the precipitation event an initial amount of rainfall is abstracted, or retained, in the watershed (I_a) as a combination of interception, infiltration, and surface storage before runoff begins (Ponce and Hawkins 1996). This amount is subtracted from the precipitation (P) and when substituted into Equation 1 results in,

$$\frac{P-I_a-Q}{S} = \frac{Q}{P-I_a}. \quad (2)$$

When solving Equation 2 for Q, the resulting function for surface runoff is

$$Q = \frac{(P-I_a)^2}{P-I_a+S}. \quad (3)$$

I_a has a linear relation with S and is described by the following equation:

$$I_a = \lambda S. \quad (4)$$

In Equation 4, λ is the initial abstraction ratio and ranges from $0.0 \le \lambda \le 0.3$ (Ponce and Hawkins 1996). Finally, when Equation 4 is substituted into Equation 3, the generalized form of the surface runoff function is

$$Q = \frac{(P-\lambda S)^2}{P+(1-\lambda)S}. \quad (5)$$

Part of the simplicity of the CN method is that the potential retention (S) can be mapped into a dimensionless CN parameter (CN) using the following relations:

$$S = \frac{25400}{\text{CN}} - 254, \quad (6)^2$$

and

$$S = \frac{1000}{\text{CN}} - 10. \quad (7)^3$$

CN values range from 0 to 100. A CN value of zero results in all precipitation being abstracted in the watershed, whereas a CN value of 100 results in no abstraction and all precipitation contributing to surface runoff.

Determining the CN value for a specific watershed and precipitation event is required to accurately estimate runoff. Because CN represents many watershed-specific variables (e.g., slope, vegetation, and regional soil characteristics) and temporally dependent variables (e.g., antecedent soil moisture), estimation of CN for a watershed can be challenging. Typically,

2. International System of Units (SI).

3. US Customary System of Units.

users of the CN method will either estimate CN values using the NRCS table of median values for varying soil, cover, and vegetation conditions (NRCS 2004b) or through local calibration of measured runoff and precipitation events (Hawkins et al. 2005). As described by Hawkins et al. (2005), there are three principal methods for using observed precipitation and streamflow to estimate CN values for a watershed. These methods are (1) asymptotic determination, (2) least squares determination, and (3) model simulation. The first two methods aim at determining an overall CN value that can be used for higher precipitation depths (i.e., large rainfall events). The third method is often used by hydrologic modelers to relate antecedent conditions of a watershed to CN values.

The asymptotic determination method rank orders P and Q separately for runoff events within a watershed over a period of interest (effectively decoupling the rainfall input from the streamflow response), S and CN are then calculated for each ranked pair. The CN values are plotted against P and an exponential decay curve is fit to the points on a linear plotting scale. If the curve asymptotically approaches a CN value, then the watershed is considered "standard" and the CN value is considered appropriate for higher precipitation depths. The details of this method are further described in Hawkins et al. (2020). Alternatively, the CN value for a watershed can be determined using the least squares method by finding an S value which minimizes the error between the calculated and observed runoff (i.e., $\sum (Q_{calc} - Q_{obs})^2$). Once the S value is determined, the CN value can be found using Equation (6) or (7) depending on the system of units. The model simulation method can be effective but generally requires in-depth knowledge of the watershed and additional information like soil moisture and vegetation health prior to the observed runoff events.

2.2 Literature Summary of Post-wildfire CN Estimation

Although the CN method is widely used in hydrologic applications, there are relatively few publications that describe how to adjust CNs following a wildfire event in a watershed. Estimated post-wildfire CNs for fires in New Mexico were published by both Livingston et al. (2005) and Springer and Hawkins (2005). Although these studies provide some insight to the magnitude of change in that specific region, their conclusion indicated that additional data were needed to determine generalized CN values for wildfire affected watersheds. Kinoshita et al. (2014) evaluated four hydrologic models for post-wildfire CN value determinations in several

western US watersheds. The four models assessed by Kinoshita et al. (2014) were (1) the USGS Linear Peak-Streamflow Regional Regression Equations (Farmer et al. 2019), (2) USDA Windows Technical Release 55 (https://data.nal.usda.gov/data set/small-watershed-hydrology-wintr-55), (3) Wildcat 5 (https://www.fs.usda.gov/research/treesearch/50557), and (4) HEC-HMS (https://www.hec.usace.army.mil/software/hec-hms/). The primary goal of their analysis was assessing the versatility and accuracy of the commonly used hydrology methods and models following wildfire. In the analysis, The Kinoshita et al. (2014) methods for adjusting the CN include a pre-wildfire modifier based on total burn area and severity. The changes in CN values were adjusted with a fixed translation between 5 to 15 units depending on burn severity. The Kinoshita et al. (2014) conclusion was that Wildcat 5 overall performed the best of the models evaluated but was limited by the maximum watershed size appropriate for the tool. Another study by Leopardi and Scorzini (2015) in Italy, also used fixed translations of CN values to test the sensitivity of the peak streamflow estimates following wildfire in a small urban wildfire affected basin. Leopardi and Scorzini (2015, p. 305) found that the ". . . lack of any consistent and verified guidelines . . ." resulted in the development of post-wildfire CN values which had a high degree of uncertainty.

Soulis (2018) evaluated three methods that used pre- and post-wildfire streamflow observations to determine CN adjustments for an experimental watershed in Greece. The three methods of CN adjustments for the entire watershed were (1) taking the arithmetic mean, median and geometric mean CN values for individual events which occurred both pre and post-wildfire and assuming $\lambda = 0.2$; (2) asymptotic CN values for both pre and post-wildfire periods following the procedure described by Hawkins et al. (2005); and (3) finding the best fit CN value by allowing λ to be treated as a free parameter in fitting Equations (5) and (6) (or 7). Using method 1, Soulis (2018) found the median CN value difference between pre- and post-wildfire periods was approximately 5 units. Method 2 resulted in a change of over 25 units, whereas method 3 with λ as a free parameter resulted in approximately a 30 unit change in the CN value. Soulis (2018) also estimated CN changes using a two-step process that split the watershed between burned and unburned areas, allowing for a spatially distributed CN estimation. Based on our review of the literature, these methods are not used in any other studies and the general applicability has not been determined. Therefore, we focused on the first of Soulis (2018) methods for this analysis.

The NRCS has published methodologies for estimating CN changes post-wildfire which are often used as background information for many federal and local government agencies reports on flood risk following wildfire (NRCS 2016). NRCS (2016) provides post-wildfire CN ranges for a limited number of USDA Forest Service regions, which are derived from individual Burned Area Emergency Response (BAER) team reports. Several tables within the NRCS (2016) report lists CN value approximations according to burn severity, CN values as high as 98 are reported in regions with high burn severity and hydrophobic soils. The NRCS (2016) report also provides a range of CN values by hydrologic soil group and burn severity. The CN changes from prewildfire conditions for hydrologic soil groups C and D are 18 and 23, respectively (assuming high burn severity). NRCS (2016, p. 15) concludes:

> The lack of field data in burned catchments and related research to verify the effect on CN hampers postfire runoff modeling with CNs. There is little research adequate to determine best-fit runoff CNs, even for unburned mountain and forested watersheds.

No additional publications reporting either CN changes or post-wildfire CN value ranges for all areas of the western US were identified. In addition, there were no studies identified that attempted to relate CN changes to watershed characteristics, which is an important step when performing simulations of post-wildfire runoff in watersheds that have no streamflow observations available.

3 Data

To complete this study we incorporated streamflow, precipitation, and snow water equivalent (SWE) (i.e., climate), wildfire perimeter, and basin characteristic data from several data sources. In this section we will describe each of the data sources.

3.1 Streamflow

The primary source of streamflow data were from the USGS streamgages (USGS 2023). Another source of streamflow data for selected gages included the Colorado Division of Water Resources (CODWR) (CODWR 2023). We also investigated data sources from the New Mexico and Wyoming State Engineer Offices, but no runoff events were identified in wildfire affected watersheds. The State of Utah relies on the USGS streamgage network and does not operate an independent streamgage network like other states. Streamgages included in the study are listed in Appendix A:.

3.2 Climate

Precipitation was the primary climate data input for estimating CN values. We used NOAA's Analysis of Record for Calibration (AORC) gridded precipitation data (NOAA 2021). This product provides hourly accumulated precipitation depths for all of the continental United States (CONUS) at a 1 km spatial resolution. These precipitation data shows reduced bias compared relatively to other hourly precipitation products (Fall et al. 2023). In addition, the AORC data set has sufficient concurrent records with the wildfire perimeter data set (Welty and Jeffries 2021) to identify multiple runoff events in each watershed and was used in other post-wildfire studies in Colorado (Giovando et al. 2023).

The SWE data set developed by Broxton et al. (2019) was used to identify runoff events that were caused by rainfall only. This data set has a 4 km spatial resolution at a daily temporal resolution for CONUS for water years 1982–2022. Dawson et al (2018) showed this data set to provide accurate representation of SWE conditions in western US watersheds.

3.3 Wildfire Perimeters

The wildfire perimeter data used to locate wildfire affected watersheds in the study area were taken from the *Combined Wildfire Datasets for the United States and Certain Territories, 1800s-Present* data set (Welty and Jeffries 2021). This data set merges 40 different wildfire and prescribed burn layers to obtain the greatest historical spatial resolution of wildfire for the United States and certain territories. For this study, we focused on fire events with perimeters greater than 1,000 acres that occurred during the period of record of the streamgages.

3.4 Land Cover and Topography

We summarized land cover and topographic characteristics of each watershed using the LANDFIRE 2022 data sets (LANDFIRE 2022a–d). We calculated and assigned each watershed the majority (mode) vegetation type based on the Existing Vegetation Type data set (LANDFIRE 2022c). A total of 17 unique existing vegetation types were assigned to the watersheds included in our analysis (Table 1). Using the LANDFIRE elevation products (30 m spatial resolution), we calculated the mean watershed elevation (meters; LANDFIRE 2022b) and slope (degrees; LANDFIRE 2022d). Additionally, using the LANDFIRE elevation (LANDFIRE 2022b) and aspect (LANDFIRE 2022a) products, we calculated the mean northness (degree to which the watershed is oriented towards the north) and eastness (degree to which the watershed is oriented east) for each watershed. North facing slopes tend to have more persistent snowpack and denser vegetation, whereas east facing watersheds can be affected by the prevailing westerly winds (Sexstone and Fassnacht 2014). The formulation for calculating northness and eastness are documented in Sexstone and Fassnacht (2014). Post-wildfire remediation efforts, including mulching, were not accounted for in the analysis because of lack of geographical information indicating the use of mulch within a burned area. Watersheds varied in mean elevation between 1,984 m and 3,460 m with a median elevation of 2,678 m. The watersheds also covered a range of aspects and slopes with northness values ranging between −0.003 and 0.90 (median of 0.01), and eastness values between −0.124 and 0.010 (median of −0.011).

Using the wildfire burn perimeters from Welty and Jeffries (2021), we calculated the percentage of each watershed that was burned. There was a total of 325 individual wildfires (Reis et al. 2024) that occurred within at

least one watershed. The percentage of burned area for individual watersheds ranged from less than 1% to over 75% with a median of 1.4% (Figure 2). Because of the relative size of the watersheds captured by the streamgages for this analysis, only 31 watersheds were burned across more than 2% of the total watershed area.

Table 1. LANDFIRE existing vegetation types (LANDFIRE 2022c) determined to be the majority (mode) existing vegetation type in the watersheds used in the analysis.

Existing Vegetation Type—ID	Existing Vegetation Type Name	Existing Vegetation Type Subclass
7011	Rocky Mountain Aspen Forest and Woodland	Deciduous open tree canopy
7016	Colorado Plateau Pinyon-Juniper Woodland	Evergreen open tree canopy
7050	Rocky Mountain Lodgepole Pine Forest	Evergreen closed tree canopy
7052	Southern Rocky Mountain Mesic Montane Mixed Conifer Forest and Woodland	Evergreen closed tree canopy
7054	Southern Rocky Mountain Ponderosa Pine Woodland	Evergreen open tree canopy
7055	Rocky Mountain Subalpine Dry-Mesic Spruce-Fir Forest and Woodland	Evergreen closed tree canopy
7059	Southern Rocky Mountain Pinyon-Juniper Woodland	Evergreen open tree canopy
7080	Inter-Mountain Basins Big Sagebrush Shrubland	Evergreen shrubland
7086	Rocky Mountain Lower Montane-Foothill Shrubland	Mixed evergreen-deciduous shrubland
7126	Inter-Mountain Basins Montane Sagebrush Steppe	Mixed evergreen-deciduous shrubland
7127	Inter-Mountain Basins Semi-Desert Shrub-Steppe	Mixed evergreen-deciduous shrubland
7146	Southern Rocky Mountain Montane-Subalpine Grassland	Perennial graminoid grassland
7147	Western Great Plains Foothill and Piedmont Grassland	Perennial graminoid grassland
7149	Western Great Plains Shortgrass Prairie	Perennial graminoid grassland
7299	Developed-Roads	Developed
9016	Rocky Mountain Alpine Bedrock and Scree	Sparsely vegetated

Figure 2. Histogram of the percentage of watershed burned by each individual wildfire used in the analysis based on the Welty and Jeffries (2021) dataset. The total number of wildfires included is 325. Note the logarithmic scale on the vertical axis.

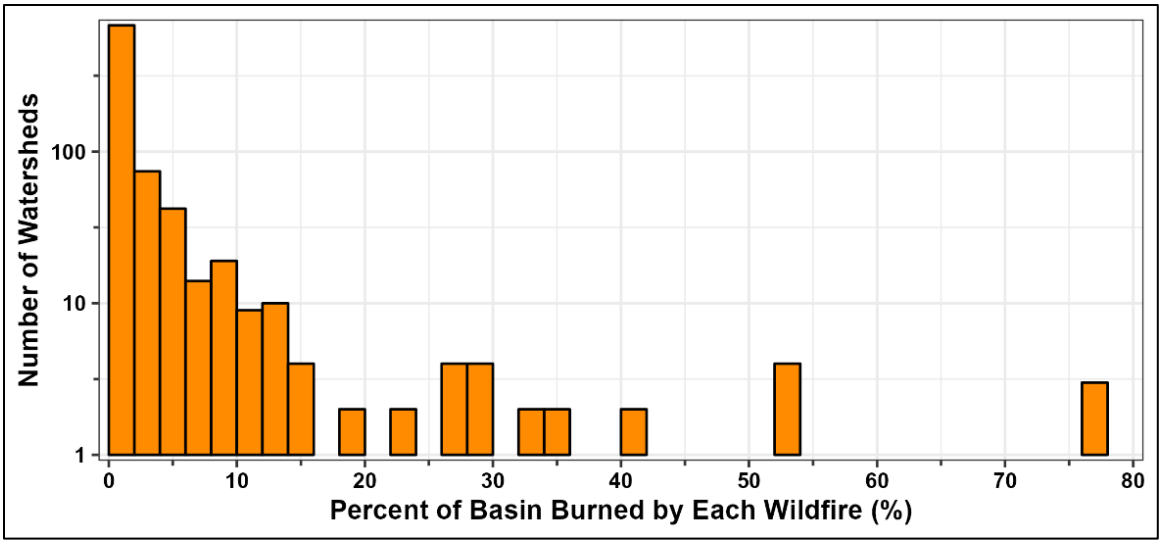

4 Methods

In the following sections we will describe in-depth the methodology used to identify rainfall driven runoff events in wildfire affected watersheds. Using the identified events the CN change is calculated following wildfire. The CN changes are then modeled using regression trees and generalized linear models to provide guidelines for how practitioners can alter CN to model runoff following wildfire. A brief methodological flow chart is included here to help visualize how each input dataset and calculated variable is used to develop the final models (Figure 3).

Figure 3. Flow chart of the methods used in the report. The flow chart includes the input data (*orange*) and the primary processes used (*blue*) to develop the curve number (CN) change models.

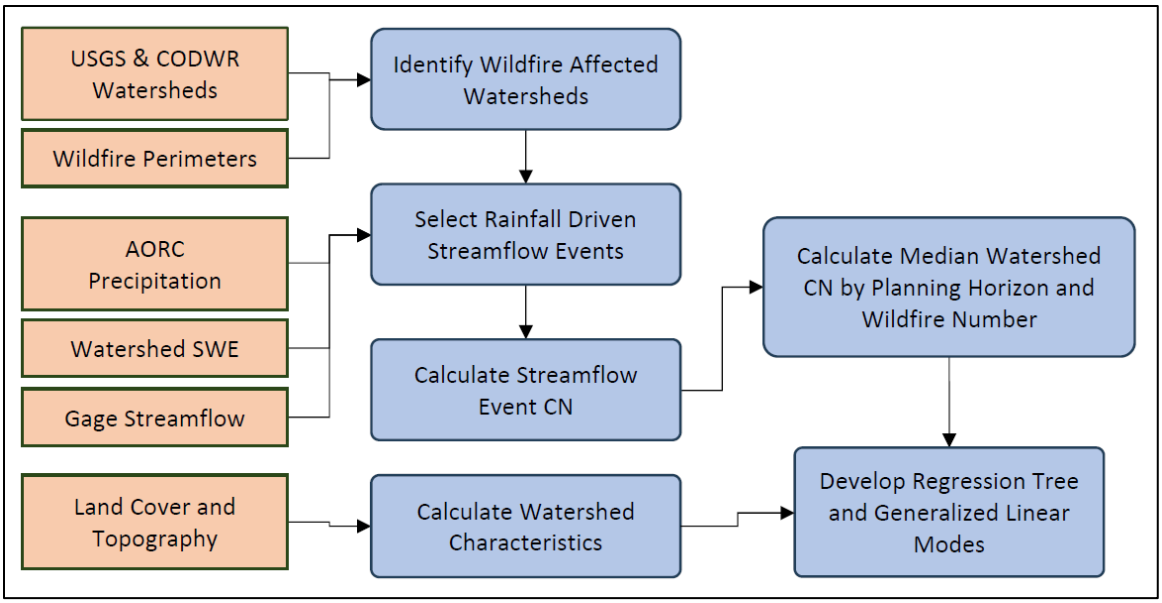

4.1 Wildfire Affected Streamgage Identification

Using the wildfire perimeter data set (Welty and Jeffries 2021), we identified all USGS and CODWR streamgage watersheds within our study area affected by at least one wildfire. This initial search provided us with several hundred potentially wildfire affected watersheds. We then filtered the watersheds by the fire type attribute (e.g., "Wildfire," "Prescribed Burn," or "Unknown") provided in the USGS data set (Welty and Jeffries 2021). This step captures only watersheds with the fire disturbance classified as Wildfire, because the hydrology effects of prescribed burns are less severe than those of wildfires (Bêche et al. 2005; Vadilonga et al. 2008). Additionally, we limited the minimum burn area to 1,000 acres to eliminate

watersheds with minimal land surface effects from wildfire burned areas. We only included wildfires from the USGS data set (Welty and Jeffries 2021) that occurred within the watershed during the period of record for the streamgage (USGS 2023). After applying these criteria, we identified 102 wildfire affected watersheds to include in the study (Reis et al. 2024).

Each of these river systems have varying levels of anthropogenic effects including dams, levees, diversions, interwatershed water transfers, and groundwater pumping. The CN method assumes rainfall input and the associated streamflow response are not influenced by any of these anthropogenic activities. Therefore, Capesius and Stephens (2009) and Kohn et al. (2016) were used to distinguish anthropogenic effects on streams and identified 24 watersheds (out of the 102) that have minimal anthropogenic effects to use in the final model development. These watersheds, referred to as "best subset" in the model naming convention, provide a comparison of both observed CN value changes and model performance to the larger sample that includes all 102 identified watersheds in the study domain. A summary table of specific streamgages used in our analysis is provided in Appendix A.

4.2 Watershed Average Precipitation

Streamflow represents a spatial integration of land surface and hydrologic processes acting upstream of a measurement point in a watershed. Therefore, to determine CN values from streamflow, we needed to spatially average precipitation data over the area upstream of the streamgage location. We completed this by delineating the upstream watersheds for each streamgage location that was identified to have been affected by wildfire and calculated the spatial average of the AORC precipitation data within the delineated watershed.

4.3 Identification of Rainfall Driven Runoff Events

The CN method was specifically designed to predict the runoff from rain events (Rallison 1980; Plummer and Woodward 1998). However, in the snowmelt dominated watersheds that are common in Colorado, most high runoff events are in response to snowmelt runoff. Because of the complexities in identifying rainfall only streamflow responses, runoff events in each of the wildfire affected watersheds, we identified each event through visual inspection of the daily mean streamflow, daily SWE, and hourly incremental precipitation timeseries (Figure 4). We selected events if there

was no SWE within the watershed and the event was a clear response to precipitation. We estimated the start and end date of each event through the visual inspection of the timeseries data. We ensured independent events by only selecting events that started and ended with an approximately equal base flow. Runoff events were identified between 1979 and 2021, with each streamgage period of record varying substantially. Event length ranged between 1 and 53 days, with a median of 8 days; however, due to the close proximity of the watersheds analyzed, many event start dates occurred within a few days of each other (median of 1 day between event start dates). Additionally, we removed streamgages from the analysis if there was a clear pattern of decoupling between the precipitation and streamflow response, typically in response to anthropogenic influences upstream from the streamgage (e.g., dams and irrigation diversions). As a result, we identified a total of 2,946 runoff events caused by rainfall in the 102 wildfire affected watersheds (Reis et al. 2024), these events were then used to evaluate the pre- and post-wildfire CN values.

Runoff events were assigned an identifier based on the following three criteria: (i) if the runoff event occurred before or after a wildfire in the watershed, (ii) if the runoff event occurred after a wildfire, the number of wildfires (i.e. “First Wildfire”, or “Second Wildfire”) that occurred before the runoff event (hereon “fire number”), and (iii) the number of years prior to the runoff event that the most recent wildfire occurred. If a runoff event occurred between two wildfires, it was assigned only to the grouping of “After” the previous fire. Only runoff events that occurred before any recorded wildfire in the watershed were described as “Before” and were used in the pre-wildfire CN value estimation. We also compared the wildfire year with the first year of operation of the streamgage to confirm if any wildfires had occurred prior to the establishment of the streamgage, removing all wildfires prior to the gage period of record. If there were no runoff events identified before the first wildfire, the streamgage was not used in the analysis due to the lack of baseline streamflow information.

Figure 4. Example runoff event selection from the Colorado Division of Water Resources (CODWR) North Inlet streamgage using timeseries data of daily mean streamflow, daily snow water equivalent (SWE), and incremental hourly precipitation. Examples of runoff events that were included in the analysis (*purple*) and those which are excluded (*yellow*) are highlighted.

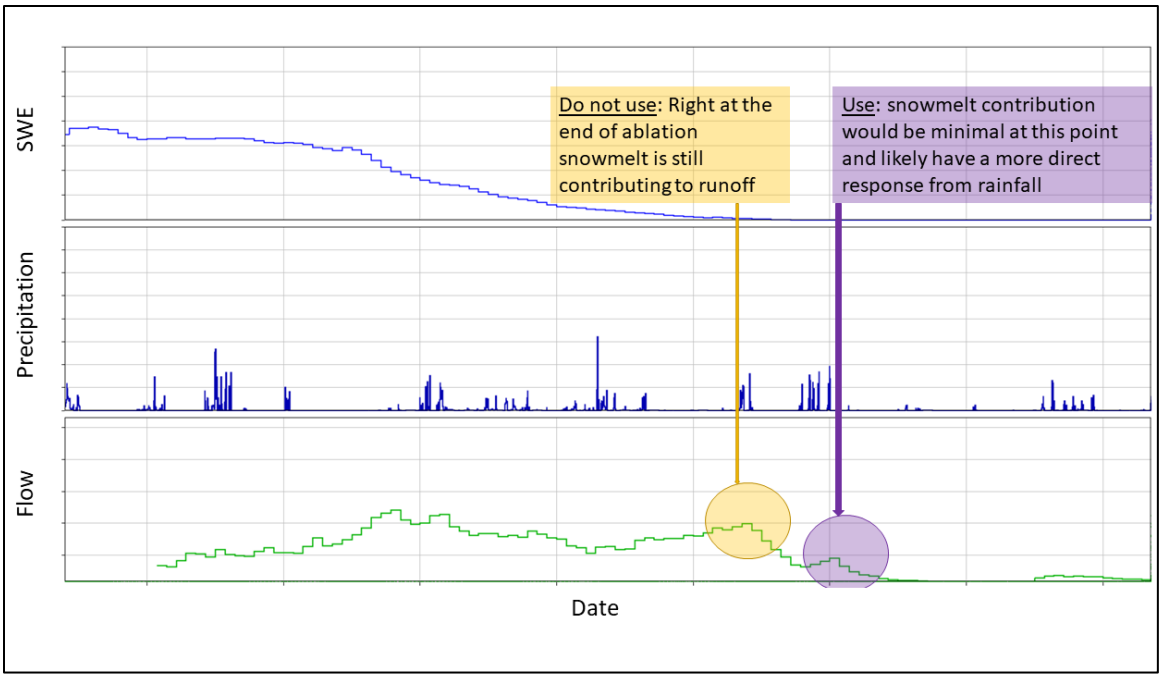

4.4 Determination of CN by Runoff Event

To calculate the CN for each runoff event, we summed the total precipitation and resulting streamflow accordant with the runoff event dates. We then converted the event precipitation and streamflow to total depth or watershed-averaged depth using the watershed area. Runoff event watershed average precipitation depth ranged between 0.3 in. and 10.4 in. (0.7 cm and 26.4 cm), with a median of 1.4 in. (3.6 cm). From the total runoff event depth of precipitation and total runoff event depth of runoff, we calculated the runoff event storage value (S) using Equation (5) for an initial abstraction ratio (λ) of 0.05 and 0.2. We then calculated the CN value using both resulting storage values (Equation 7). The historical formulation of the CN equation used an initial abstraction ratio of 0.2; however, more recent studies have found the initial abstraction ratio of 0.05 to be more appropriate (Hawkins et al. 2020). By calculating the CN using both storage values, we were able to link our changes in CN to historical values commonly found in the literature while also providing a range in the estimated CN changes following wildfire.

4.5 Development of Relation of CN Change to Watershed Characteristics

From the runoff event-based CN values, we then calculated the median CN values within each watershed for each runoff event period. The "Before" wildfire period represents the years prior to any wildfire event occurring within a watershed when streamflow measurements were available. In contrast, the "After" wildfire period was assigned to five unique planning horizons (0–4 years, 5–9 years, 10–14 years, 15+ years, and all years) following the first or second wildfire event (Figure 5). For example, "After First Fire 0–4 yrs" are runoff events immediately following the first identified wildfire in the watershed up to 4 years later.

We then calculated the watershed median change in CN by subtracting the after-wildfire CN median value from the before-wildfire median CN value. A median CN change was calculated for both the 5% and 20% initial abstraction storage values (S05 and S20, respectively) for each runoff event. CN changes were identified for at least one post-wildfire period in 102 watersheds. We further subset the number of total watersheds to those with two or fewer wildfires for a total of 77 watersheds which were then used for our model development. Depending on the specific watershed, runoff events did not occur within each planning horizon (i.e., Before Fire, 0–4 years After First Fire, etc.), which further reduced the sample size to between 19 and 68 of all 77 watersheds (Reis et al. 2024).

Figure 5. The histogram of the number of runoff events included in calculating the median CN for each period used for analysis in the CN change estimates following wildfire. The total number (*n*) of runoff events for each planning horizon is based on the number of fires per watershed.

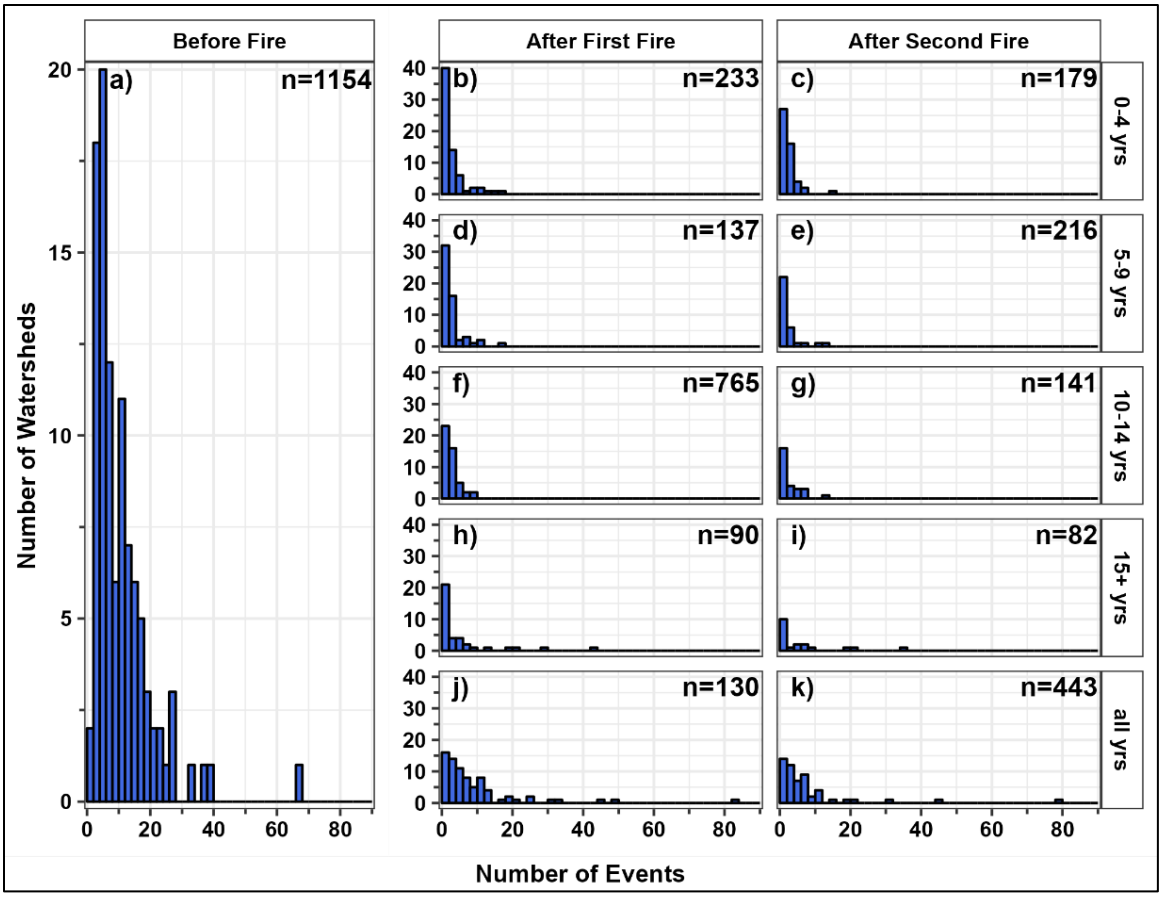

4.6 Model Development

Using the change in CN, we developed generalized linear models and regression tree models to identify the characteristics of the watersheds and wildfire alterations that resulted in the CN change between pre- and post-wildfire conditions. These models were developed so they could be used in future burned watersheds to predict the increase in runoff expected following a wildfire.

4.6.1 Linear Model

We developed generalized linear models (GLM) of the change in CN for rainfall driven runoff events in a watershed for each of the five planning horizons (e.g., 0–4 yr and 5–9 yr) and fire number (e.g., First wildfire). For each linear model, the equations were defined by the general form,

$$Y = \beta_0 + \beta_1 X_1 + \beta_2 X_2 + \ldots + \beta_i X_i \quad (8)$$

where Y is the change in CN (ΔCN), β_0 is the y-intercept, or base CN change, β is the coefficient for each dependent variable term (X) included in the GLM. GLMs can use both continuous, categorical, and binary variables. For example, if the GLM equation was

$$\Delta CN = 25 + 5(\text{Mean Elevation}) + 45(\text{Landcover} = 7011) \quad (9)$$

to identify the predicted change in CN for a watershed (ΔCN), the mean elevation of the watershed would be multiplied by the coefficient (5) and a binary operator (0 = no) or (1 = yes) based on if the majority of landcover type of the watershed is Rocky Mountain Aspen Forest and Woodland (7011) multiplied by the landcover coefficient (45).

The input variables included in the GLM development are mean watershed elevation, slope, eastness, northness, LANDFIRE mode landcover type, and wildfire burn percentage. Our initial step in the process of developing the GLMs was to identify the input variables which resulted in the best performance metrics. Using the *leaps* package (Lumley 2020) in R (R Core Team 2023), we conducted an exhaustive evaluation of input variable combinations while also implementing a 5-fold, k-fold cross validation process to determine the root-mean-square error (RSME) for each model. The k-fold process subdivides a dataset into k subsets and the model is trained and evaluated k times; the k-fold process was implemented using the *caret* package in R (Kuhn et al. 2023). The 5-fold cross validation produces robust results for high variance data sets (James et al. 2013). For each model that was produced, we calculated the mean absolute error (MAE), Kling-Gupta efficiency (KGE) (Gupta et al. 2009), and coefficient of determination (R^2) along with the RMSE. Using these statistical metrics, we then selected the final linear models based on minimizing RMSE while also keeping the number of input variables limited to 1 per 10–15 response variable values as recommended by Jenkins and Quintana-Ascencio (2020). GLM models were created for all planning horizons, fire numbers, and storage values (S) for the full set of watersheds along with the "best subset" of watersheds that are known to have minimal anthropogenic influenced streamflows. Using both sets of watersheds (i.e., "full set" of 102 analyzed and 24 "best subset" with limited anthropogenic influence) resulted in 30 unique models.

4.6.2 Regression Tree Model

Regression tree models are a form of machine learning that allows for partitioning of the data set for identification of input variable groupings associated with similar responses values (Figure 6). These partitions (Figure 6*h*) are recursive, and the tree is a simple visualization of the recursive model with each terminal node (Figure 6*d*), representing the end point of a singular path through the data, allowing for complex systems to be described through simple flow-chart type logic. The splits in the tree model are identified by incremental improvement in the coefficient of determination (R^2). For this project, we identified the top five preforming regression trees for each runoff event period and storage value using an iterative search of the minimum number of data points required for a split (1 to 20), the minimum number of data points required in a terminal node (1 to 10), and maximum number of split levels allowed in the trees (1 to 5). The regression trees were created using the *rpart* package in R (Therneau et al. 2023). From the top five best performing models, we selected the final models based on RMSE, MAE, KGE, and R^2. During this selection process, we emphasized the statistical validity of the models along with the applicability of the models for practitioners. The output of final regression tree models was then created from R using the *rattle* package (Williams et al. 2022). The k-fold process was not used in the creation of the regression trees due to compatibility issues between the *rpart* and *caret* packages, which did not allow the user to have control over the final tree output and resulted in oversimplifying some models. In total, 30 regression tree models were constructed with 20 trees for the full data set (102 watersheds) based on the runoff event period and the storage value. An additional 10 regression trees were constructed for the known low anthropogenic influence watersheds (24 “best subset” watersheds).

The interpretation of a regression tree model diagram is important for understanding the results and how the models can be used for estimating streamflow changes in the 102 wildfire affected watersheds. Figure 6 shows an example of a regression tree diagram. Several important pieces of information are labeled in the figure. The primary components of a tree model are the root node (*a*), branches (*b* and *c*), and leaf or terminal nodes (*d*). Every tree model has a root node that contains information about the entire sample used in training of the model. This information includes the sample size (*e*), the percentage of the total sample grouped at the node (*f*), and the average CN change value of the sample (*g*). When the tree model splits the input sample based on incremental

improvement of the R^2, branches are formed based on the splitting criterion (h). In Figure 6, the splitting criterion is evaluating if the mean watershed elevation is less than 3,118 m. From the original sample of 71 watersheds, there are 57 watersheds that have a mean elevation less than this threshold and have an average CN value change of 0.032 units. In contrast, only 14 watersheds have a mean elevation greater than the 3,118 m elevation and have a mean CN value change of 9.5 units.

Figure 6. Example regression tree model diagram with labels of important information.

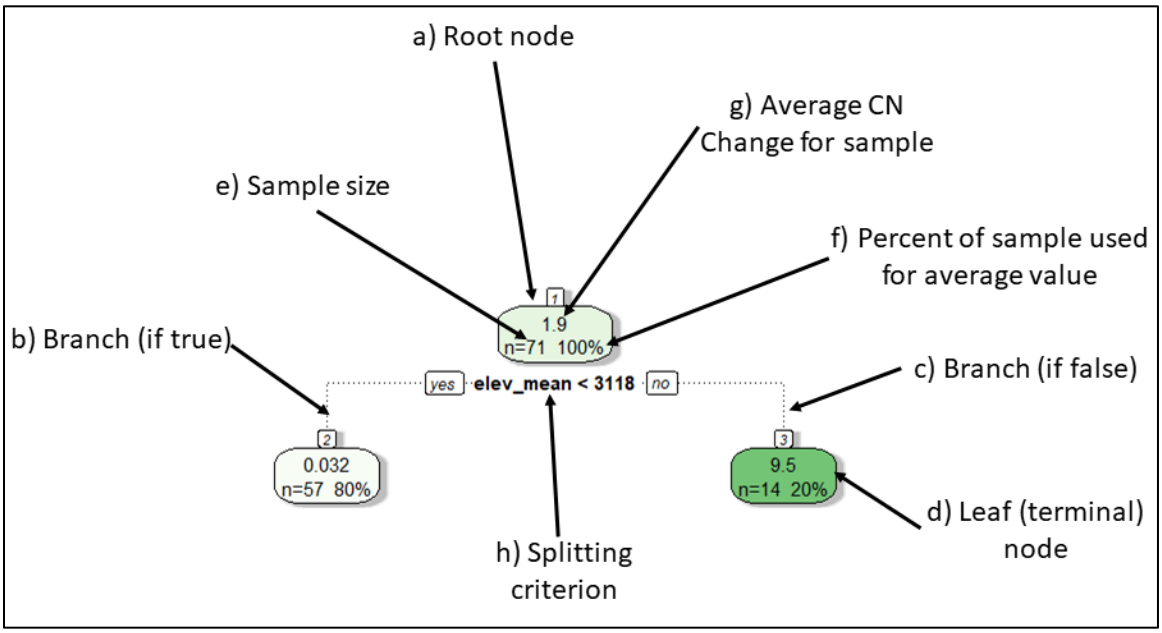

5 Results

5.1 Wildfire Affected Streamgages

The 102 wildfire affected watersheds are in 12 four-digit hydrologic unit codes (HUC4) (Figure 7). These 12 HUC4 watersheds include six states and the headwaters to major river systems in the western US (Figure 7). The "best subset" of fire affected watersheds are in nine HUC4 watersheds, primarily in north- and south-central Colorado. The watershed size distribution has a similar range between the "all watersheds" and "best subset" data sets (Figure 8), with the total area for the majority of watersheds analyzed falling below 1,000 km^2. In the "best subset" watersheds, only two watersheds are greater than 4,000 km^2 (Figure 8*b*), while the full watershed data set includes several more sites (Figure 8*a*).

Figure 7. Map of four-digit hydrologic unit code (HUC4) watersheds within the study domain. The 102 analyzed watersheds are included along with the subset of 24 watersheds (best subset) known to have minimal anthropogenic influence.

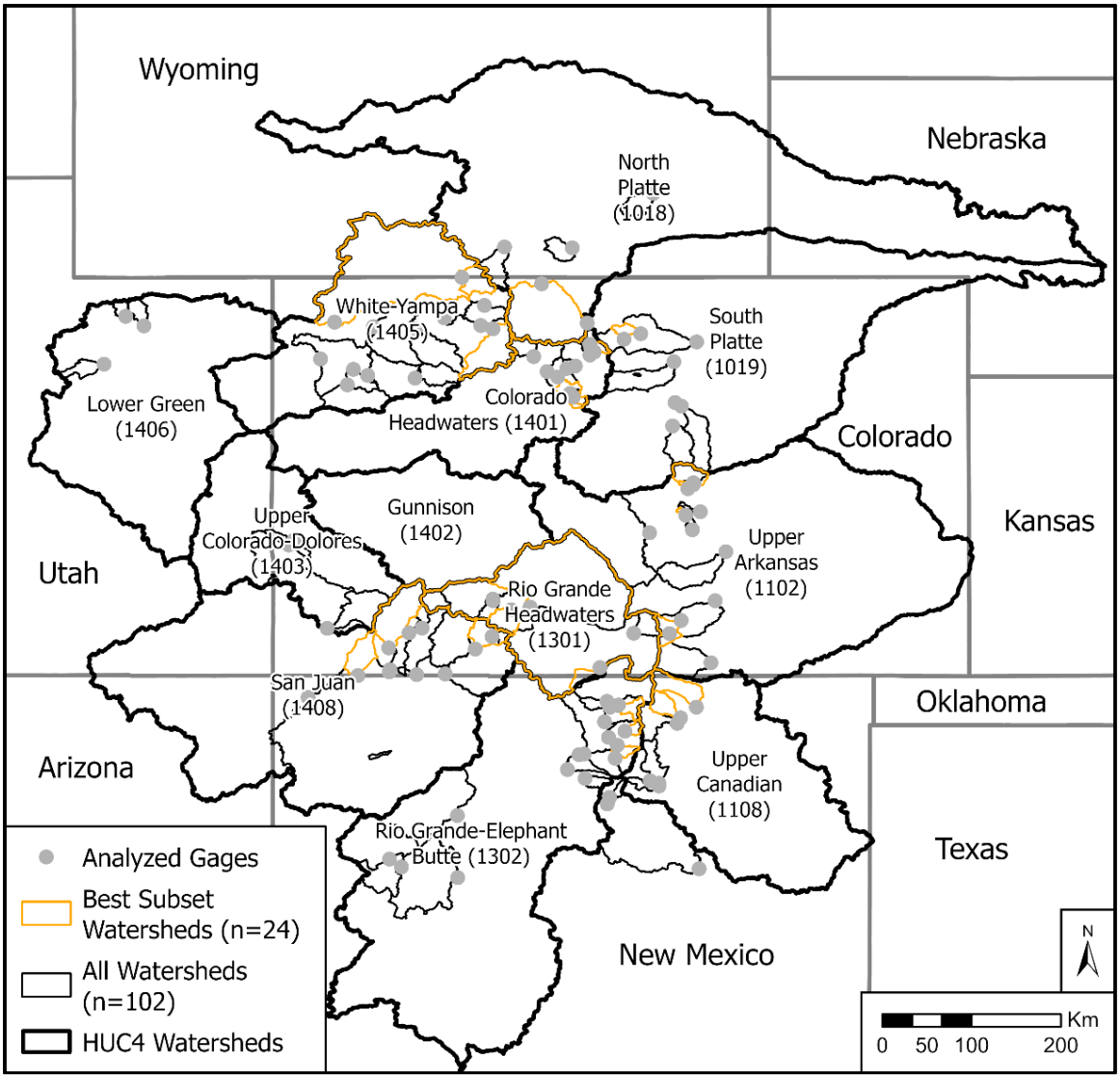

Figure 8. Histogram of watershed area for all 102 analyzed watersheds (*a*). Histogram of watershed area for the 24 "best subset" watersheds that have minimal anthropogenic influence (*b*).

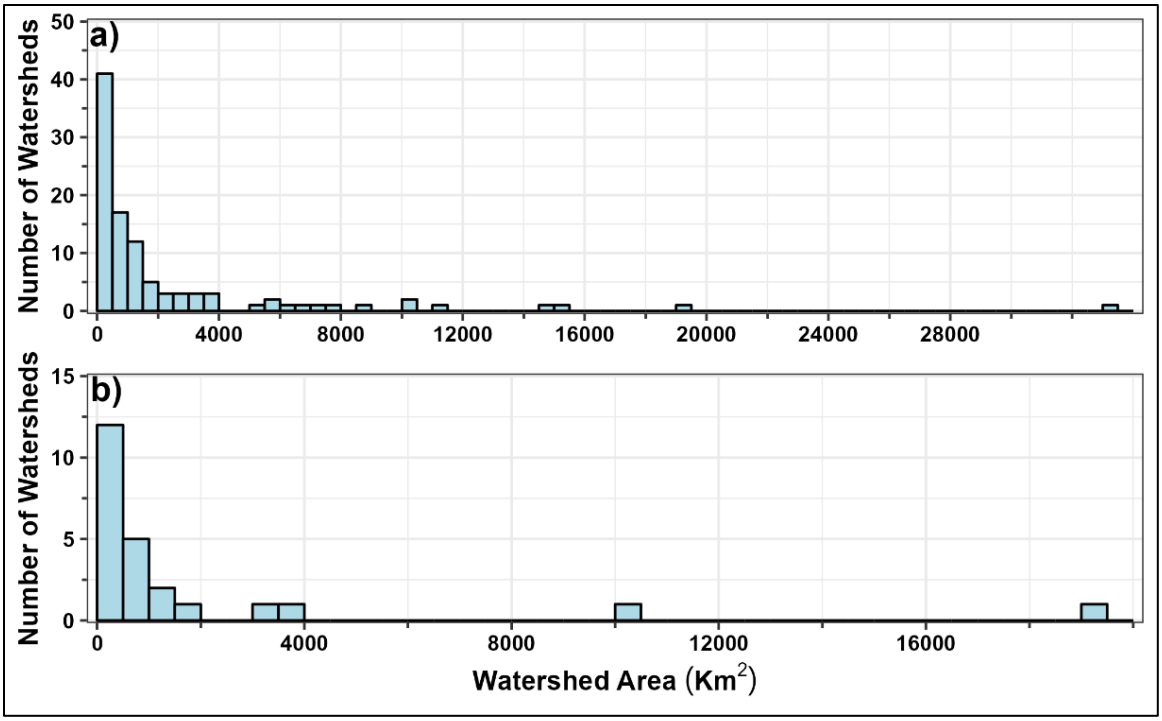

5.2 Observed CN Changes

In the 102 wildfire affected watersheds, the observed changes in CN values vary by both storage (S) and HUC4 (Figure 9). In the majority of the HUC4 locations, the change in CN values is both negative and positive, indicating runoff both decreases and increases, respectively, following wildfire. The only exceptions are the Lower Green (Figure 9*b*) and Upper Pecos (Figure 9*k*) HUC4 watersheds which have only positive or negative CN value changes, respectively. The largest CN value ranges for both S05 and S20 are in the Yampa-White HUC4 (Figure 9*l*). In contrast, the minimum range for both S levels was the Lower Green HUC4 (Figure 9*b*). The median CN change values for the S05 and S20 storage levels are positive for the Colorado Headwaters, Lower Green, North Platte, Rio Grande-Elephant Butte, Rio Grande Headwaters, Upper Arkansas (S05 only), and Upper Colorado-Dolores (Figure 9*a*–e, Figure 9*h*, and Figure 9*j*). The rest of the median CN change values for HUC4 watersheds are negative. The South Platte HUC4, which includes large portions of the Colorado Front Range, has negative CN value changes following wildfire except for only a few individual watersheds (Figure 9*g*). The San Juan HUC4 has a median CN value change of approximately zero for both storage levels (Figure 9*f*).

Figure 9. Boxplot of the median CN pre-fire, post-fire, and change for each HUC4 watershed within the study domain (*a*–*l*) and for all 102 wildfire affected watersheds (*m*). Each HUC4 watershed contains individual watersheds delineated for specific streamgages. The CN value distributions are for all years following the first wildfire. The number of runoff events and sites included within each HUC4. CN change distribution is reported for each runoff event period following the wildfire using both storage levels (S05, S20).

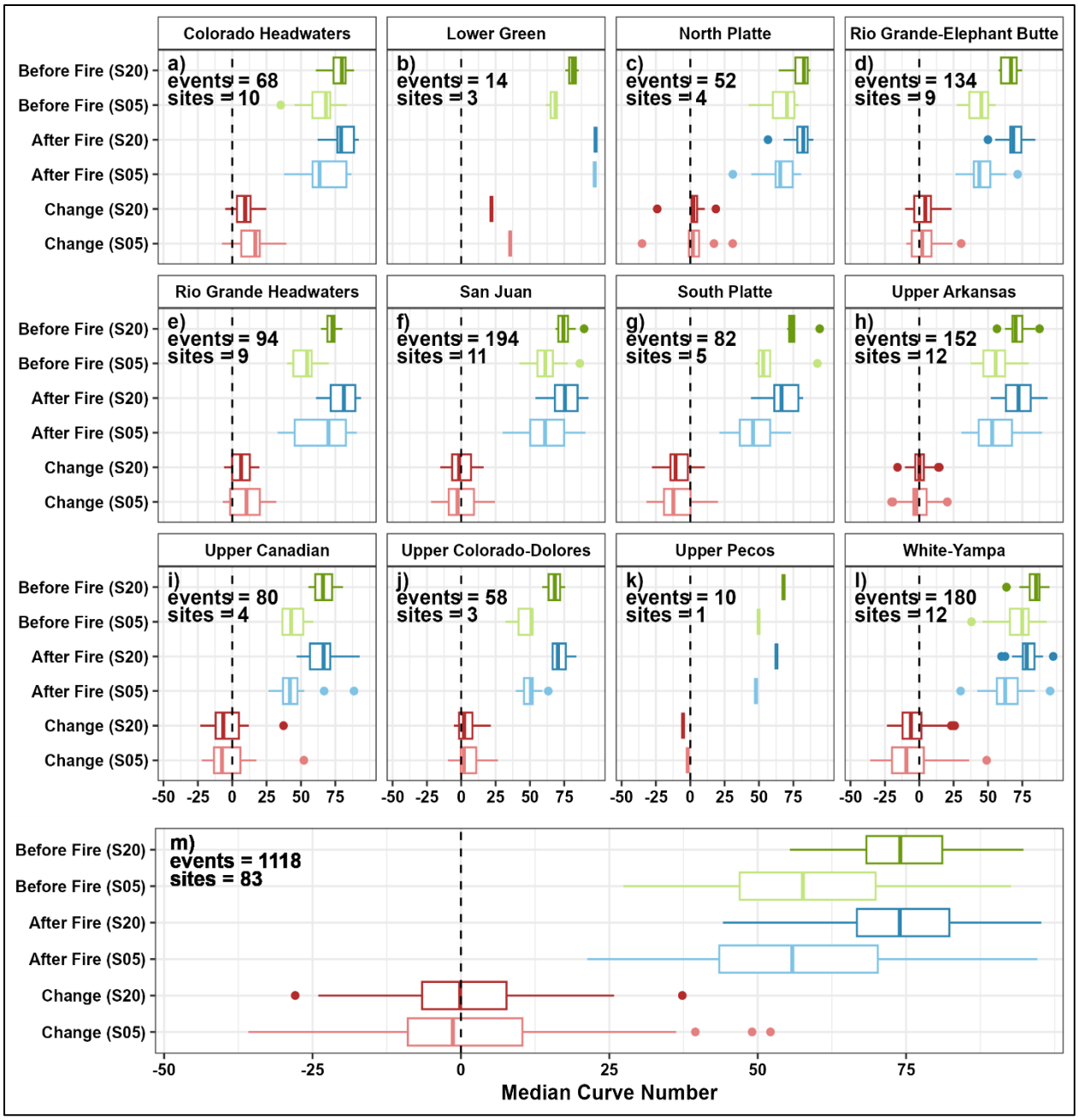

Figure 10 shows the distribution of CN value changes by period. The distribution for most periods is generally normally distributed around zero with some notable exceptions. These exceptions include the periods 10–14 years and more than 15 years following the second fire which appear to approach a uniform distribution (Figure 10*m*, *n*, and *r*–*s*). This may be

due to the limited sample size of watersheds with post-wildfire periods extending beyond 10 years. In addition, the *all yrs* distributions (Figure 10*j*, Figure 10*o*, and Figure 10*t*) do not resemble a normally distributed data set and appear to be positively skewed.

The post-wildfire period 0–4 years immediately after a wildfire is likely the most critical for emergency response and infrastructure vulnerability assessment (Ebel et al. 2012; Ebel et al. 2016). From our analysis, the 0–4 years following the first fire indicates there are an equal number of watersheds that have CN value increases (more runoff) and decreases (less runoff; Figure 10*a* and Figure 10*f*). In contrast, after the second fire there is a slight shift to most watersheds in our analysis showing positive CN value changes (Figure 10*k* and Figure 10*p*).

Using the "best subset" watersheds data, a uniform distribution is evident for nearly all periods and both storage levels (Figure 11). However, when considering all post-wildfire years, there is a difference between the S05 and S20 storage levels (Figure 11*e* and Figure 11*j*). The S20 storage level (Figure 11*j*) is more consistent with a positively skewed distribution, similar to that found in Figure 10*j*. In contrast, the distribution for S05 can be described as a discontinuous uniform distribution with a shift near the zero CN change value (Figure 11*e*).

Figure 10. Histogram of the change in CN following the first and second wildfire in each of the 102 watersheds. CN change distribution is reported for each runoff event period following the wildfire using both storage levels. CN change distribution is reported for each runoff event period following the wildfire using both storage levels (S05, S20).

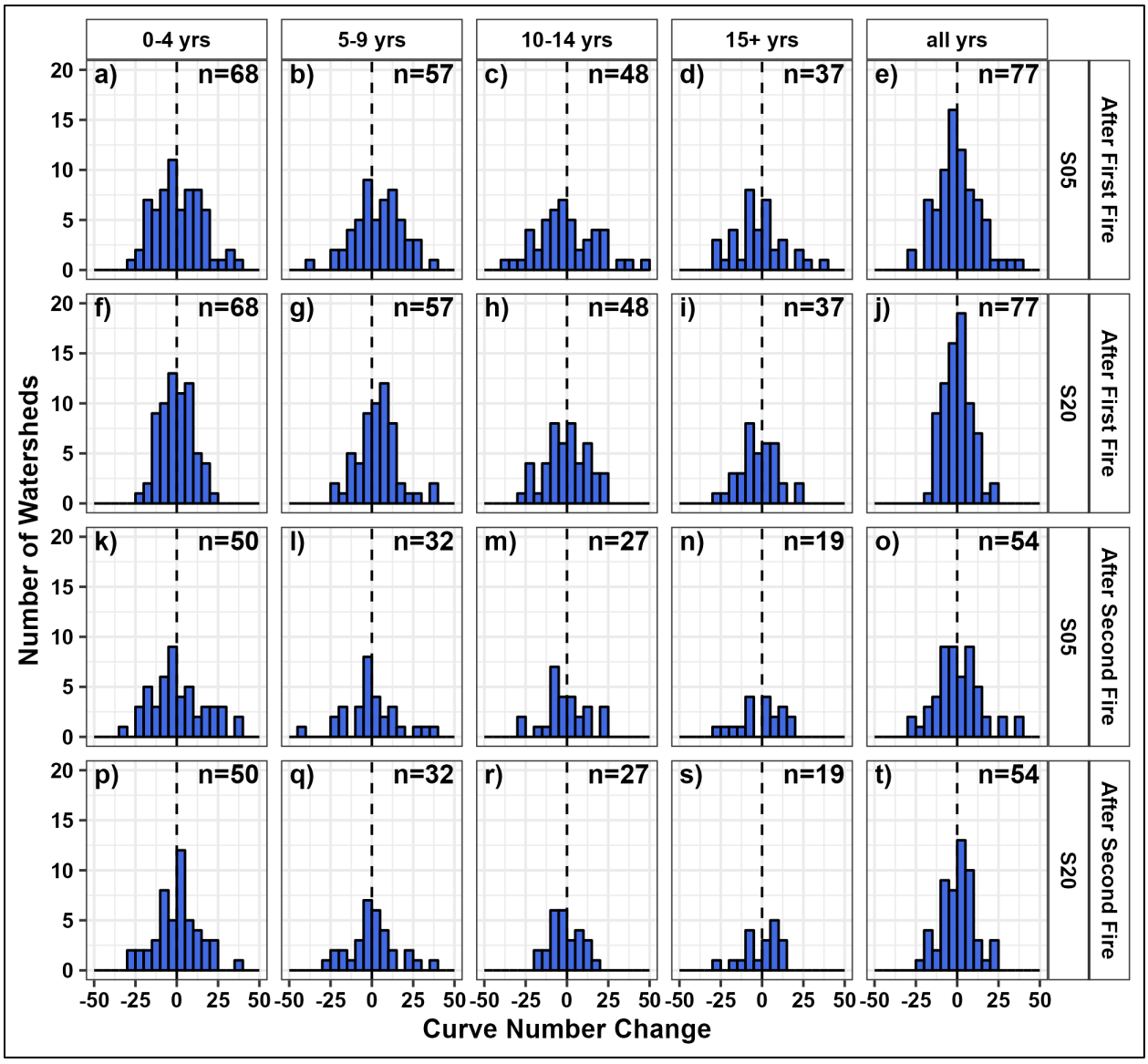

Figure 11. Histogram of CN change following wildfire using the "best subset" of 24 watersheds known to have minimal anthropogenic influence. CN change distribution is reported for each runoff event period following the wildfire using both storage levels (S05, S20).

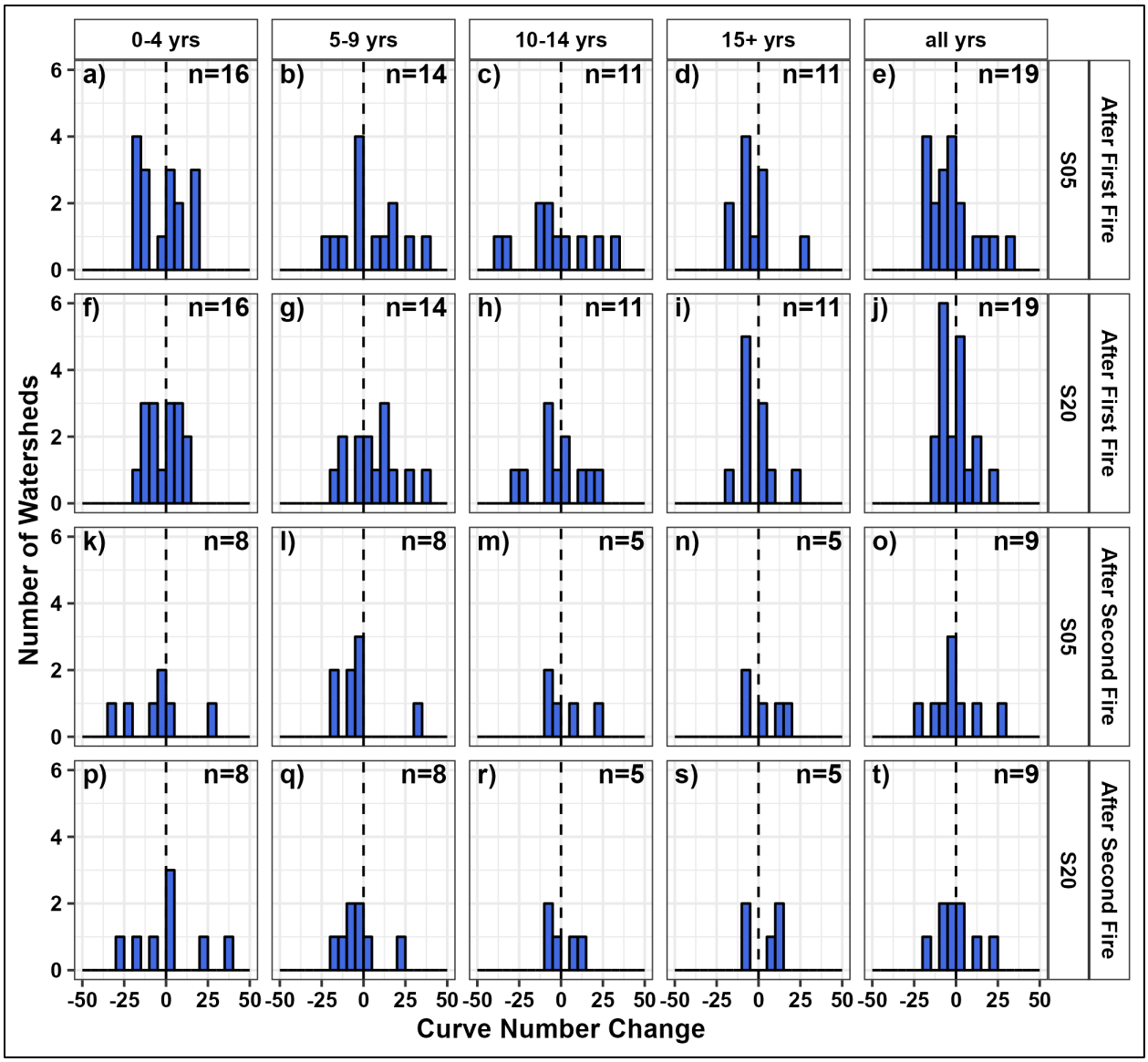

5.3 Prediction Models CN Changes

The estimated median CN changes for all planning horizons are discussed in this section. However, only models for the planning horizon of 0–4 years post-wildfire are discussed in detail because the most urgent need for assessing flood risk is immediately following the wildfire event. Additional results for other planning horizons for the GLM and regression tree models are shown in Appendix B: and Appendix C:, respectively.

5.3.1 Linear Models

The GLMs provide estimated changes in the CN following the first and second wildfire for all planning horizons. To better understand the input variables that had the greatest effect on the creation of the GLMs, we tallied the input variables for each fire number and for each storage value that was used (Figure 12). Each storage value and fire had five GLMs in total (i.e., *0–4 yrs, 5–9 yrs, 10–14 yrs, +15 yrs, and all yrs*). From this analysis, we determined that mean elevation and landcover type classified as Rocky Mountain Subalpine Dry-Mesic Spruce-Fir Forest and Woodland (7055) were used in 3 of the 5 GLMs following the first fire for both storage values (Figure 12*a* and 12*c*). Inter-Mountain Basins Big Sagebrush Shrubland (7080) was included in three models following both the first fire and assuming S05 (Figure 12*a*). The percentage of watershed area burned was only included in the After First Fire and S20 (Figure 12*c*).

While the GLMs for the full watershed data set used 18 unique input variables, the "best subset" watersheds models only used 5 variables (Figure 13). The "best subset" models did not use of burn percentage and an input variable following the first fire (Figure 13). In addition, watershed mean elevation was used less in the "best subset" watershed models (2 models; Figure 13) than it was in the full data set (102 watersheds) models (10 models; Figure 12). Mean watershed slope, a variable used in 4 models in the full data set (102 watersheds), was not used in any models for the "best subset" watershed data set. Additionally, only 3 landcover types, Rocky Mountain Lodgepole Pine Forest (7050), Rocky Mountain Subalpine Dry-Mesic Spruce-Fir Forest and Woodland (7055), and Inter-Mountain Basins Big Sagebrush Shrubland (7080) were included in the "best subset" watershed models while 13 landcover types were included in the full data set (102 watersheds) models.

Figure 12. The number of times each variable was used by the 102-watersheds generalized linear model (GLM) equations based on the fire number in each watershed and the storage (S) value. Five models were created for the number of fires and storage values using all identified watersheds with fire occupancy in the study domain.

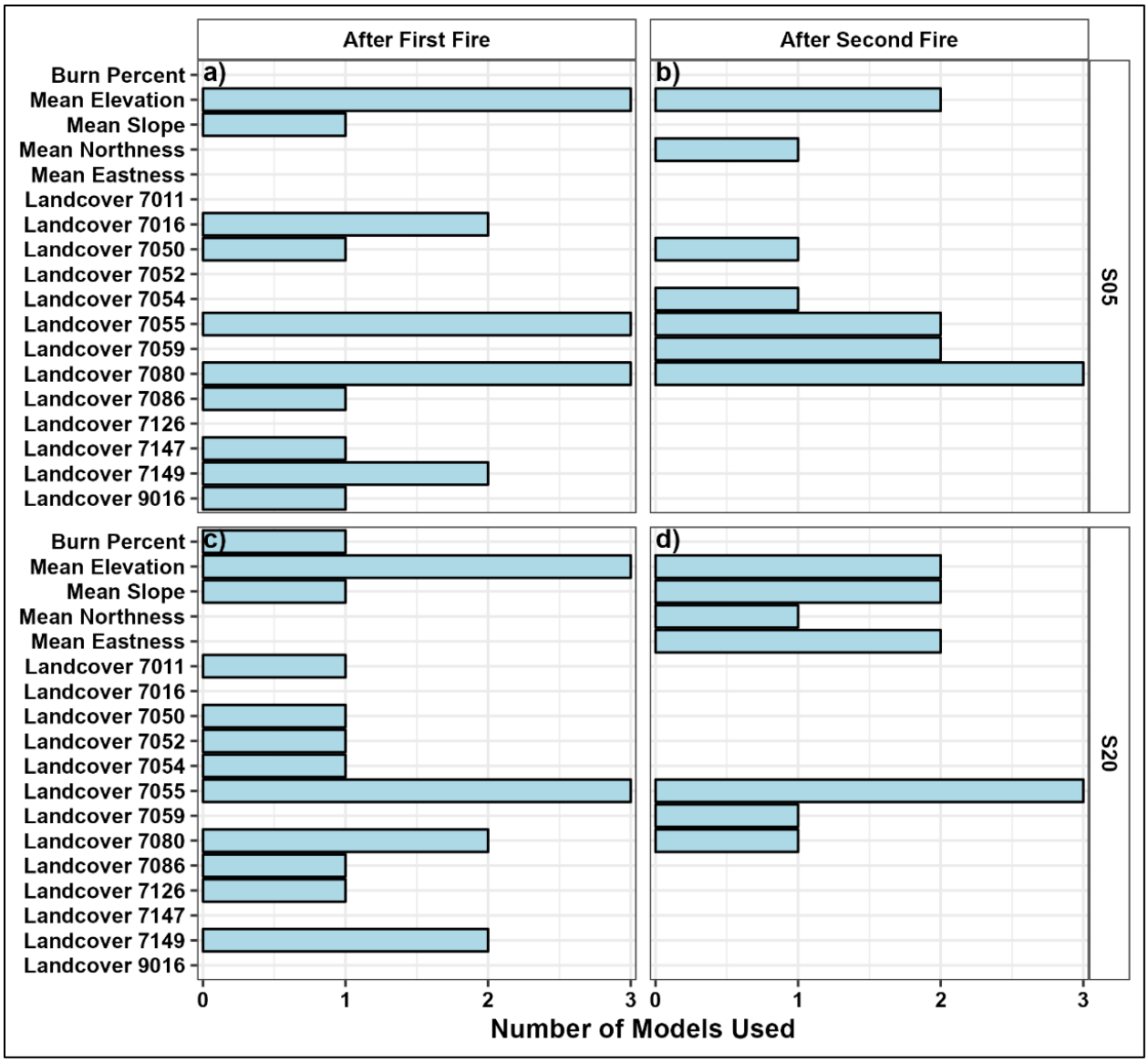

Figure 13. The number of times each variable was used by the GLM equations for the 24 "best subset" watersheds that are known to have minimal anthropogenic influence data set following the first fire in each watershed for both storage (S) values. Five models were created for each number of fires and storage values using the 24 "best subset" watersheds with fire occupancy in the study domain. The plot is limited to the variables used in the "best subset" watersheds models.

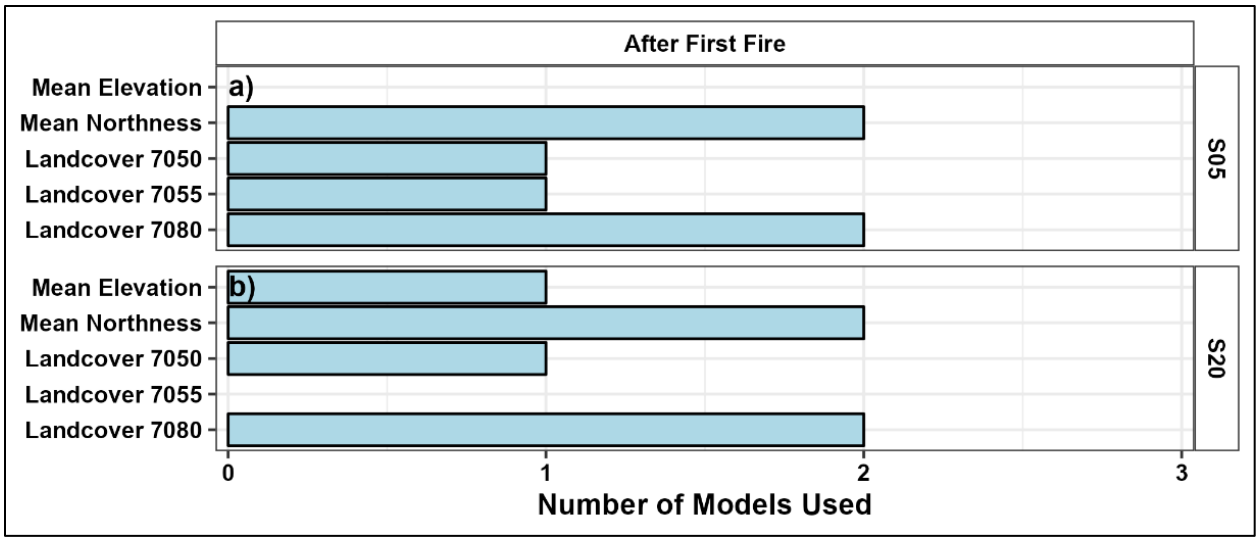

5.3.1.1 All Watersheds Linear Models

The final GLMs for the 0–4 years planning horizon following the first and second fires in all 102 watersheds are included in Table 2, and linear equations for all 102 analyzed watersheds for all scenarios can be found in Table 2. The linear model that we developed for the first wildfire 0–4 Year planning horizon assuming S05, relied on watershed mean elevation, mean slope, and binary operators based on if the majority landcover type is Rocky Mountain Subalpine Dry-Mesic Spruce-Fir Forest and Woodland (7055), Rocky Mountain Lower Montane-Foothill Shrubland (7086), or Rocky Mountain Alpine Bedrock and Scree (9016; Table 2). Landcover names and numbers can be found in Table 1. The change in CN for the immediate 4 years following the first fire, assuming S05, is positively correlated with mean elevation, Rocky Mountain Lower Montane-Foothill Shrubland (7086), and Rocky Mountain Alpine Bedrock and Scree (9016) landcover types, but negatively correlated with mean watershed slope, and Rocky Mountain Subalpine Dry-Mesic Spruce-Fir Forest and Woodland (7055) landcover. The RMSE of the CNs estimated by the GLM is 14.3 units (Table 4).

The GLM for 0–4 years following the first fire with S20, is very similar to the S05 GLM (Table 2). The GLM for the S20 relies on the watershed

mean elevation, and landcover types of Rocky Mountain Subalpine Dry-Mesic Spruce-Fir Forest and Woodland (7055) or Rocky Mountain Lower Montane-Foothill Shrubland (7086) as input variables. For this model, the only negatively correlated coefficient is the landcover type Rocky Mountain Subalpine Dry-Mesic Spruce-Fir Forest and Woodland (7055). All other variables are positively correlated to CN change. This model produces an RMSE of 9.7 units (Table 4).

For the first 4 years following the second fire in a watershed, mean elevation along with Rocky Mountain Subalpine Dry-Mesic Spruce-Fir Forest and Woodland (7055) landcover types are included in the linear models for both S05 and S20 (Table 2). For S05, the model also includes landcover types of Rocky Mountain Lodgepole Pine Forest (7050), Southern Rocky Mountain Pinyon-Juniper Woodland (7059), and Inter-Mountain Basins Big Sagebrush Shrubland (7080). Mean elevation is positively correlated to CN change in the models for both storage values while all landcover types are negatively correlated with the exception of Inter-Mountain Basins Big Sagebrush Shrubland (7080) in the S05 model. The S05 and S20 models had similar RSME values, 16.2 and 13.2 units, respectively (Table 4).

Table 2. Linear models for the change in CN for the 0–4 yr planning horizon following the first and second wildfire within each watershed. Landcover type definitions are included in Table 1. Statistical metrics are included in Table 4.

Wildfire Scenario	Storage Value	Linear Equation
After First Fire: 0–4 years	S05	ΔCN = −38.27 + 0.02(Mean Elevation) −0.87(Mean Slope) −9.07(Landcover=7055) +34.42(Landcover=7086) +22.77(Landcover=9016)
After Second Fire: 0–4 years	S05	ΔCN = −63.48 + 0.03(Mean Elevation) −22.62(Landcover=7050) −25.20(Landcover=7055) −18.07(Landcover=7059) +30.27(Landcover=7080)
After First Fire: 0–4 years	S20	ΔCN = −24.48 + 0.01(Mean Elevation) −7.36(Landcover=7055) +21.71(Landcover=7086)
After Second Fire: 0–4 years	S20	ΔCN = −27.93 + 0.01(Mean Elevation) −11.59(Landcover=7055)

5.3.1.2 "Best Subset" Watersheds Linear Models

The linear models for the 0–4 years planning horizon following the first fire in the 24 "best subset" watershed subsets are included in Table 3. All linear equations for the "best subset" watersheds can be found in Table 3. The final linear models for the "best subset" watersheds generally used fewer variables than the same models used to capture the full watershed data set, primarily because the sample size of the "best subset" watershed subset is limiting the appropriate number of variables used to fit the models. The S05 storage value linear model only includes mean northness and landcover type of Rocky Mountain Subalpine Dry-Mesic Spruce-Fir Forest and Woodland (7055; Table 3). Both variables are negatively correlated with the predicted change in CN for the first four years following the first wildfire.

The final linear model created for the S20 following the first fire uses the mean elevation and northness of the watershed with both variables being positively correlated with the change in CN (Table 3). The RMSE resulting from the S05 is 13.7 units, whereas the S20 RMSE is 9.4 units (Table 5).

Table 3. Linear models for the 0–4 yr planning horizon following the first fire within each of the 24 "best subset" watersheds.

Wildfire Scenario	Storage Value	Linear Equation
After First Fire: 0–4 years	S05	ΔCN = 2.74 −5.29(Mean Northness) −4.50(Landcover=7055)
After First Fire: 0–4 years	S20	ΔCN = −11.66 + 0.004(Mean Elevation) +42.86(Mean Northness)

5.3.2 Regression Tree Models

5.3.2.1 All Watersheds Tree Models

The final tree models for the planning horizon of 0–4 years immediately following the wildfire using all watersheds are shown in Figure 14 through Figure 17. The tree model in Figure 14 uses a starting sample size of 68 watersheds that only had one wildfire event and assumed a storage value S05. The variables used for splitting in this tree model are land cover type, northness, eastness, and elevation. In this tree model, any watershed with a northness at approximately 0.0 would have a negative CN value change whereas all other watersheds would have an average CN value increase of 2.5. The next splitting criterion was based on land cover type (Table 1). If the land cover type is Rocky Mountain Aspen Forest and

Woodland (7011), Colorado Plateau Pinyon-Juniper Woodland (7016), Southern Rocky Mountain Mesic Montane Mixed Conifer Forest and Woodland (7052), Southern Rocky Mountain Ponderosa Pine Woodland (7054), Rocky Mountain Subalpine Dry-Mesic Spruce-Fir Forest and Woodland (7055), Southern Rocky Mountain Pinyon-Juniper Woodland (7059), Inter-Mountain Basins Montane Sagebrush Steppe (7126), Inter-Mountain Basins Semi-Desert Shrub-Steppe (7127), Western Great Plains Foothill and Piedmont Grassland (7147), Western Great Plains Shortgrass Prairie (7149), or Developed-Roads (7299), the average CN value change is 27 units. If the land cover type does not match those listed, then northness of the watershed is considered. If the watershed northness is very close to 0.0 (north facing) then the CN value change is −15 units; however, if the watershed is oriented slightly east or west, then the average CN value change is 0.46 units and can be further split into additional branches. Eastness is the next splitting criteria and for watersheds that have an eastness value of less than 0.0012 (very close to due east orientation), the average CN value change is −0.73 units whereas watersheds with an eastness value greater than the threshold have an average CN value change of 13 units. Finally for watersheds that have an eastness value of less than 0.0012 and an elevation less than 3,171 m, then the average CN value change is 13 units. For watersheds with an elevation of greater than 3,171 m, the CN value change averages −1.8 units. The RMSE for this tree model is 10.8 units (Table 4).

The tree diagram in Figure 15 is based on CN change values using an assumed storage value S20 for the planning horizon of 0–4 years following the first wildfire (68 total watersheds). The initial variables used for splitting in this tree model are land cover type, northness, elevation, and slope. For watersheds with land cover types Rocky Mountain Aspen Forest and Woodland (7011), Colorado Plateau Pinyon-Juniper Woodland (7016), Southern Rocky Mountain Mesic Montane Mixed Conifer Forest and Woodland (7052), Southern Rocky Mountain Ponderosa Pine Woodland (7054), Rocky Mountain Subalpine Dry-Mesic Spruce-Fir Forest and Woodland (7055), Southern Rocky Mountain Pinyon-Juniper Woodland (7059), Inter-Mountain Basins Montane Sagebrush Steppe (7126), Inter-Mountain Basins Semi-Desert Shrub-Steppe (7127), Western Great Plains Foothill and Piedmont Grassland (7147), Western Great Plains Shortgrass Prairie (7149), or Developed-Roads (7299), the average CN value change is 17 units, otherwise the average is −0.87 units. Stepping through the tree model results for the majority of watersheds have a predicted positive CN value change slightly greater than zero. The RMSE for this tree model is 7.3 units (Table 4).

Figure 14. Regression tree diagram for CN change in 68 analyzed watersheds (*n*) that had runoff events in the 0–4 years following the first wildfire. The storage value was assumed to be 5% (S05). Landcover types are listed in Table 1.

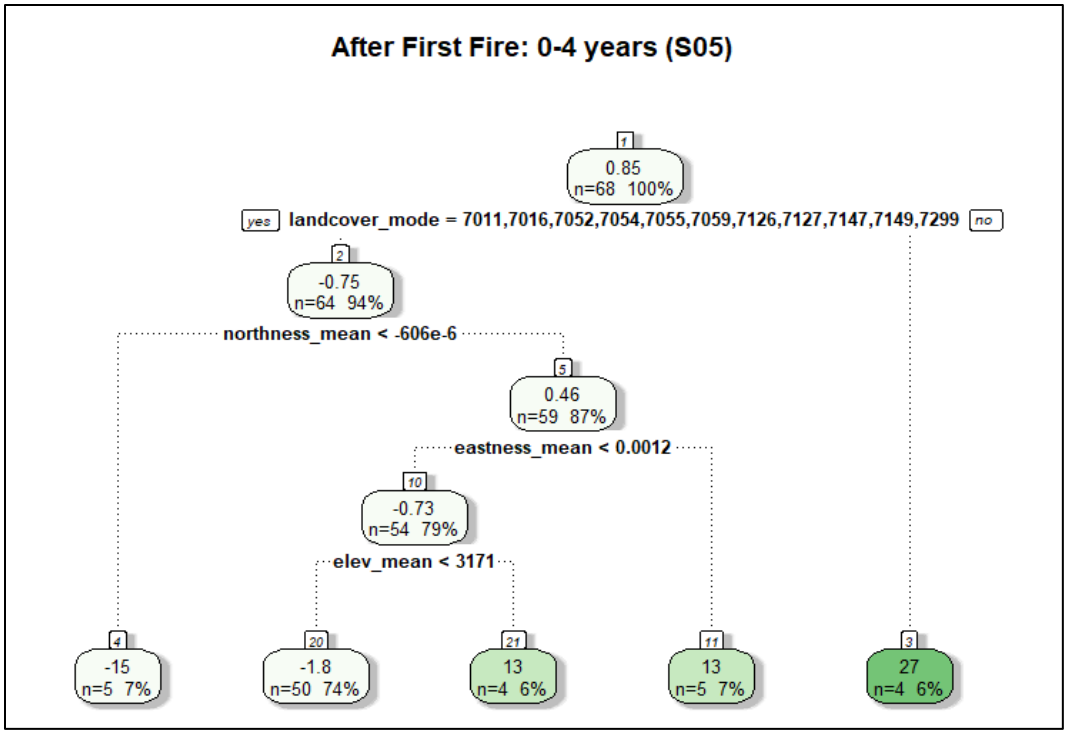

Figure 15. Regression tree diagram for CN change in 68 analyzed watersheds (*n*) that had runoff events between 0 to 4 years following the first wildfire. The storage value was assumed to be 20% (S20). Landcover types are listed in Table 1.

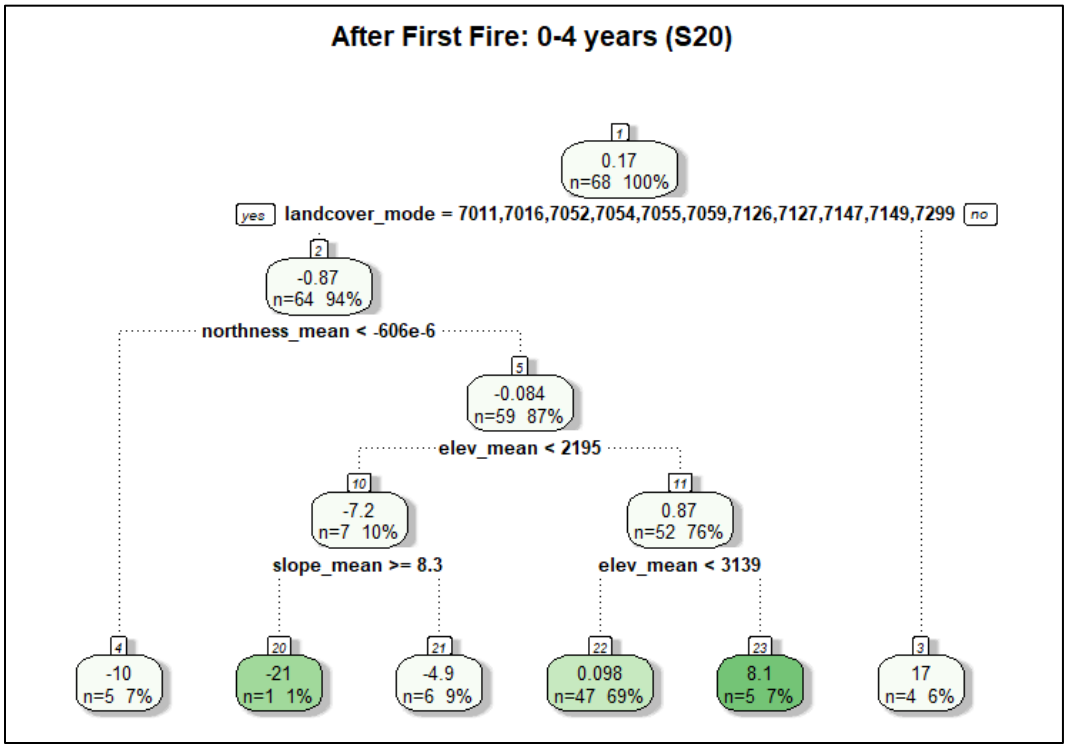

The tree diagram in Figure 16 assumes S05 and was created for the planning horizon of 0–4 years following the second wildfire within each watershed. The total number of analyzed watersheds that recorded a runoff event following the second wildfire within the watershed during the streamgage period of record is 50. This is a reduction of approximately 26% relative to the total number of watersheds used in Figure 14. The variables used for splitting in this tree model are land cover type and northness. For watersheds that do not have land cover type Rocky Mountain Aspen Forest and Woodland (7011), Rocky Mountain Lodgepole Pine Forest (7050), Rocky Mountain Subalpine Dry-Mesic Spruce-Fir Forest and Woodland (7055), Southern Rocky Mountain Pinyon-Juniper Woodland (7059), Western Great Plains Foothill and Piedmont Grassland (7147), or Western Great Plains Shortgrass Prairie (7149), and northness of greater than or equal to 0.0014, the average CN value is 5.2 units. The majority of watershed CN value changes are predicted to be positive after stepping through the tree model. The RMSE for the tree model following the second wildfire assuming S05 is 14.2 units (Table 4).

Figure 16. Regression tree diagram for CN change in 50 analyzed watersheds (*n*) that had runoff events for 0–4 years following the second wildfire. The storage level was assumed to be 5% (S05). Landcover types are listed in Table 1.

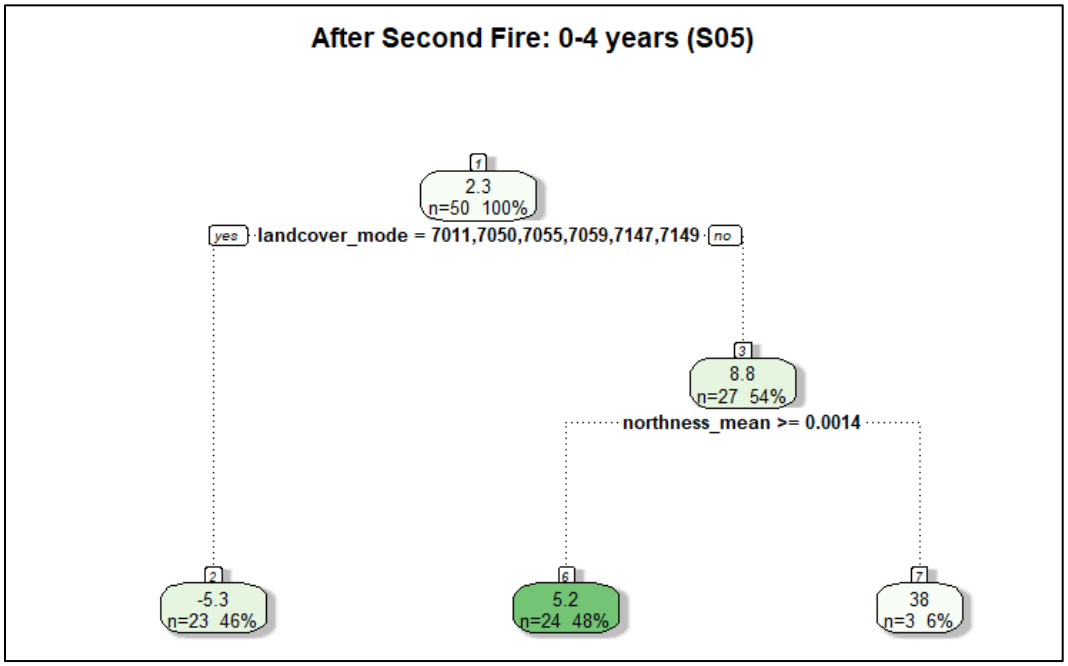

The tree diagram in Figure 17 is for the 0–4 year planning horizon following the second wildfire with an assumed S20. The variables used for splitting in this tree model are burn percentage, land cover type, mean elevation, and mean slope. These results indicate that a single watershed

with a relatively low total burn percentage had a CN value change of 37 units following the second wildfire event. Otherwise, the rest of the watersheds follow a similar first splitting criterion of land cover type. If the watershed has a land cover type of Rocky Mountain Aspen Forest and Woodland (7011), Colorado Plateau Pinyon-Juniper Woodland (7016), Rocky Mountain Lodgepole Pine Forest (7050), Southern Rocky Mountain Ponderosa Pine Woodland (7054), Rocky Mountain Subalpine Dry-Mesic Spruce-Fir Forest and Woodland (7055), Southern Rocky Mountain Pinyon-Juniper Woodland (7059), Rocky Mountain Lower Montane-Foothill Shrubland (7086), Inter-Mountain Basins Semi-Desert Shrub-Steppe (7127), Western Great Plains Foothill and Piedmont Grassland (7147), or Western Great Plains Shortgrass Prairie (7149), and the slope is between 14% and 16%, then the average CN value change is 9.9 units. If the slope is less than 14% then the average is –2.2 units. If the slope is greater than 16% and the elevation is 3,058 m, then the average change is 2.5 units. The results of this model indicate the majority of watersheds are predicted to have a negative CN value change. Both slope and elevation have an impact on the magnitude and direction of the CN value change. The RMSE for the tree model in Figure 17 is 8.5 units (Table 4).

Figure 17. Regression tree diagram for CN change in 50 analyzed watersheds (*n*) that had runoff events for 0–4 years following the second wildfire. The storage level was assumed to be 20% (S20). Landcover types are listed in Table 1.

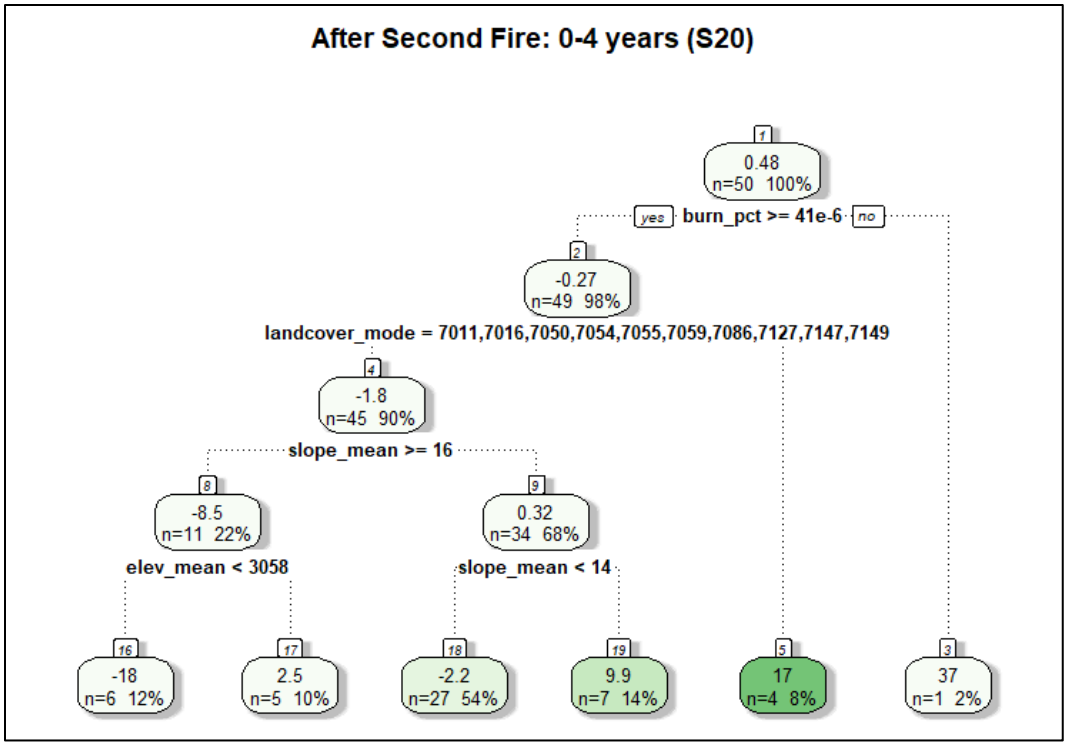

5.3.2.2 "Best Subset" Watersheds Tree Models

The 24 "best subset" watersheds that have minimal anthropogenic effects final regression tree models for the first four years (0–4 years) immediately following the first wildfire are shown in Figure 18 and Figure 19. Models following the second fire in 24 "best subset" watersheds that have minimal anthropogenic effects were not constructed due to a lack of data for those watersheds. Both figures have an initial watershed sample size of 16 and begin by splitting the watersheds based on the mean northness (Figure 18 and Figure 19). The 5% storage value (S05) identifies watersheds with a mean northness value less than 0.0048 (Figure 18). If the mean northness is less than −0.0024, the average CN change is −18 units (three watersheds). If northness is greater than or equal to 0.0011 but less than 0.0048, CN changes by −11 units, however when mean northness is between −0.0024 and 0.0011 average CN change is approximately 0 units (0.19). When northness is greater than 0.0048, mean watershed slope is less than 11%, and burn percentage is greater than or equal to 0.41, average CN change is −17 units. If the watershed meets the same northness and slope conditions but burn percentage is less than 0.41, the average CN change is 3.4 units. When watershed northness is greater than or equal to 0.0048 and slope is greater than or equal to 11%, the CN changes by 15 units. The RMSE for the tree model shown in Figure 18 is 2.6 units (Table 5).

When using the S20, we found that if the watershed northness was less than −0.0024, the average median CN change is −12 units. Otherwise, when northness is greater than (inclusive) −0.0024 and the watershed mean elevation is greater than (inclusive) 3,167 m, the average CN change was 11 units. If the northness was between −0.0024 and 0.052, watershed elevation is less than 3,167 m, and watershed eastness is less than −0.0014 the CN change was −7.7 units. However, if the eastness is greater than or equal to −0.0014, average CN change was 3.4 units. For watersheds with a mean elevation less than 3,167 m and a mean northness greater than 0.052, average CN change was 8.4 units following the first wildfire. The RMSE for the tree model shown in Figure 19 was 3.1 units (Table 5).

Figure 18. Regression tree diagram for median CN change following first wildfire and using 0–4 years post-wildfire in the 24 "best subset" watersheds that have minimal anthropogenic effects. The storage level was assumed to be 5% (S05).

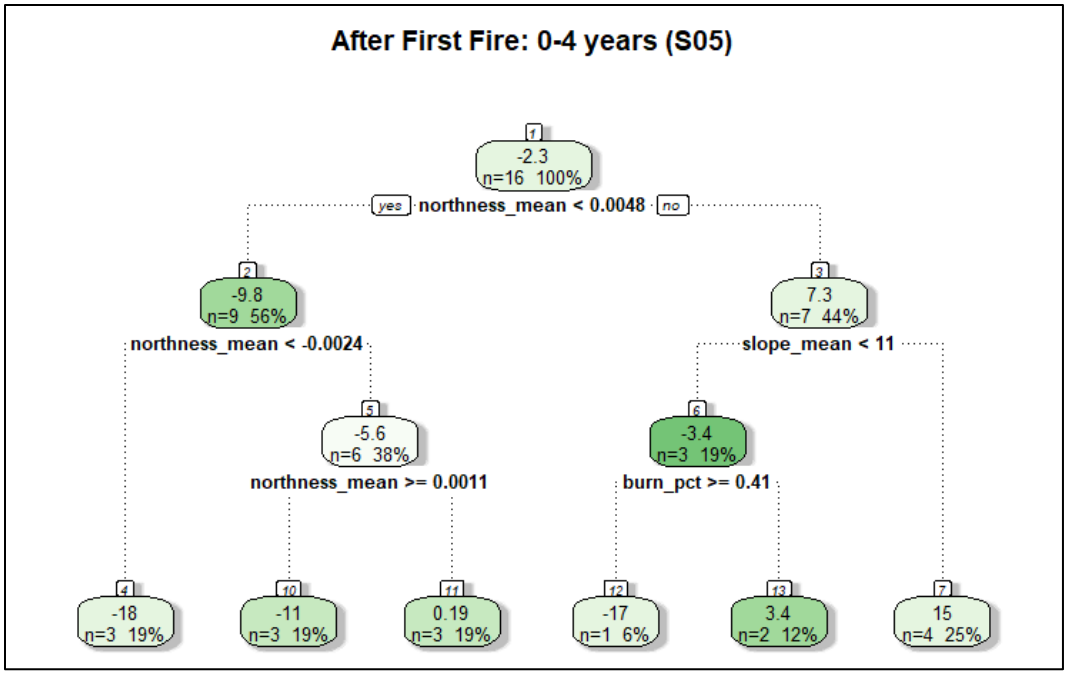

Figure 19. Regression tree diagram for median CN change following first wildfire and using 0–4 years post-wildfire in the USGS "best subset" watersheds. The storage level was assumed to be 20% (S20).

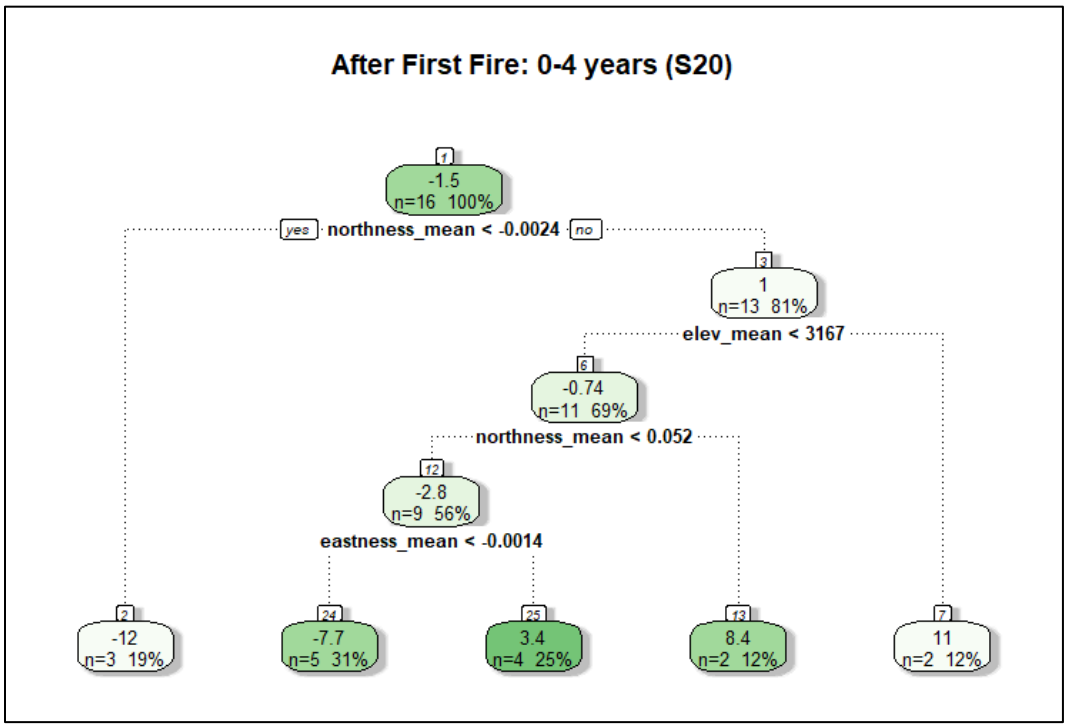

5.3.3 Summary of Model Performance

Using the final models for both the linear (GLM) and regression tree methods, the predicted CN change values using all watersheds were plotted against the observed CN changes for all 102 watersheds (Figure 20). The 1:1 line (perfect fit) was also displayed to help evaluate the model performance. Our overall results indicate both model structures have similar ranges for changes of CN values following wildfire. The overall accuracy of the tree models was slightly better compared to the GLM for several of the post-wildfire periods. For example, periods 10–14 years and 15+ years the tree models show substantial improvement over the linear models (Figure 20*c*–*d*, Figure 20*h*–*i*, Figure 20*m* and *n*, and Figure 20*r*–*s*) based on the smaller residuals from the 1 to 1 line. There was also improved model accuracy for the important period immediately following a wildfire (0–4 years) (Figure 20*a*, Figure 20*f*, Figure 20*k*, and Figure 20*p*).

Figure 21 shows the regression tree model results using the subset of the 24 "best subset" watersheds that have minimal anthropogenic effects. Because of the reduced sample size of the "best subset" watersheds, results following only the first wildfire event were developed. Instead of using all watersheds (Figure 20), the accuracy of regression tree model results was substantially improved compared to linear models for the "best subset" watersheds. The predicted CN value changes using the tree models match observed values closely for a majority of periods and storage levels (Figure 21).

The regression tree models had lower RMSE values for each post-wildfire period and storage value combination compared to the GLMs (Figure 22). The difference in RMSE between the GLM and tree model was larger for the "best subset" watershed models when compared to using all watersheds. When comparing model error using the "best subset" of watersheds, the tree model RMSE values were less than half of GLM values (Figure 22*k*–*o*). Model RMSE, MAE, KGE, and R^2 statistics for all GLM and regression tree models are listed in Table 4 (All Watersheds) and Table 5 ("best subset" Watersheds).

Figure 20. Predicted and observed CN change using the GLMs and the regression tree models for all 102 watersheds included in the analysis.

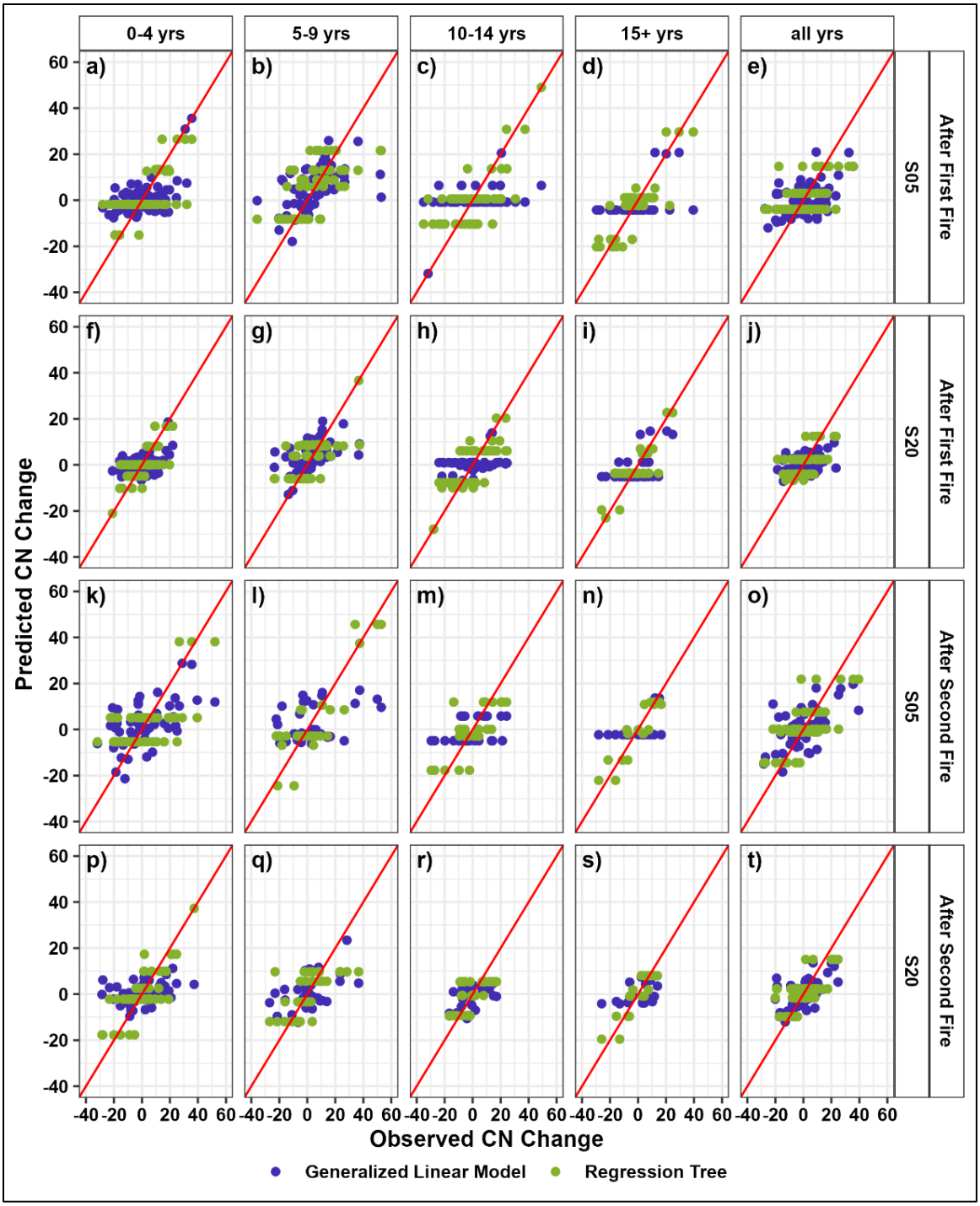

Figure 21. Predicted and observed CN change using the GLMs and the regression tree models for the subset of 24 watersheds known to have minimal anthropogenic influence.

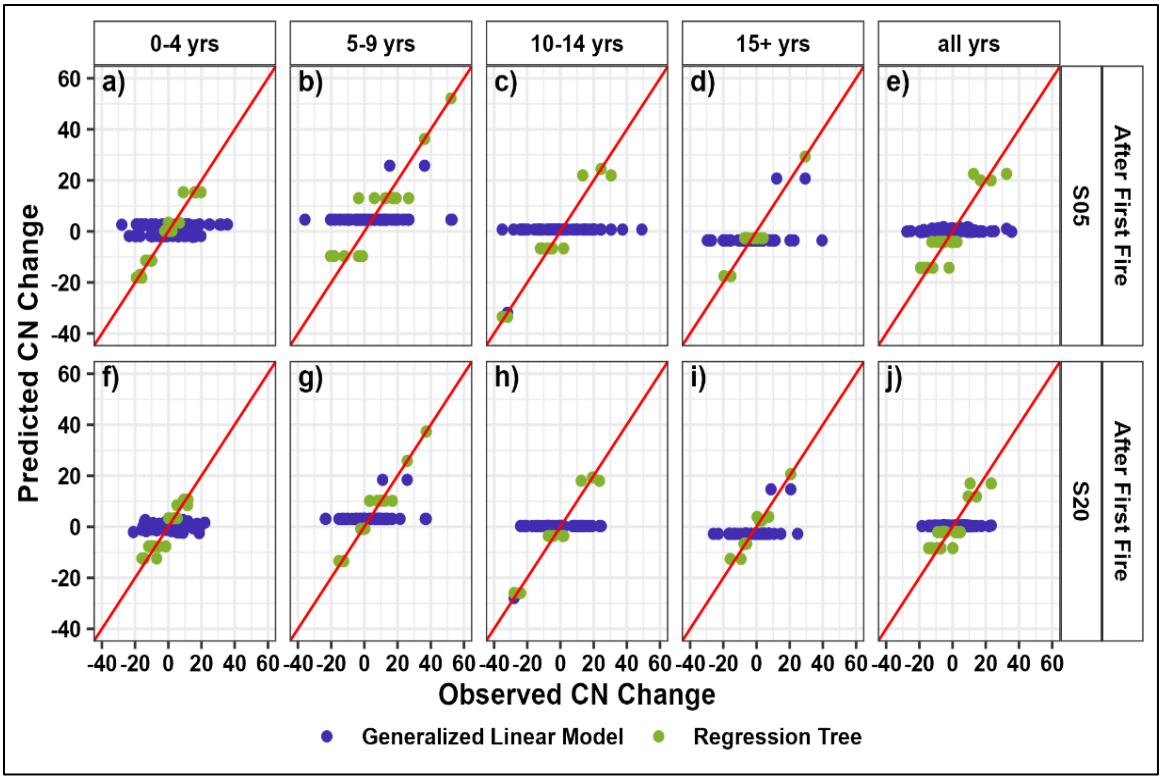

Figure 22. Root-mean-square error (RMSE) of the final regression tree and GLMs for the first and second fire during each period following fire for both storage scenarios (S05 and S20).

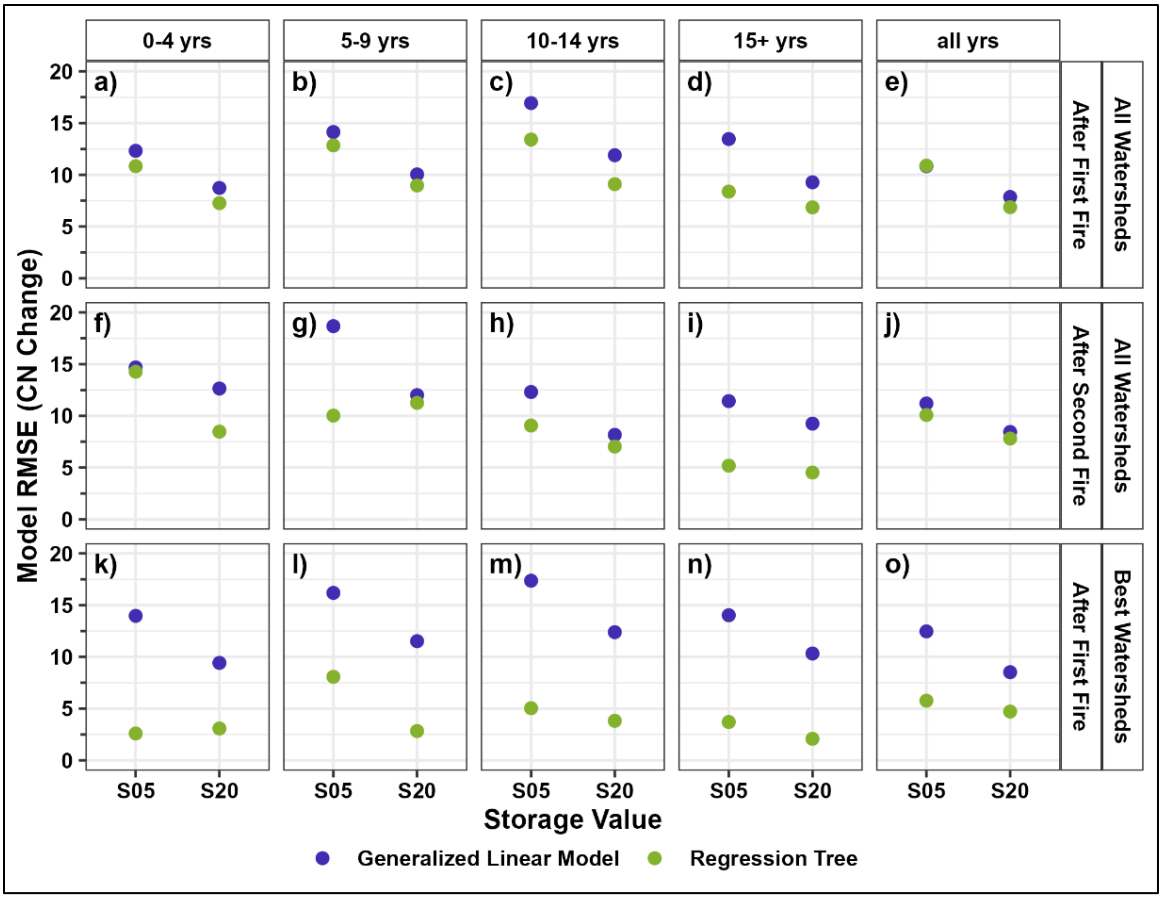

Table 4. GLM and regression tree model statistics for the models developed using all watersheds data set. The RSME, mean absolute error (MAE), Kling-Gupta efficiency (KGE), and R^2 statistics are included for all planning horizons using the 20% (S20) and 5% (S05) storage values.

Model Type	Fire Number	Planning Horizon Years	Storage Value	RMSE	MAE	KGE	R^2
GLM	First	0–4	S05	12.32	10.26	0.28	0.24
GLM	First	0–4	S20	8.74	7.26	0.15	0.16
Tree	First	0–4	S05	10.84	8.23	0.49	0.41
Tree	First	0–4	S20	7.26	5.88	0.50	0.42
GLM	First	5–9	S05	14.14	10.09	0.33	0.28
GLM	First	5–9	S20	10.04	6.96	0.34	0.28
Tree	First	5–9	S05	12.84	10.24	0.49	0.41
Tree	First	5–9	S20	8.97	6.63	0.51	0.43
GLM	First	10–14	S05	16.94	13.09	0.06	0.11
GLM	First	10–14	S20	11.89	9.20	0.16	0.17
Tree	First	10–14	S05	13.41	11.06	0.53	0.44

Table 4 (cont.). GLM and regression tree model statistics for the models developed using all watersheds data set. The RSME, mean absolute error (MAE), Kling-Gupta efficiency (KGE), and R^2 statistics are included for all planning horizons using the 20% (S20) and 5% (S05) storage values.

Model Type	Fire Number	Planning Horizon Years	Storage Value	RMSE	MAE	KGE	R^2
Tree	First	10–14	S20	9.10	7.71	0.60	0.51
GLM	First	+15	S05	13.46	9.93	0.22	0.20
GLM	First	+15	S20	9.28	7.52	0.36	0.30
Tree	First	15+	S05	8.38	6.86	0.76	0.69
Tree	First	+15	S20	6.85	5.21	0.70	0.62
GLM	First	all yrs	S05	10.83	8.52	0.29	0.25
GLM	First	all yrs	S20	7.86	6.17	0.13	0.15
Tree	First	all yrs	S05	10.89	8.74	0.28	0.24
Tree	First	all yrs	S20	6.87	5.43	0.42	0.35
GLM Average (First Fire)			S05	13.54	10.38	0.24	0.22
GLM Average (First Fire)			S20	9.56	7.42	0.23	0.21
Tree Average (First Fire)			S05	11.27	9.03	0.51	0.44
Tree Average (First Fire)			S20	7.81	6.17	0.55	0.46
GLM	Second	0–4	S05	14.69	11.46	0.37	0.31
GLM	Second	0–4	S20	12.65	9.45	0.04	0.10
Tree	Second	0–4	S05	14.27	11.32	0.42	0.35
Tree	Second	0–4	S20	8.47	6.98	0.68	0.60
GLM	Second	5–9	S05	18.67	14.33	0.13	0.15
GLM	Second	5–9	S20	12.01	9.21	0.32	0.27
Tree	Second	5–9	S05	10.03	7.89	0.82	0.76
Tree	Second	5–9	S20	11.26	8.54	0.44	0.36
GLM	Second	10–14	S05	12.31	9.46	0.13	0.15
GLM	Second	10–14	S20	8.16	7.03	0.27	0.23
Tree	Second	10–14	S05	9.06	7.32	0.62	0.54
Tree	Second	10–14	S20	7.03	5.90	0.51	0.43
GLM	Second	+15	S05	11.43	9.44	0.14	0.16
GLM	Second	+15	S20	9.25	7.66	0.17	0.17
Tree	Second	+15	S05	5.18	4.51	0.87	0.83
Tree	Second	+15	S20	4.52	4.16	0.85	0.80
GLM	Second	all yrs	S05	11.20	8.84	0.42	0.34
GLM	Second	all yrs	S20	8.44	6.61	0.35	0.29
Tree	Second	all yrs	S05	10.08	8.09	0.55	0.47
Tree	Second	all yrs	S20	7.81	6.22	0.48	0.40
GLM Average (Second Fire)			S05	13.66	10.71	0.24	0.22
GLM Average (Second Fire)			S20	10.10	7.99	0.23	0.21
Tree Average (Second Fire)			S05	9.72	7.83	0.66	0.59
Tree Average (Second Fire)			S20	7.82	6.36	0.59	0.52

Table 5. GLM and regression tree model statistics for the models developed using the "best subset" watershed data set. The RSME, MAE, KGE, and R^2 statistics are included for all planning horizons using the 20% (S20) and 5% (S05) storage values. No models were created for any planning horizons following the second fire due to lack of data.

Model Type	Fire Number	Planning Horizon Years	Storage Value	RMSE	MAE	KGE	R2
GLM	First	0–4	S05	13.97	11.50	−0.20	0.02
GLM	First	0–4	S20	9.42	7.75	−0.22	0.02
Tree	First	0–4	S05	2.60	2.04	0.97	0.96
Tree	First	0–4	S20	3.08	2.65	0.91	0.88
GLM	First	5–9	S05	16.19	12.59	−0.08	0.06
GLM	First	5–9	S20	11.52	8.78	−0.08	0.06
Tree	First	5–9	S05	8.08	6.50	0.88	0.84
Tree	First	5–9	S20	2.83	1.80	0.97	0.96
GLM	First	10–14	S05	17.37	13.65	−0.05	0.07
GLM	First	10–14	S20	12.39	9.91	0.02	0.10
Tree	First	10–14	S05	5.04	3.86	0.95	0.93
Tree	First	10–14	S20	3.82	3.30	0.96	0.94
GLM	First	+15	S05	14.03	10.62	0.10	0.13
GLM	First	+15	S20	10.33	8.26	0.09	0.13
Tree	First	+15	S05	3.70	3.22	0.93	0.91
Tree	First	+15	S20	2.08	1.52	0.97	0.95
GLM	First	all yrs	S05	12.47	9.73	−0.35	0.00
GLM	First	all yrs	S20	8.52	6.81	−0.39	0.00
Tree	First	all yrs	S05	5.77	4.85	0.88	0.83
Tree	First	all yrs	S20	4.71	4.20	0.82	0.76
GLM Average (First Fire)			S05	14.80	11.62	−0.12	0.06
GLM Average (First Fire)			S20	10.43	8.30	−0.12	0.06
Tree Average (First Fire)			S05	5.04	4.09	0.92	0.89
Tree Average (First Fire)			S20	3.30	2.69	0.92	0.90

6 Discussion

The CN value changes resulting from the data at the 102 streamgages used in our study indicate both positive and negative CN value changes. We would expect the CN values to increase, especially immediately after a wildfire due to increase runoff in burned watersheds (Ebel et al. 2012; Moody and Martin 2001; Neary et al. 2003; Stoof et al. 2012).; however, our results show there are substantial variations. There are likely several potential causes for negative change in CN values related to the data used in our analysis. First, the sample size of rainfall driven runoff events and watersheds (full set of 102 and "best subset" of 24) for this study is relatively small. Because of most streams in our study area are being driven by snowmelt hydrology, the period for rainfall runoff events is limited to the summer months. Second, the rainfall events that are typical of the region, especially outside the snowmelt period, are convective storms that can be highly localized, and the effects of localized storms on streamflow response may not be apparent when averaged over the larger watersheds represented by the streamgage data. Third, wildfires typically are small relative to the watershed size (Figure 2) and affect headwater streams (Figure 1) that often are ephemeral or have minimal perennial streamflow whereas the streamgage network in Colorado and across much of the western US is focused on large perennial streams. This network configuration results in relatively few streamgages that have watershed areas affected by wildfire. In addition, wildfire effects as a percentage of the total watershed area are typically very small (Figure 2). Additionally, runoff most likely flows over areas not affected by wildfire which allows for infiltration of the runoff in arid regions with high infiltration losses. Finally, the initial soil moisture conditions for each runoff event were not considered in our analysis. Not considering soil moisture means that runoff events with similar rainfall could produce different runoff responses regardless of the area of watershed affected by wildfire.

Although there are some modeled soil moisture products that could help inform antecedent conditions for each runoff event we identified, there are challenges with directly integrating those estimates to the storage or initial abstraction values used in the CN method and there is uncertainty in the best value for predicting the streamflow magnitude of future runoff events. Quantification of the uncertainty for each of the aforementioned factors is challenging; however, Monte Carlo simulations using hydrology modeling

software (e.g., HEC-HMS) may be useful in identifying both total and variable specific uncertainty for the post-wildfire CN value changes.

The negative change in CN value may also have some physical basis. One potential explanation is vegetation recovery during the post-wildfire period could results in soil moisture regime changes (Hamilton and Burton 2023). This would be consistent with a forested area being converted to grasslands following wildfire. The change in vegetation could result in decreased soil moisture between rainfall events compared to the pre-wildfire condition which could potentially decrease surface runoff (increased soil storage). To confirm this could be a cause of decreased CN values, a remote sensing analysis along with collection of field data could be beneficial.

Three approaches (i.e., historical runoff event observations, linear regression model, and regression tree model) were used to help estimate a post-wildfire curve number from watershed and wildfire parameters. Although we have lower confidence in linear models, we have moderate confidence in the tree model results based on the observed CN value changes and using the tree models for post-wildfire analysis are highly beneficial. Using all watersheds, the RMSE of the tree models was reduced by 20%–30% for the majority of post-wildfire periods compared to the GLMs. In addition, the R^2 values for the tree models are typically 2–3 times greater than the GLM for the same post-wildfire period and storage level (Table 2). This indicates the regression tree models produce less error and greater correlations to observed CN value changes. The KGE values are also approximately double those produced by the GLMs (Table 2). The differences are even more pronounced with the "best subset" of watersheds. The RMSE values for the tree models are less than half the GLMs and the KGE is relatively high at 0.92 (1.0 is perfect agreement) (Table 3). Again, these results indicate the tree models perform substantially better for the subset of watersheds that have minimal anthropogenic influences.

Using the tree models still involves judgement, lowering the CN values while performing a post-wildfire flood risk assessment may not be advisable provided the many publications that seem to indicate otherwise. However, our results indicate more variability between burned watersheds than previously described in the literature. The predicted positive changes provided by the tree models can provide guidance on the magnitude of the CN value change based on specific land cover and watershed characteristics. Based on the information in Hawkins et al. (2020), using

an initial abstraction storage value of 0.05 (S05) is preferred when developing both the pre- and post-wildfire CN values. The positive CN change values produced in our study follow the same magnitudes as produced by the NRCS (2016) ranging between 5 and 15 units. The results within this report provide additional resolution for important variables to consider other than the burn severity when performing a post-wildfire runoff analysis.

7 Conclusions and Additional Research

7.1 Conclusions

The study used observed runoff events from wildfire affected watersheds in the Southern Rocky Mountain region to estimate changes in CN values from pre- to post-wildfire conditions. Three approaches (i.e., historical runoff event observations, linear regression model, and regression tree model) were used to help estimate a post-wildfire curve number from watershed and wildfire parameters. The computed CN value changes from the observed runoff events indicate there is variation in both magnitude and direction of the CN value change following wildfire. Limitations in this study could help account for the large variation in CN found post-fire. The CN value changes estimated from observed runoff events do not account for antecedent conditions (e.g., soil moisture) before the runoff events, which could be contributing to the unexpected negative CN value after wildfire. In addition, the relatively limited sample size for rainfall only runoff events (both pre- and post-wildfire) could also be contributing to the range of estimated values. Even with these uncertainties and limitations, the empirically derived CN values demonstrate that selecting a single CN value for modeling all rainfall events in a watershed is likely not appropriate, and simple translations of the CN values for post-wildfire conditions based only on burn area and severity are also likely to have high uncertainty. Therefore, using watershed characteristics (i.e., elevation, slope, northness, and eastness) combined with the wildfire information (i.e., burn extents) could allow for watershed specific CN value changes to be used by hydrologic modelers and emergency managers when wildfire events occur in Southern Rocky Mountain watersheds.

7.2 Additional Research

The runoff event identification and model development process we used can be applied to other geographic regions where data are available. The precipitation, SWE, wildfire, land cover, and topographic data sets used are available for other regions of CONUS which allows for prediction models of CN value changes to be developed anywhere in CONUS that has streamflow data. From our results the regression tree models have the overall best performance, especially when using streamflow information not affected by anthropogenic activities. For streamflow data sets which do have anthropogenic influences (e.g., reservoir regulation, irrigation

diversions, trans-watershed diversions, etc.), careful consideration may be given to how much these factors decouple the streamflow response from the precipitation input.

There are several areas for additional research indicated from this analysis that could improve CN estimates and improve modelling results:

- Consider adding antecedent soil moisture information for each runoff event and using those values in the development of the regression tree models.
- Develop hydrology models calibrated to observed runoff events to test the computed CN value changes.
- Increase the number of streamgages and the availability of streamflow data for watersheds affected by wildfire.
- Repeat our analysis in a region where rainfall is the dominant hydrologic driver which could provide a larger sample size of runoff events.
- Repeat our analysis using only large precipitation events (e.g., greater than 5-year return period).
- Implement the equations developed in this report into an online calculator where a user could easily compute the expected CN and thus streamflow value based on the characteristics of the basin of interest for future wildfire affected watersheds.

Applying this analysis to other regions and watersheds affected by greater percent burned areas relative to the watershed size could be important for comparing the CN variability found in our results. The comparison can confirm that the variability in Colorado watersheds is common or perhaps unique to the region. In addition, application of these methods to regions affected primarily by rainfall-runoff events rather than snowmelt-dominated runoff could help inform the range of observed CN value changes in context of larger domains (e.g., western US).

Bibliography

Bart, R. R., M. C. Kennedy, C. L. Tague, and D. McKenzie. 2020. "Integrating Fire Effects on Vegetation Carbon Cycling Within an Ecohydrologic Model." *Ecological Modelling* 416:1–15. https://doi.org/10.1016/j.ecolmodel.2019.108880.

Bêche, L. A., S. L. Stephens, and V. H. Resh. 2005. "Effects of Prescribed Fire on a Sierra Nevada (California, USA) Stream and Its Riparian Zone." *Forest Ecology and Management* 218 (1–3): 37–59. https://doi.org/10.1016/j.foreco.2005.06.010.

Brown, E. K., J. Wang, Y. Feng. 2021. "US Wildfire Potential: A Historical View and Future Projection Using High-Resolution Climate Data." *Environmental Research Letters* 16 (3): 1–11. https://doi.org/10.1088/1748-9326/aba868.

Broxton, P., X. Zeng, and N. Dawson. 2019. *Daily 4 km Gridded SWE and Snow Depth from Assimilated In-Situ and Modeled Data over the Conterminous US, Version 1* [Data Set], accessed July 15, 2023. Data Set NSIDC-0719. Boulder, CO: NASA National Snow and Ice Data Center Distributed Active Archive Center. https://doi.org/10.5067/0GGPB220EX6A.

Canfield, H. E., D. C. Goodrich, and I. S. Burns. 2005. "Selection of Parameters Values to Model Postfire Runoff and Sediment Transport at the Watershed scale in Southwestern Forests." *Proceedings of the 2005 Watershed Management Conference–Managing Watersheds for Human and Natural Impacts: Engineering, Ecological, and Economic Challenges*, 561–572. https://doi.org/10.1061/40763(178)48.

Capesius, J.P., and V.C. Stephens. 2009. *Regional Regression Equations for Estimation of Natural Streamflow Statistics in Colorado*. US Geological Survey Scientific Investigations Report 2009–5136. Reston, VA: USGS. https://pubs.usgs.gov/sir/2009/5136/pdf/SIR09-5136.pdf.

Chen, L., M. Berli, and K. Chief. 2013. "Examining Modeling Approaches for the Rainfall-Runoff Process in Wildfire-Affected Watersheds: Using San Dimas Experimental Forest." *Journal of the American Water Resources Association* 49 (4): 851–866. https://doi.org/10.1111/jawr.12043.

Colorado Division of Water Resources (CODWR). 2023. "Stations-Current Conditions." Colorado Decision Support Systems, accessed March 17, 2023. https://dwr.state.co.us/tools/stations.

Cydzik, K., and T. S. Hogue. 2009. "Modeling Postfire Response and Recovery Using the Hydrologic Engineering Center Hydrologic Modeling System (HEC-HMS)." *Journal of the American Water Resources Association* 45 (3): 702–714. https://doi.org/10.1111/j.1752-1688.2009.00317.x.

Dawson, N., P. Broxton, and X. Zeng. 2018. "Evaluation of Remotely Sensed Snow Water Equivalent and Snow Cover Extent over the Contiguous United States." *Journal of Hydrometeorology* 19 (11): 1777–1791. https://doi.org/10.1175/JHM-D-18-0007.1.

Dennison, P. E., S. C. Brewer, J. D. Arnold, and M. A. Moritz. 2014. "Large Wildfire Trends in the Western United States, 1984–2011." Geophysical Research Letters 41 (8): 2928–2933. https://doi.org/10.1002/2014GL059576.

De Roo, A. P. J., Wesseling, C. G., & Ritsema, C. J. 1996. "LISEM: A Single-Event Physically Based Hydrological and Soil Erosion Model for Drainage Basins. I: Theory, Input and Output." *Hydrological Processes* 10 (8): 1107–1117). https://doi.org/10.1002/(sici)1099-1085(199608)10:8<1107::aid-hyp415>3.0.co;2-4.

Ebel, B. A., J. A. Moody, and D. A. Martin. 2012. "Hydrologic Conditions Controlling Runoff Generation Immediately After Wildfire." *Water Resources Research*, 48 3: 1–13. https://doi.org/10.1029/2011WR011470.

Ebel, B. A., F. K. Rengers, and G. E. Tucker. 2016. "Observed and Simulated Hydrologic Response for a First-Order Catchment During Extreme Rainfall 3 Years After Wildfire Disturbance." *Water Resources Research* 52 (12): 9367–9389. https://doi.org/10.1002/2016WR019110.

Ebel, B. A., Z. M. Shephard, M. A. Walvoord, S. F. Murphy, T. F. Partridge, and K. S. Perkins. 2023. "Modeling Post-Wildfire Hydrologic Response: Review and Future Directions for Applications of Physically Based Distributed Simulation." *In Earth's Future* 11 (2): 1–23. https://doi.org/10.1029/2022EF003038.

Ellis, T. M., D. M. J. S. Bowman, P. Jain, M. D. Flannigan, and G. J. Williamson. 2022. "Global Increase in Wildfire Risk due to Climate-Driven Declines in Fuel Moisture." *Global Change Biology* 28 (4): 1444–1559. https://doi.org/10.1111/gcb.16006.

Fall, G., D. Kitzmiller, S. Pavlovic, Z. Zhang, N. Patrick, M. St. Laurent, C. Trypaluk, W. Wu, and D. Miller. 2023. "The Office of Water Prediction's Analysis of Record for Calibration, Version 1.1: Dataset Description and Precipitation Evaluation." *Journal of the American Water Resources Association* 59 (6): 1246–1272. https://doi.org/10.1111/1752-1688.13143.

Farmer, W. H., J. E. Kiang, T. D. Feaster, and K. Eng. 2019. "Regionalization of Surface-Water Statistics Using Multiple Linear Regression." *US Geological Survey Techniques and Methods* 4 (A12). https://doi.org/10.3133/tm4a12.

Giovando, J., E. Heisman, and K. Seefus. 2023. "Monte Carlo Simulation of Post-Fire Flood Hazard Probabilities." *Sedimentation and Hydrologic Modeling 2023 Conference* 6D2 (247). https://www.sedhyd.org/2023Program/s247.html.

Gupta, H. V., H. Kling, K. K. Yilmaz, and G. F. Martinez. 2009. "Decomposition of the Mean Squared Error and NSE Performance Criteria: Implications for Improving Hydrological Modelling." *Journal of Hydrology* 377 (1–2): 80–91. https://doi.org/10.1016/j.jhydrol.2009.08.003.

Hamilton, N. P., and P. J. Burton. 2023. "Wildfire Disturbance Reveals Evidence of Ecosystem Resilience and Precariousness in a Forest–Grassland Mosaic." *Ecosphere* 14 (3): 1–24. https://doi.org/10.1002/ecs2.4460.

Havel, A., A. Tasdighi, and M. Arabi. 2018. "Assessing the Hydrologic Response to Wildfires in Mountainous Regions." *Hydrology and Earth System Sciences* 22 (4): 2527–2550. https://doi.org/10.5194/hess-22-2527-2018.

Hawkins, R. H., G. E. Moglen, T. J. Ward, and D. E. Woodward. 2020. "Updating the Curve Number: Task Group Report." *Watershed Management 2020: A Clear Vision of Watershed Management*, 131–140. https://ascelibrary.org/doi/pdf/10.1061/9780784483060.012.

Hawkins, R. H., T. J. Ward, D. E. Woodward, and J. A. VanMullem. 2005. "Progress Report: ASCE Task Committee on Curve Number hydrology." P*roceedings of the 2005 Watershed Management Conference–Managing Watersheds for Human and Natural Impacts: Engineering, Ecological, and Economic Challenges* 2: 1755–1766. https://doi.org/10.1061/40763(178)150.

Holden, Z. A., A. Swanson, C. H. Luce, W. M. Jolly, M. Maneta, J. W. Oyler, D. A. Warren, R. Parsons, and D. Affleck. 2018. "Decreasing Fire Season Precipitation Increased Recent Western US Forest Wildfire Activity." *Proceedings of the National Academy of Sciences of the United States of America* 115 (36): E8349–E8357. https://doi.org/10.1073/pnas.1802316115.

James, G., D. Witten, T. Hastie, and R. Tibshirani. 2013. *An Introduction to Statistical Learning with Application in R*. New York, NY: Springer.

Jenkins, D. G., and P. F. Quintana-Ascencio. 2020. "A Solution to Minimum Sample Size for Regressions." *PLoS ONE* 15 (2): 1–15. https://doi.org/10.1371/journal.pone.0229345.

Jolly, M. W., M. A. Cochrane, P. H. Freeborn, Z. A. Holden, T. J. Brown, G. J. Williamson, and D. M. J. S. Bowman. 2015. " Climate-Induced Variations in Global Wildfire Danger From 1979 to 2013." *Nature Communications* 6 (7537): 1–11. https://doi.org/10.1038/ncomms8537.

Kinoshita, A. M., T. S. Hogue, and C. Napper. 2014. "Evaluating Pre- and Post-Fire Peak Discharge Predictions across Western US Watersheds." *Journal of the American Water Resources Association* 50 (6): 1540–1557. https://doi.org/10.1111/jawr.12226.

Kohn, M. S., M. R. Stevens, T. M. Harden, J. E. Godaire, R. E. Klinger, and A. Mommandi. 2016. *Paleoflood Investigations to Improve Peak-Streamflow Regional-Regression Equations for Natural Streamflow in Eastern Colorado, 2015*." USGS Scientific Investigations Report 2016–5099. Reston, VA: USGS. https://doi.org/10.3133/sir20165099.

Kuhn, M., J. Wing, S. Weston, A. Williams, C. Keefer, A. Engelhardt, T. Cooper, et al. 2023. *caret: Classification and Regression Training*. R package version 6.0-94. https://cran.r-project.org/package=caret.

LANDFIRE. 2022a. *LANDFIRE Aspect Layer*, accessed August 2, 2023. US Department of Interior, USGS, and USDA. https://www.landfire.gov/viewer/.

LANDFIRE. 2022b. *LANDFIRE Elevation Layer*, accessed August 2, 2023. US Department of Interior, USGS, and USDA. https://www.landfire.gov/viewer/.

LANDFIRE. 2022c. *LANDFIRE Existing Vegetation Type Layer*, Accessed November 20, 2023.US Department of Interior, USGS, and USDA. https://www.landfire.gov/viewer/.

LANDFIRE. 2022d. *LANDFIRE Slope Layer*, accessed August 2, 2023. US Department of Interior, USGS, and USDA. https://www.landfire.gov/viewer/.

Leopardi, M., and A. R. Scorzini. 2015. "Effects of Wildfires on Peak Discharges in Watersheds." *IForest* 8: 302–307. https://doi.org/10.3832/ifor1120-007.

Livingston, R. K., T. A. Earles, and K. R. Wright. 2005. "Los Alamos Postfire Watershed Recovery: A Curve-Number-Based Evaluation." *Proceedings of the 2005 Watershed Management Conference–Managing Watersheds for Human and Natural Impacts: Engineering, Ecological, and Economic Challenges*, 471–481. https://doi.org/10.1061/40763(178)41.

Lumley, T. 2020. *Package 'leaps': Regression Subset Selection*. R package Version 3.1. https://cran.r-project.org/web/packages/leaps/leaps.pdf.

Moody, J. A., and D. A. Martin. 2001. "Postfire, Rainfall Intensity-Peak Discharge Relations for Three Mountainous Watersheds in the Western USA." *Hydrological Processes* 15 (15): 2981–2993. https://doi.org/10.1002/hyp.386.

Neary, D. G., G. J. Gottfried, and P. F. Ffolliott. 2003. "Post-Wildfire Watershed Flood Responses." *Second International Fire Ecology and Fire Management Congress, Orlando, Florida, 16-20 November 2003* 1B7, 1–8. https://www.researchgate.net/publication/228510172_Post-wildfire_watershed_flood_responses.

NOAA. 2021. *Analysis of Record for Calibration Version 1.1–Sources, Methods, and Verification*. Silver Spring, MD: NOAA, NWS, and Office of Water Prediction. https://hydrology.nws.noaa.gov/aorc-historic/Documents/AORC-Version1.1-SourcesMethodsandVerifications.pdf.

NRCS (National Resources Conservation Service). 2004a. "Chapter 10: Estimation of Direct Runoff from Storm Rainfall," in *National Engineering Handbook–Part 630*. Washington, DC: USDA. https://directives.sc.egov.usda.gov/17752.wba.

NRCS (National Resources Conservation Service). 2004b. "Chapter 9: Hydrologic Soil-Cover Complexes," in *National Engineering Handbook–Part 630*. Washington, DC: USDA. https://directives.sc.egov.usda.gov/17758.wba.

NRCS (National Resources Conservation Service). 2016. *Hydrologic Analyses of Post-Wildfire Conditions*. Hydrology Technical Note No. 4. *ional Engineering Handbook–Part 630*. Washington, DC: USDA. https://afterthefirewa.org/wp-content/uploads/2019/04/USDA-NRCS-Hydrologic-Analyses-of-Post-Wildfire-Conditions-August-2016.pdf.

Omernik, J. M., and G. E. Griffith. 2014. "Ecoregions of the Conterminous United States: Evolution of a Hierarchical Spatial Framework." *Environmental Management* 54 (6): 1249–1266. https://doi.org/10.1007/s00267-014-0364-1.

Plummer, A., and D. E. Woodward. 1998 "Origin and Derivation of Ia/S in the Runoff Curve Number System." *International Water Resources Engineering Conference Proceedings*, ASCE, Reston, VA. Vol. 2.

Ponce, V. M., and R. H. Hawkins. 1996. "Runoff Curve Number: Has It Reached Maturity?" *Journal of Hydrologic Engineering* 1 (1): 11–19. https://doi.org/10.1061/(ASCE)1084-0699(1996)1:1(11).

Rallison, R. E. 1980. "Origin and Evolution of the SCS Runoff Equation." Proc., ASCE Irrig. and Drain. Div. Symp. on Watershed Mgmt., ASCE, New York, N.Y., Vol. II, 912–924.

Robichaud, P. R., and L. E. Ashmun. 2013. "Tools to Aid Post-wildfire Assessment and Erosion-Mitigation Treatment Decisions." *International Journal of Wildland Fire* 22 (1): 95–105. http://dx.doi.org/10.1071/WF11162.

Sexstone, G. A., and S. R. Fassnacht. 2014. "What Drives Basin Scale Spatial Variability of Snowpack Properties in Northern Colorado?" *Cryosphere* 8 (2): 329–344. https://doi.org/10.5194/tc-8-329-2014.

Smith, R. E., D. C. Goodrich, D. A. Woolhiser, and C. L. Unkrich. 1995. "Chapter 20: KINEROS–A Kinematic Runoff and Erosion Model," in *Computer Models of Watershed Hydrology*, ed. V. J. Singh. Littleton, CO: Water Resources Publications, 697–632. https://www.researchgate.net/profile/David-Goodrich-3/publication/43266900_KINEROS-a_kinematic_runoff_and_erosion_model/links/5f835dc1458515b7cf79d90b/KINEROS-a-kinematic-runoff-and-erosion-model.pdf.

Smith, R. E., and J. N. Quinton. 2000. "Dynamics and Scale in Simulating Erosion by Water," in *Soil Erosion: Application of Physically Based Models*, ed. J. Schmidt. Berlin, Germany: Springer-Verlag, 283–294. https://link.springer.com/chapter/10.1007/978-3-662-04295-3_13.

Reis W. K., J. E. Smith IV, J. J. Giovando, and M. S. Kohn. 2024. *Post-Wildfire Curve Number Estimates for the Southern Rocky Mountains Data*. US Geologic Survey.

Soulis, K. X. 2018. "Estimation of SCS Curve Number Variation Following Forest Fires." *Hydrological Sciences Journal* 63 (9): 1332–1346. https://doi.org/10.1080/02626667.2018.1501482.

Springer, E. P., and R. H. Hawkins. 2005. "Curve Number and Peakflow Responses Following the Cerro Grande Fire on a Small Watershed." *Proceedings of the 2005 Watershed Management Conference–Managing Watersheds for Human and Natural Impacts: Engineering, Ecological, and Economic Challenges*, 459–470. https://doi.org/10.1061/40763(178)40.

Stavi, I. 2019. "Wildfires in Grasslands and Shrublands: A Review of Impacts on Vegetation, Soil, Hydrology, and Geomorphology." *Water* 11 (5): 1–20. https://doi.org/10.3390/w11051042.

Stoof, C. R., R. W. Vervoort, J. Iwema, E. van den Elsen, A. J. D. Ferreira, and C. J. Ritsema. 2012. "Hydrological Response of a Small Catchment Burned by Experimental Fire." *Hydrology and Earth System Sciences* 16 (2): 267–285. https://doi.org/10.5194/hess-16-267-2012.

Therneau, T., B. Atkinson, and B. Ripley. 2023. *Package rpart: Recursive Partitioning and Regression Trees*. R package version 4.1.23. https://cran.r-project.org/web/packages/rpart/rpart.pdf.

USGS. 2023. "USGS Water Data for the Nation." US Geological Survey National Water Information System database, accessed March 16, 2023. https://doi.org/10.5066/F7P55KJN.

Vadilonga, T., X. Úbeda, P. F. Germann, and M. Lorca. 2008. "Effects of Prescribed Burnings on Soil Hydrological Parameters." *Hydrological Processes* 22 (21): 4249–56. https://doi.org/10.1002/hyp.7032.

VanderKwaak, J. E. 1999. "Numerical Simulation of Flow and Chemical Transport in Integrated Surface-Subsurface Hydrologic Systems." PhD dissertation, University of Waterloo. http://hdl.handle.net/10012/412.

Van Eck, C. M., J. P. Nunes, D. C. S. Vieira, S. Keesstra, and J. J. Keizer. 2016. "Physically Based Modelling of the Post-Fire Runoff Response of a Forest Catchment in Central Portugal: Using Field Versus Remote Sensing Based Estimates of Vegetation Recovery." *Land Degradation and Development* 27 (5): 1535–1544. https://doi.org/10.1002/ldr.2507.

Wang, J., T. A. Endreny, and J. M. Hassett. 2005. "A Flexible Modeling Package for Topographically Based Watershed Hydrology." *Journal of Hydrology* 314 (1–4): 78–91. https://doi.org/10.1016/j.jhydrol.2005.03.030.

Wang, J., M. A. Stern, V. M. King, C. N. Alpers, N. W. T. Quinn, A. L. Flint, and L. E. Flint. 2020. "PFHydro: A New Watershed-Scale Model for Post-Fire Runoff Simulation." *Environmental Modelling and Software* 123 (104555): 1–15. https://doi.org/10.1016/j.envsoft.2019.104555.

Welty, J.L., and M. I. Jeffries. 2021. *Combined Wildland Fire Data Sets for the United States and Certain Territories, 1800s-Present*. USGS data release, December 12, 2021. https://doi.org/10.5066/P9ZXGFY3.

Westerling, A. L. R. 2016. "Increasing Western US Forest Wildfire Activity: Sensitivity to Changes in the Timing of Spring." *Philosophical Transactions of the Royal Society B: Biological Sciences* 371 (1696): 1–10. https://doi.org/10.1098/rstb.2015.0178.

Westerling, A. L., H. G. Hidalgo, D. R. Cayan, and T. W. Swetnam. 2006. "Warming and Earlier Spring Increase Western US Forest Wildfire Activity." *Science* 313 (5789): 940–943. https://doi.org/10.1126/science.1128834.

Williams, G., M. Vere Culp, E. Cox, A. Nolan, D. White, D. Medri, A. Waljee, et al. 2022. *rattle: Graphical User Interface for Data Science in R*. R package version 3.5.1. https://cran.r-project.org/web/packages/rattle/index.html.

Wine, M. L., and D. Cadol. 2016. "Hydrologic Effects of Large Southwestern USA Wildfires Significantly Increase Regional Water Supply: Fact or Fiction?" *Environmental Research Letters* 11 (8): 1–13. https://doi.org/10.1088/1748-9326/11/8/085006.

Wine, M. L., D. Cadol, and O. Makhnin. 2018. "In Ecoregions Across Western USA Streamflow Increases During Post-wildfire Recovery." *Environmental Research Letters* 13 (1): 1–14. https://doi.org/10.1088/1748-9326/aa9c5a.

Appendix A: : Wildfire Affected Streamgages Used for CN Analysis

Table 1. A list of all 102 wildfire-affected streamgages used in the curve number (CN) analysis. Watersheds with two streamgages listed indicate incremental watersheds, and only the area between the two gages was used for analysis.

Streamgage Name	Streamgage Number	Watershed Area (km^2)	Streamgage Agency	Streamgage Latitude (°)	Streamgage Longitude (°)
Animas River at Durango, Colorado	09361500	1817	USGS	37.2792	−107.8803
Animas River near Cedar Hill, New Mexico	09363500	2855	USGS	37.0366	−107.8753
Arkansas River at Canon City, Colorado	07096000	7935	USGS	38.4339	−105.2572
Arroyo Chico nr Guadalupe, New Mexico[1]	08340500	3564	USGS	35.5923	−107.1894
Big Thompson River at Estes Park, Colorado	06733000	355	USGS	40.3783	−105.5139
Big Thompson River at Mouth near La Salle	BIGLASCO	2150	CODWR[1]	40.3500	−104.7850
Boulder Creek At Mouth near Longmont, Colorado	06730500	1160	USGS	40.1388	−105.0202
Bummers Gulch near El Vado, Colorado	06726900	10	USGS	40.0117	−105.3486
Camp Creek At Garden of the Gods, Colorado	07103703	25	USGS	38.8769	−104.8728
Cherry Creek at Denver, Colorado	06713500	1062	USGS	39.7425	−105.0000
Cherry Creek at Glendale, Colorado	06713300	1048	USGS	39.7061	−104.9375
Cimarron River near Cimarron, New Mexico	07207000	707	USGS	36.5198	−104.9786
Colorado River at Grand Lake (North Fork)	COLGRAND	264	CODWR	40.2189	−105.8575
Colorado River at Hot Sulphur Springs, Colorado	COLSULCO	2134	CODWR	40.0833	−106.0881
Colorado River at K Barger Ditch Near Kremmling	COLKBDCO	3091	CODWR	40.0545	−106.2877
Colorado River at Windy Gap, near Granby, Colorado	09034250	2041	USGS	40.1083	−106.0042
Colorado River below Baker Gulch nr Grand Lake, Colorado	09010500	165	USGS	40.3258	−105.8567
Colorado River near Grand Lake, Colorado	09011000	264	USGS	40.2189	−105.8575

Table 1 (cont.). A list of all 102 wildfire-affected streamgages used in the curve number (CN) analysis. Watersheds with two streamgages listed indicate incremental watersheds, and only the area between the two gages was used for analysis.

Streamgage Name	Streamgage Number	Watershed Area (km^2)	Streamgage Agency	Streamgage Latitude (°)	Streamgage Longitude (°)
Cottonwood Creek at Mouth at Pikeview, Colorado	07103990	48	USGS	38.9272	−104.8142
Coyote Creek near Golondrinas, New Mexico	07218000	626	USGS	35.9165	−105.1641
Cucharas River at Boyd Ranch near Louisiana, Veta	CRBRLVCO	137	CODWR	37.4200	−105.0528
Cucharas River at Harrison Bridge near La Veta, Colorado	CRHBLVCO	511	CODWR	37.4500	−105.0372
Dolores River at Bedrock, Colorado	09169500	5254	USGS	38.3103	−108.8854
Dolores River at Dolores, Colorado	09166500	1308	USGS	37.4725	−108.4976
Dolores River near Bedrock, Colorado	09171100	5570	USGS	38.3569	−108.8334
Ef San Juan R Ab Sand Creek, nr Pagosa Spgs, Colorado[1]	09339900	169	USGS	37.3897	−106.8412
Elk River at Clark, Colorado	09241000	561	USGS	40.7175	−106.9159
Elk River near Milner, Colorado	09242500	1190	USGS	40.5147	−106.9539
Elkhead Creek above Long Gulch, near Hayden, Colorado	09246200	444	USGS	40.5916	−107.3209
Embudo Creek at Dixon, New Mexico	08279000	829	USGS	36.2109	−105.9136
Encampment River at mouth, near Encampment, Wyoming	06625000	678	USGS	41.3033	−106.7153
Florida River above Lemon Reservoir Near Durango	FLOALECO	136	CODWR	37.4267	−107.6744
Florida River at Bondad, Colorado	FLOBONCO	572	CODWR	37.0567	−107.8698
Goose Creek at Wagonwheel Gap, Colorado	GOOWAGCO	236	CODWR	37.7520	−106.8300
Joe Wright Creek above Joe Wright Reservoir, Colorado	06746095	8	USGS	40.5400	−105.8828
La Plata River at Colorado-New Mexico State Line	09366500	802	USGS	36.9997	−108.1887
Lake Fork River ab Moon Lake, nr Mountain Home, Utah	09289500	203	USGS	40.6066	−110.5271
Little Fountain Creek near Fountain, Colorado	07105940	69	USGS	38.6427	−104.7484
Little Laramie River near Filmore, Wyoming	06661000	411	USGS	41.2950	−106.0347

Table 1 (cont.). A list of all 102 wildfire-affected streamgages used in the curve number (CN) analysis. Watersheds with two streamgages listed indicate incremental watersheds, and only the area between the two gages was used for analysis.

Streamgage Name	Streamgage Number	Watershed Area (km^2)	Streamgage Agency	Streamgage Latitude (°)	Streamgage Longitude (°)
Little Snake River near Lily, Colorado	09260000	10455	USGS	40.5490	−108.4243
Little Snake River near Slater, Colorado	09253000	652	USGS	40.9994	−107.1434
Los Pinos River at La Boca, Colorado	09354500	1346	USGS	37.0094	−107.5995
Monument Cr abv Woodmen Rd at Colorado Springs, Colorado	07103970	467	USGS	38.9339	−104.8172
Mora River at La Cueva, New Mexico	07215500	464	USGS	35.9451	−105.2557
Mora River near Golondrinas, New Mexico	07216500	689	USGS	35.8909	−105.1636
Muddy Creek above Antelope Creek nr Kremmling, Colorado	09041090	374	USGS	40.2025	−106.4225
North Fork Big Thompson River at Drake, Colorado	BTNFDRCO	220	CODWR	40.4329	−105.3387
North Fork White River at Buford, Colorado	09303000	672	USGS	39.9875	−107.6145
North Inlet Creek	NORINLET	119	CODWR	40.2509	−105.8144
North Platte River near Northgate, Colorado	06620000	3699	USGS	40.9366	−106.3392
Pecos River above Santa Rosa Lake, New Mexico	08382650	6041	USGS	35.0594	−104.7611
Pecos River near Pecos, New Mexico	08378500	444	USGS	35.7084	−105.6827
Piceance Creek at White River, Colorado	09306222	1689	USGS	40.0780	−108.2365
Piceance Creek bl Ryan Gulch, nr Rio Blanco, Colorado[1]	09306200	1310	USGS	39.9211	−108.2976
Piedra River near Arboles, Colorado	09349800	1692	USGS	37.0883	−107.3978
Plum Creek at Titan Road near Louviers, Colorado	06709530	817	USGS	39.5074	−105.0245
Ponil Creek near Cimarron, New Mexico	07207500	480	USGS	36.5737	−104.9468
Purgatoire River at Madrid, Colorado	07124200	1305	USGS	37.1295	−104.6400
Red River below Fish Hatchery, near Questa, New Mexico	08266820	466	USGS	36.6828	−105.6541

Table 1 (cont.). A list of all 102 wildfire-affected streamgages used in the curve number (CN) analysis. Watersheds with two streamgages listed indicate incremental watersheds, and only the area between the two gages was used for analysis.

Streamgage Name	Streamgage Number	Watershed Area (km^2)	Streamgage Agency	Streamgage Latitude (°)	Streamgage Longitude (°)
Red River near Questa, New Mexico	08265000	290	USGS	36.7033	−105.5684
Rio Grande above San Juan Pueblo, New Mexico	08281100	15096	USGS	36.0570	−106.0822
Rio Grande at Embudo, New Mexico	08279500	14696	USGS	36.2056	−105.9640
Rio Grande at Thirty Mile Bridge near Creede, Colorado, to Wagon Wheel Gap, Colorado	Upstream: RIOMILCO Downstream: RIOWAGCO	1568	Upstream: CODWR Downstream: CODWR	Upstream: 37.7247 Downstream: 37.7670	Upstream: -107.2550 Downstream: -106.8314
Rio Grande at Wagon Wheel Gap	RIOWAGCO	1679	CODWR	37.7670	−106.8314
Rio Grande Del Rancho near Talpa, New Mexico	08275500	208	USGS	36.3031	−105.5810
Rio Grande near Arroyo Hondo, New Mexico	08268700	11388	USGS	36.5345	−105.7100
Rio Grande near Cerro, New Mexico	08263500	10366	USGS	36.7400	−105.6834
Rio Grande near Del Norte, Colorado	08220000	3396	USGS	37.6886	−106.4599
Rio Grande near Lobatos, Colorado	08251500	19378	USGS	37.0786	−105.7569
Rio Mora near Terrero, New Mexico	08377900	139	USGS	35.7771	−105.6580
Rio Mora near Terrero, New Mexico, to Pecos River near Pecos, New Mexico	Upstream: 08377900 Downstream: 08378500	306	Upstream: USGS Downstream: USGS	Upstream: 35.7771 Downstream: 35.7084	Upstream: -105.6580 Downstream: -105.6827
Rio Pueblo de Taos below Los Cordovas, New Mexico	08276300	1004	USGS	36.3793	−105.6678
Rio Pueblo de Taos near Taos, New Mexico	08269000	163	USGS	36.4394	−105.5036
Rio Pueblo nr Penasco, New Mexico	08277470	258	USGS	36.1685	−105.6028
Rio San Jose at Acoma Pueblo, New Mexico	08343500	3723	USGS	35.0744	−107.7511
Rio San Jose at Correo, New Mexico	08351500	7278	USGS	34.9681	−107.1870
Rio San Jose at Grants, New Mexico	08343000	2620	USGS	35.1545	−107.8703

Table 1 (cont.). A list of all 102 wildfire-affected streamgages used in the curve number (CN) analysis. Watersheds with two streamgages listed indicate incremental watersheds, and only the area between the two gages was used for analysis.

Streamgage Name	Streamgage Number	Watershed Area (km^2)	Streamgage Agency	Streamgage Latitude (°)	Streamgage Longitude (°)
San Juan River at Pagosa Springs, Colorado	09342500	727	USGS	37.2655	−107.0110
San Juan River at Shiprock, New Mexico	09368000	33097	USGS	36.7767	−108.6831
San Juan River near Carracas, Colorado	09346400	3238	USGS	37.0136	−107.3123
Sangre de Cristo Creek Near Fort Garland, Colorado	SANFTGCO	474	CODWR	37.4250	−105.4144
Santa Cruz River near Cundiyo, New Mexico	08291000	239	USGS	35.9647	−105.9047
South Fork Rio Grande at South Fork, Colorado	08219500	546	USGS	37.6569	−106.6492
St Charles River at Vineland, Colorado	07108900	1226	USGS	38.2456	−104.4864
Strawberry River near Soldier Springs, Utah, to Pinnacles near Fruitland, Utah	Upstream: 09285000 Downstream: 09285900	414	Upstream: USGS Downstream: USGS	Upstream: 40.1333 Downstream: 40.1272	Upstream: -111.0249 Downstream: -110.7418
Sybille Creek ab Mule Creek, near Wheatland, Wyoming	06664400	504	USGS	41.8441	−105.2214
Turkey Creek ab Teller Res near Stone City, Colorado	07099230	161	USGS	38.4650	−104.8272
Turkey Creek near Fountain, Colorado	07099215	34	USGS	38.6117	−104.8947
Turkey Creek near Fountain, Colorado, to ab Teller Res Near Stone City, Colorado[1]	Upstream: 07099215 Downstream: 07099230	128	Upstream: USGS Downstream: USGS	Upstream: 38.4650 Downstream: 38.4650	Upstream: -104.8272 Downstream: -104.8272
Vallecito Creek near Bayfield, Colorado	09352900	188	USGS	37.4775	−107.5437
Vermejo River near Dawson, New Mexico	07203000	893	USGS	36.6810	−104.7864
White River below Boise Creek, near Rangely, Colorado	09306290	6559	USGS	40.1797	−108.5654
White River below Meeker, Colorado	09304800	2652	USGS	40.0226	−108.1199
Williams Fork above Darling Creek, near Leal, Colorado	09035700	91	USGS	39.7972	−106.0256

Table 1 (cont.). A list of all 102 wildfire-affected streamgages used in the curve number (CN) analysis. Watersheds with two streamgages listed indicate incremental watersheds, and only the area between the two gages was used for analysis.

Streamgage Name	Streamgage Number	Watershed Area (km^2)	Streamgage Agency	Streamgage Latitude (°)	Streamgage Longitude (°)
Williams Fork at Mouth, near Hamilton, Colorado	09249750	1184	USGS	40.4372	−107.6478
Williams Fork near Leal, Colorado	09036000	232	USGS	39.8339	−106.0564
Williams Fork near Parshall, Colorado	09037500	477	USGS	40.0002	−106.1804
Yampa River at Steamboat Springs, Colorado	09239500	1470	USGS	40.4830	−106.8324
Yampa River below Craig, Colorado	09247600	5514	USGS	40.4808	−107.6142
Yampa River near Maybell, Colorado	09251000	8763	USGS	40.5027	−108.0334
Yellowstone River near Altonah, Utah	09292500	337	USGS	40.5119	−110.3415

[1] nr (near), Ef (East fork), Ab (above), Spgs (Springs), bl (below), Res (reservoir). CODWR (Colorado Division of Water Resources).

Appendix B: : Linear Models

The final set of linear models for all scenarios using all analyzed watersheds are shown below in Table 2, and the "best subset" watershed models are included in Table B-2. The input variables and model parameters vary by scenario and can be used for the appropriate planning horizon following wildfire impacts to a watershed.

Table 2. Generalized linear models (GLMs) for median curve number (CN) change following the first and second wildfire for each planning horizon and storage value (S05 and S20) at all 102 analyzed watersheds.

Wildfire Scenario	Storage Value	Linear Equation
After First Fire: 0–4 years	S05	ΔCN = −38.27 + 0.02 (Mean Elevation) −0.87 (Mean Slope) −9.07 (Landcover = 7055) +34.42 (Landcover = 7086) +22.77 (Landcover = 9016)
After First Fire: 5–9 years	S05	ΔCN = −54.87 + 0.03 (Mean Elevation) +8.02 (Landcover = 7016) −18.80 (Landcover = 7055) +26.12 (Landcover = 7080) −14.40 (Landcover = 7149)
After First Fire: 10–14 years	S05	ΔCN = −0.76 + 7.19 (Landcover = 7016) −31.08 (Landcover = 7050) +21.28 (Landcover = 7149)
After First Fire: 15+ years	S05	ΔCN = −4.21 + 24.96 (Landcover = 7016) +24.39 (Landcover = 7147)
After First Fire: All years	S05	ΔCN = −41.04 + 0.02 (Mean Elevation) −13.56 (Landcover = 7055) +24.10 (Landcover = 7080)
After Second Fire: 0–4 years	S05	ΔCN = −63.48+ 0.03 (Mean Elevation) −22.62 (Landcover = 7050) −25.20 (Landcover = 7055) −18.07 (Landcover = 7059) +30.27 (Landcover = 7080)
After Second Fire: 5–9 years	S05	ΔCN = −5.74 + 297.52 (Mean Northness)
After Second Fire: 10–14 years	S05	ΔCN = −4.88 + 10.72 (Landcover = 7054)
After Second Fire: 15+ years	S05	ΔCN = −2.26 + 15.94 (Landcover = 7080)
After Second Fire: All years	S05	ΔCN = −47.32 + 0.02 (Mean Elevation) −18.86 (Landcover = 7055) −15.05 (Landcover = 7059) +19.79 (Landcover = 7080)

Table 2 (cont.). Generalized linear models (GLMs) for median curve number (CN) change following the first and second wildfire for each planning horizon and storage value (S05 and S20) at all 102 analyzed watersheds.

Wildfire Scenario	Storage Value	Linear Equation
After First Fire: 0–4 years	S20	ΔCN = −24.48 + 0.01 (Mean Elevation) −7.36 (Landcover = 7055) +21.71 (Landcover = 7086)
After First Fire: 5–9 years	S20	ΔCN = −26.61 + 0.01 (Mean Elevation) +0.47 (Mean Slope) −9.71 (Landcover = 7011) −13.04 (Landcover = 7055) +17.66 (Landcover = 7080) −13.02 (Landcover = 7149)
After First Fire: 10–14 years	S20	ΔCN = 1.11 −0.62 (Percent Burn) −27.29 (Landcover = 7050) +13.81 (Landcover = 7052) +13.06 (Landcover = 7149)
After First Fire: 15+ years	S20	ΔCN = −5.08 + 6.29 (Landcover = 7054) +19.75 (Landcover = 7080) +18.30 (Landcover = 7126)
After First Fire: All years	S20	ΔCN = −24.38 + 0.01 (Mean Elevation) −8.80 (Landcover = 7055)
After Second Fire: 0–4 years	S20	ΔCN = −27.93 + 0.01 (Mean Elevation) −11.59 (Landcover = 7055)
After Second Fire: 5–9 years	S20	ΔCN = −21.79 + 1.00(Mean Slope) +987.05 (Mean Northness) +491.43 (Mean Eastness)
After Second Fire: 10–14 years	S20	ΔCN = −3.89 + 0.54 (Mean Slope) −11.32 (Landcover = 7055)
After Second Fire: 15+ years	S20	ΔCN = −3.89 −102.88(Mean Eastness)
After Second Fire: All years	S20	ΔCN = −28.37 + 0.01 (Mean Elevation) −12.43(Landcover = 7055) −10.24(Landcover = 7059) +14.41 (Landcover = 7080)

Table 3. GLMs for median CN change following the first wildfire for each planning horizon and storage value (S05 and S20) using the 24 "best subset" watersheds that have minimal anthropogenic affect.

Wildfire Scenario	Storage Value	Linear Equation
After First Fire: 0–4 years	S05	ΔCN = 2.74 −5.29 (Mean Northness) −4.50(Landcover = 7055)
After First Fire: 5–9 years	S05	ΔCN = 4.62 + 21.15 (Landcover = 7080)
After First Fire: 10–14 years	S05	ΔCN = 0.76 −32.60 (Landcover = 7050)
After First Fire: 15+ years	S05	ΔCN = −3.52 + 24.26 (Landcover = 7080)
After First Fire: All years	S05	ΔCN = −0.15 + 20.82 (Mean Northness)
After First Fire: 0–4 years	S20	ΔCN = −11.66 + 0.004 (Mean Elevation) + 42.86 (Mean Northness)
After First Fire: 5–9 years	S20	ΔCN = 3.09 + 15.32(Landcover = 7080)
After First Fire: 10–14 years	S20	ΔCN = 0.27 − 28.18 (Landcover = 7050)
After First Fire: 15+ years	S20	ΔCN = −2.78 + 17.45 (Landcover = 7080)
After First Fire: All years	S20	ΔCN = 0.22 + 5.20 (Mean Northness)

Appendix C: : Regression Tree Diagrams

The regression tree diagrams from the all watersheds data set for all scenarios with planning horizons longer than 4 years are shown in Figure 1 through Figure 16. Figure 1 through Figure 8 represent median curve number (CN) changes after one wildfire and Figure 9 through Figure 16 median CN changes after two wildfires in a watershed. The 24 "best subset" watershed regression trees following one fire for all scenarios with planning horizons greater than 4 years are shown in Figure 17 through Figure 24. No models were created using the "best subset" watersheds following two wildfires due to a lack of data. The interpretation of these diagrams is consistent with the description provided in Section 5.3.2. Landcover data for these figures are from LANDFIRE (2022c).

Figure 1. Regression tree diagram for median curve number (CN) change in 77 analyzed watersheds that recorded runoff events all years following the first wildfire in the watershed. The storage value was assumed to be 5% (S05).

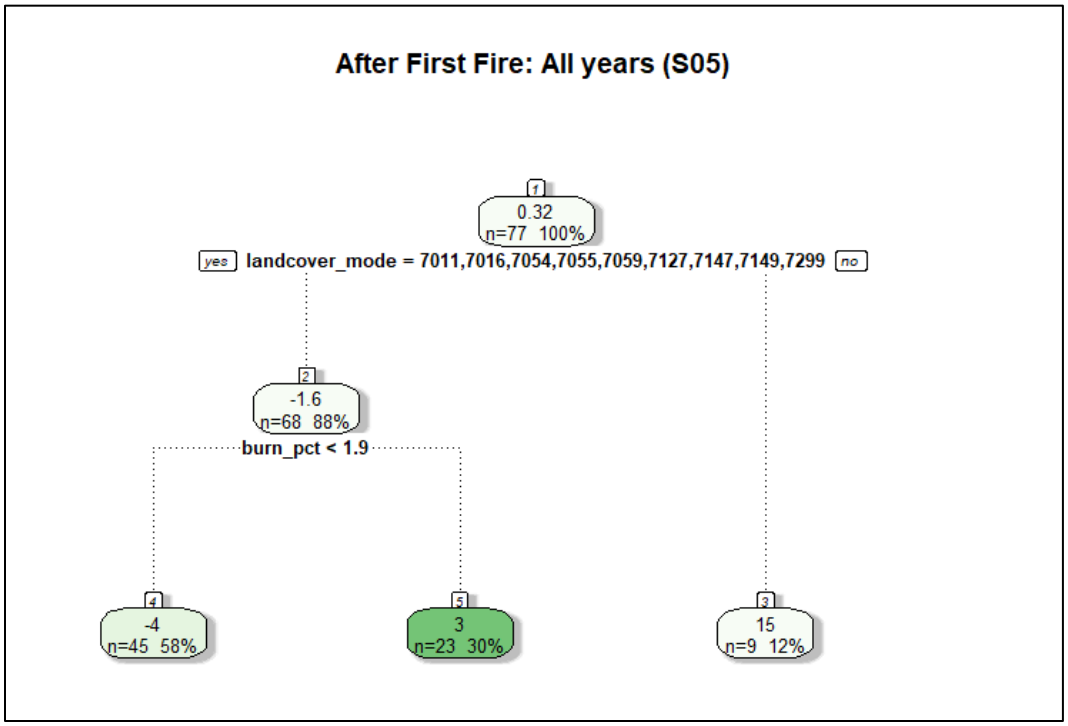

Figure 2. Regression tree diagram for median CN change in 77 analyzed watersheds that recorded runoff events all years following the first wildfire in the watershed. The storage value was assumed to be 20% (S20).

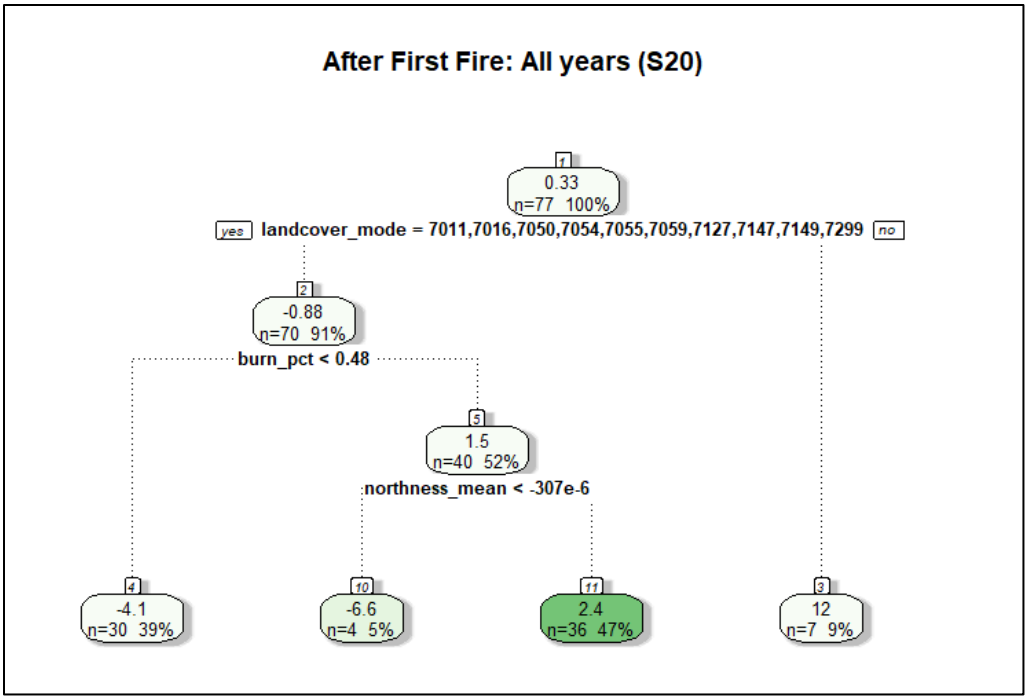

Figure 3. Regression tree diagram for median CN change in 57 analyzed watersheds that recorded runoff events 5–9 years following the first wildfire in the watershed. The storage value was assumed to be 5% (S05).

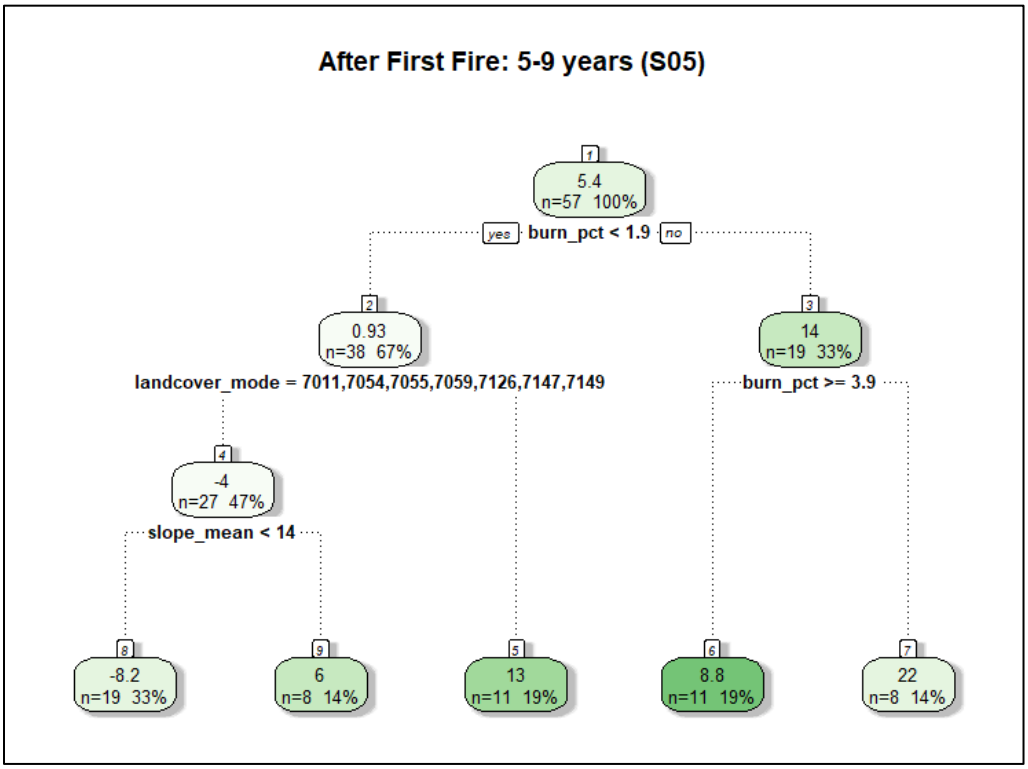

Figure 4. Regression tree diagram for median CN change in 57 analyzed watersheds that recorded runoff events 5–9 years following the first wildfire in the watershed. The storage value was assumed to be 20% (S20).

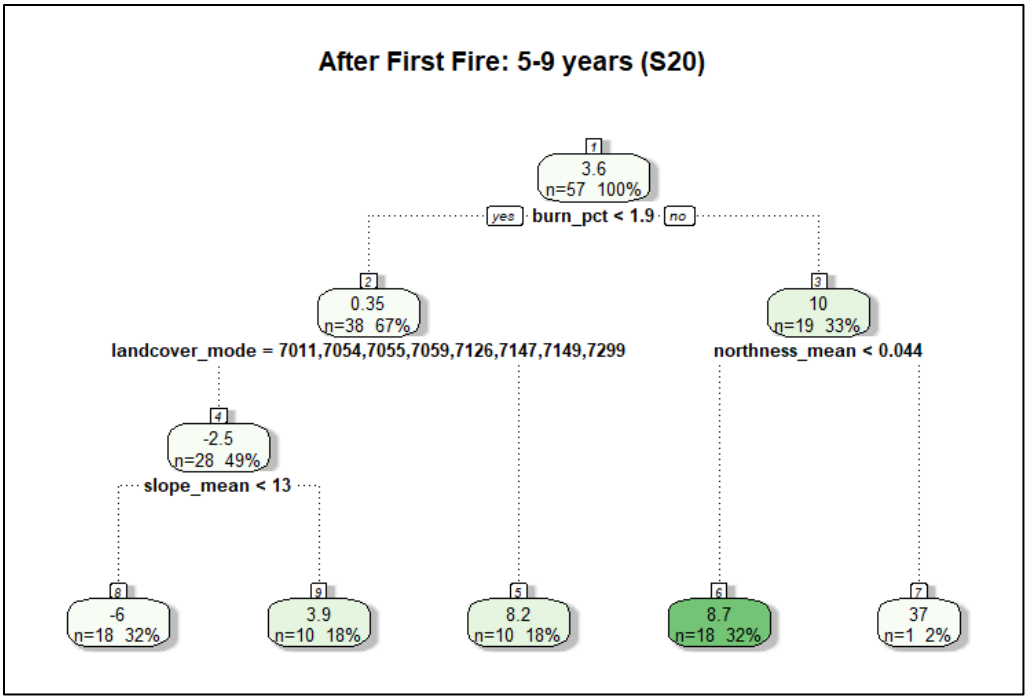

Figure 5. Regression tree diagram for median CN change in 48 analyzed watersheds that recorded runoff events 10–14 years following the first wildfire in the watershed. The storage value was assumed to be 5% (S05).

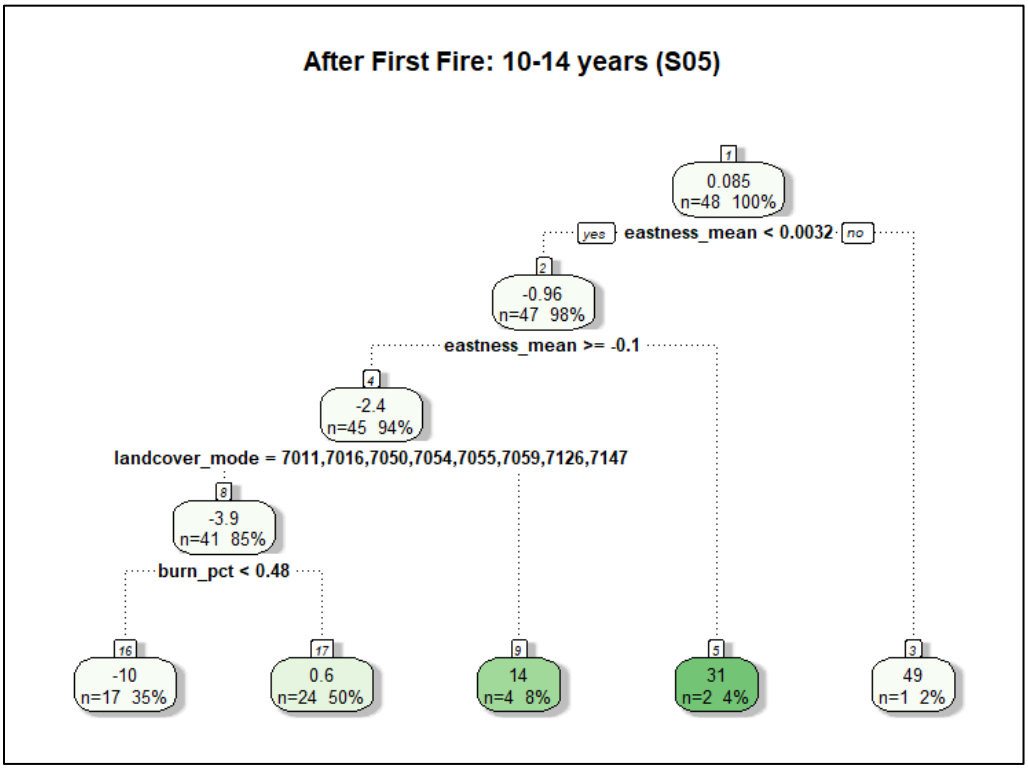

Figure 6. Regression tree diagram for median CN change in 48 analyzed watersheds that recorded runoff events 10–14 years following the first wildfire in the watershed. The storage value was assumed to be 20% (S20).

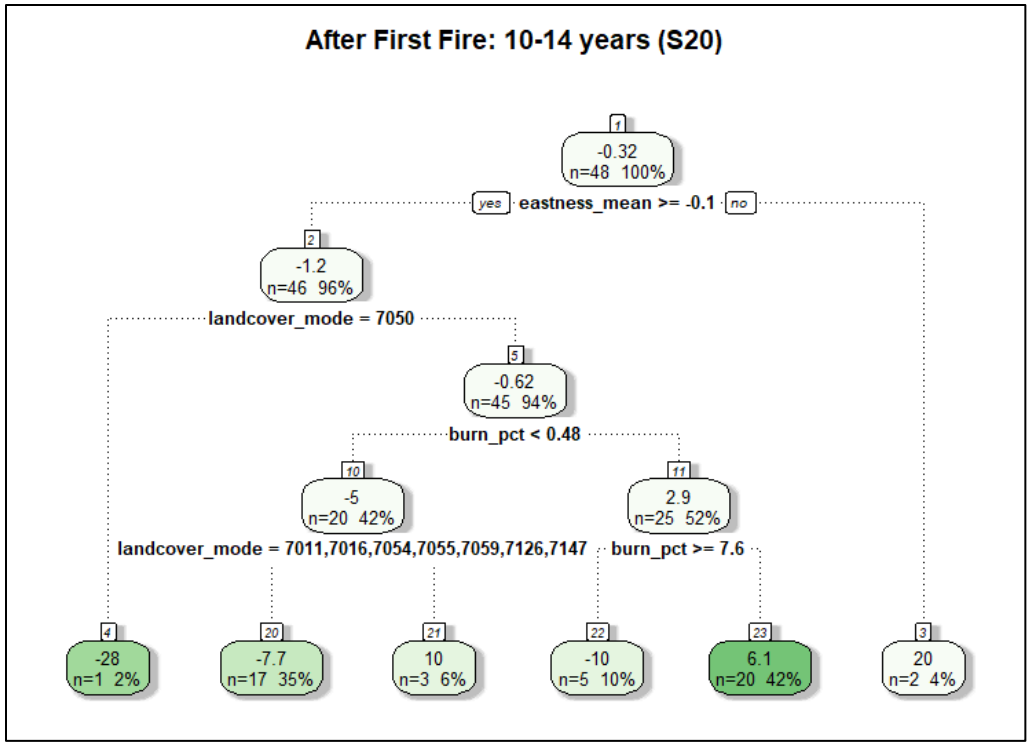

Figure 7. Regression tree diagram for median CN change in 37 analyzed watersheds that recorded runoff events 15+ years following the first wildfire in the watershed. The storage value was assumed to be 5% (S05).

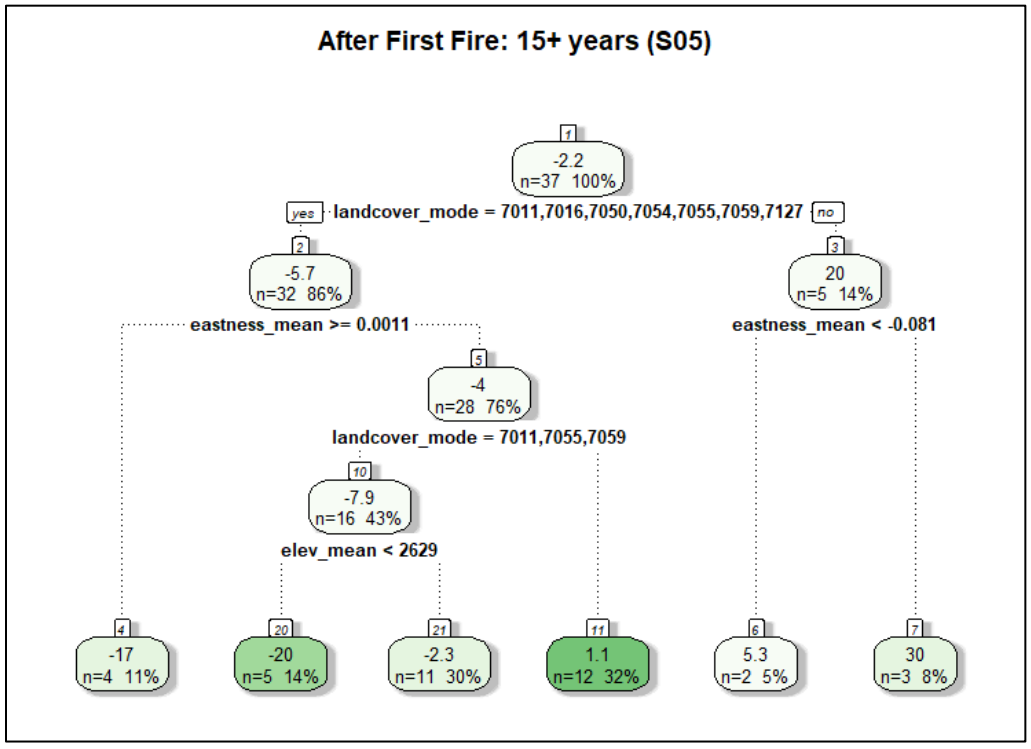

Figure 8. Regression tree diagram for median CN change in 37 analyzed watersheds that recorded runoff events 15+ years following the first wildfire in the watershed. The storage value was assumed to be 20% (S20).

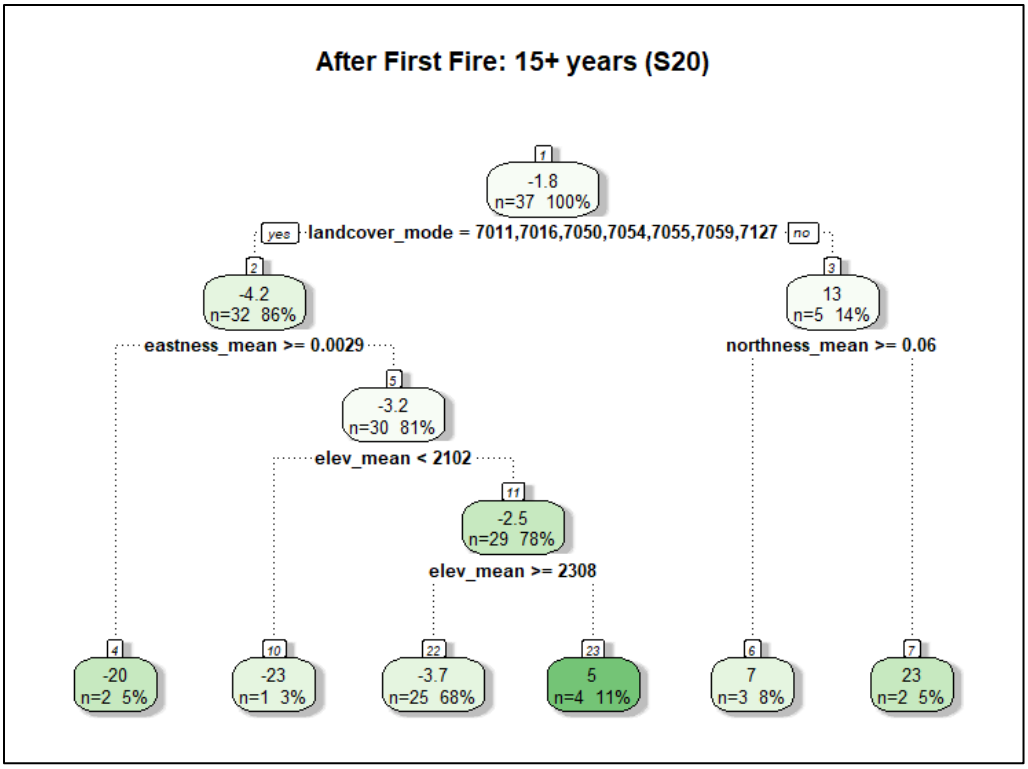

Figure 9. Regression tree diagram for median CN change in 54 analyzed watersheds that recorded runoff events all years following the second wildfire in the watershed. The storage value was assumed to be 5% (S05).

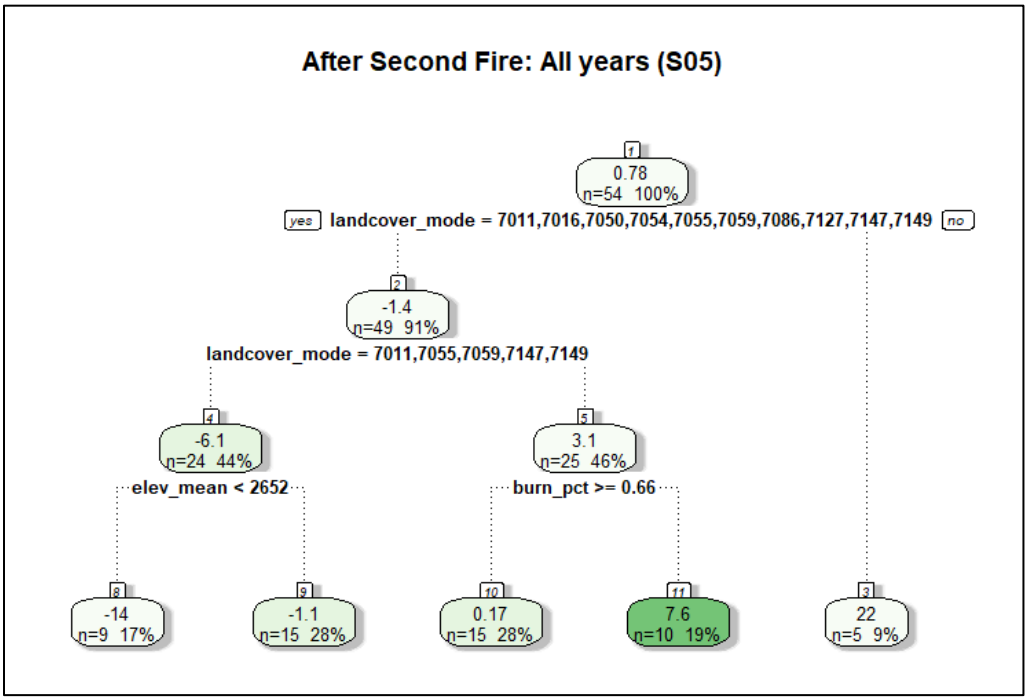

Figure 10. Regression tree diagram for median CN change in 54 analyzed watersheds that recorded runoff events all years following the second wildfire in the watershed. The storage value was assumed to be 20% (S20).

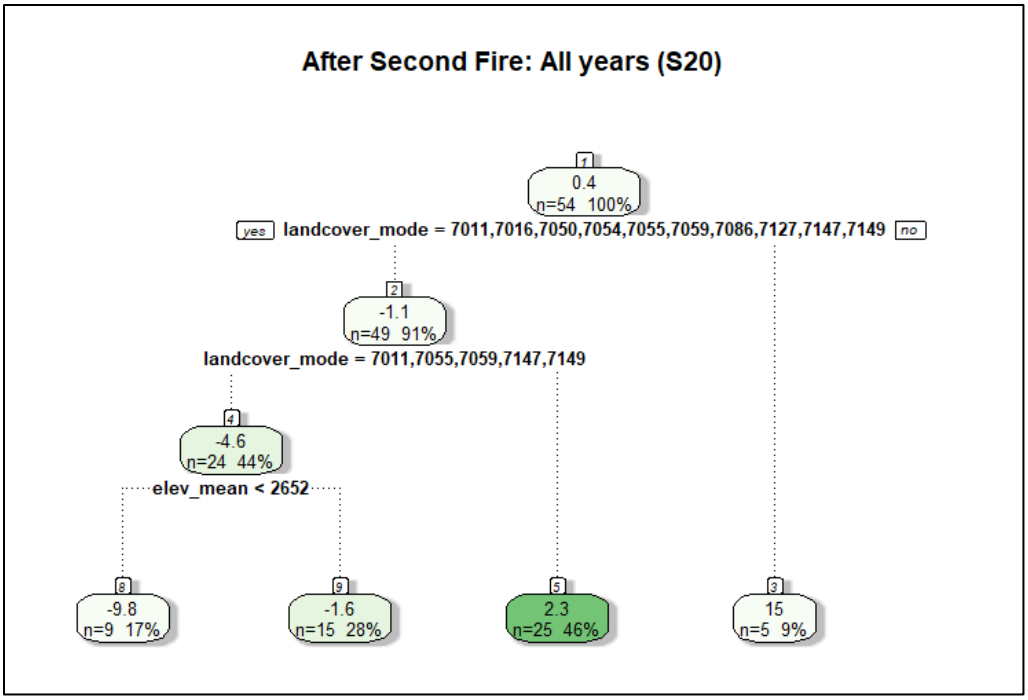

Figure 11. Regression tree diagram for median CN change in 32 analyzed watersheds that recorded runoff events 5–9 years following the second wildfire in the watershed. The storage value was assumed to be 5% (S05).

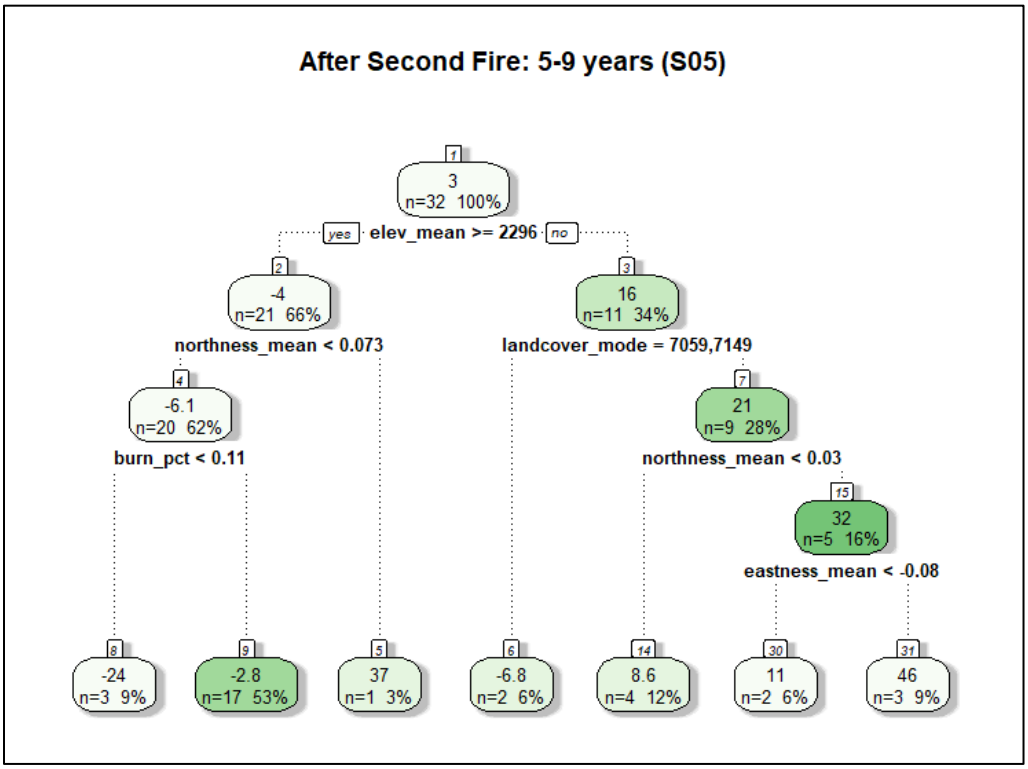

Figure 12. Regression tree diagram for median CN change in 32 analyzed watersheds that recorded runoff events 5–9 years following the second wildfire in the watershed. The storage value was assumed to be 20% (S20).

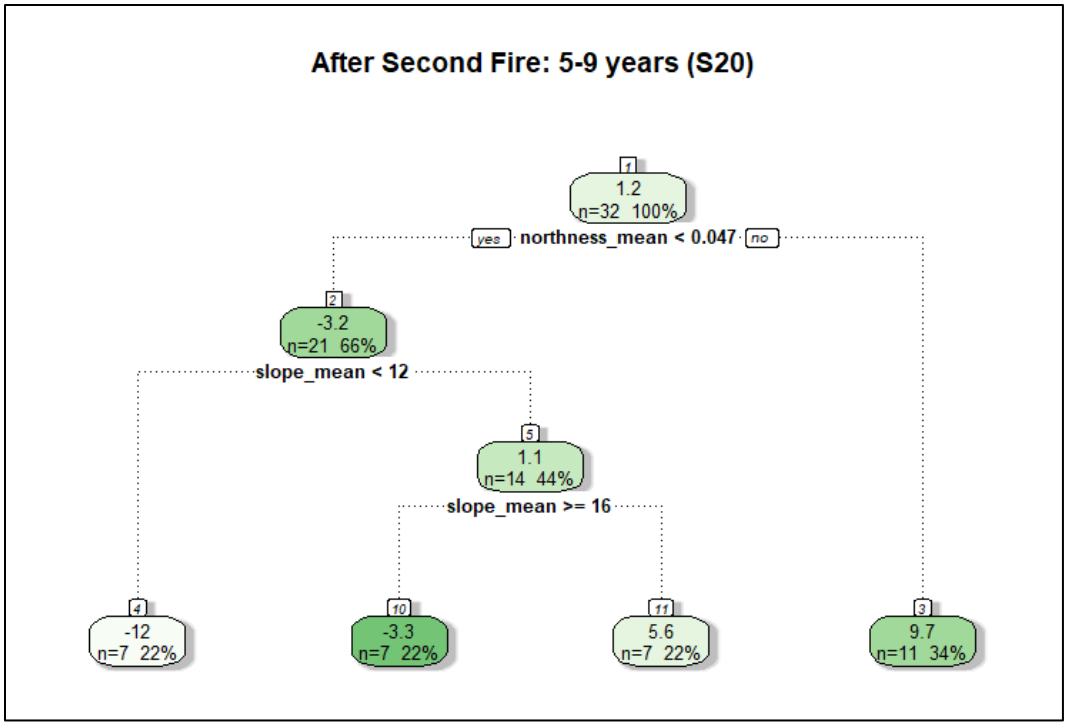

Figure 13. Regression tree diagram for median CN change in 27 analyzed watersheds that recorded runoff events 10–14 years following the second wildfire in the watershed. The storage value was assumed to be 5% (S05).

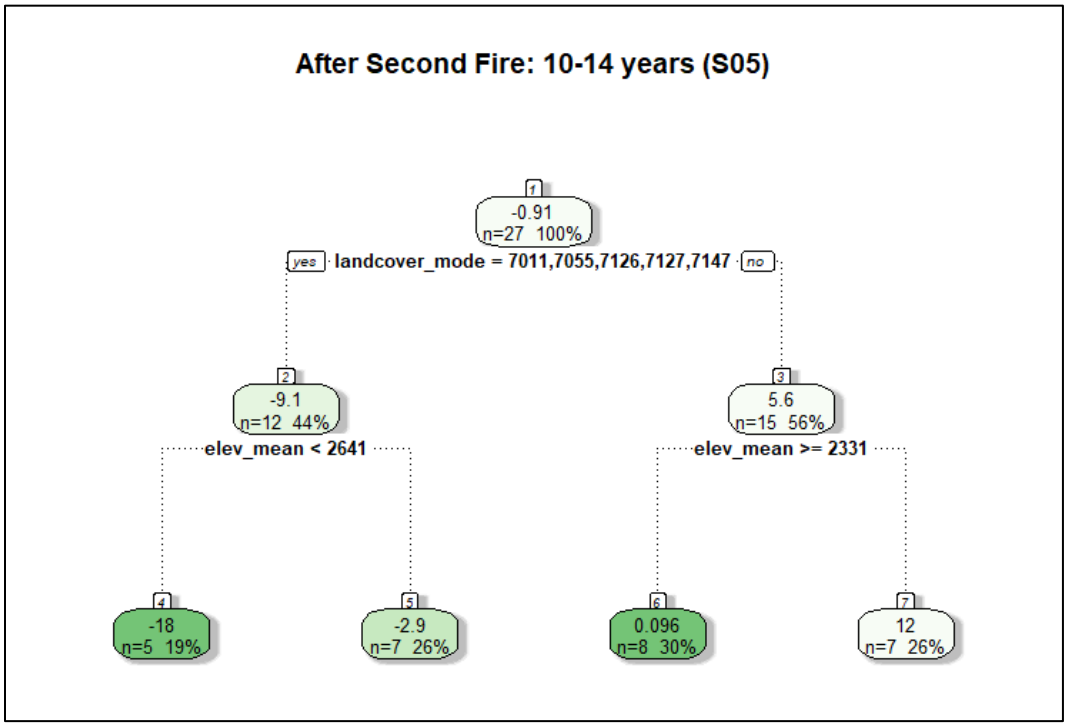

Figure 14. Regression tree diagram for median CN change in 27 analyzed watersheds that recorded runoff events 10–14 years following the second wildfire in the watershed. The storage value was assumed to be 20% (S20).

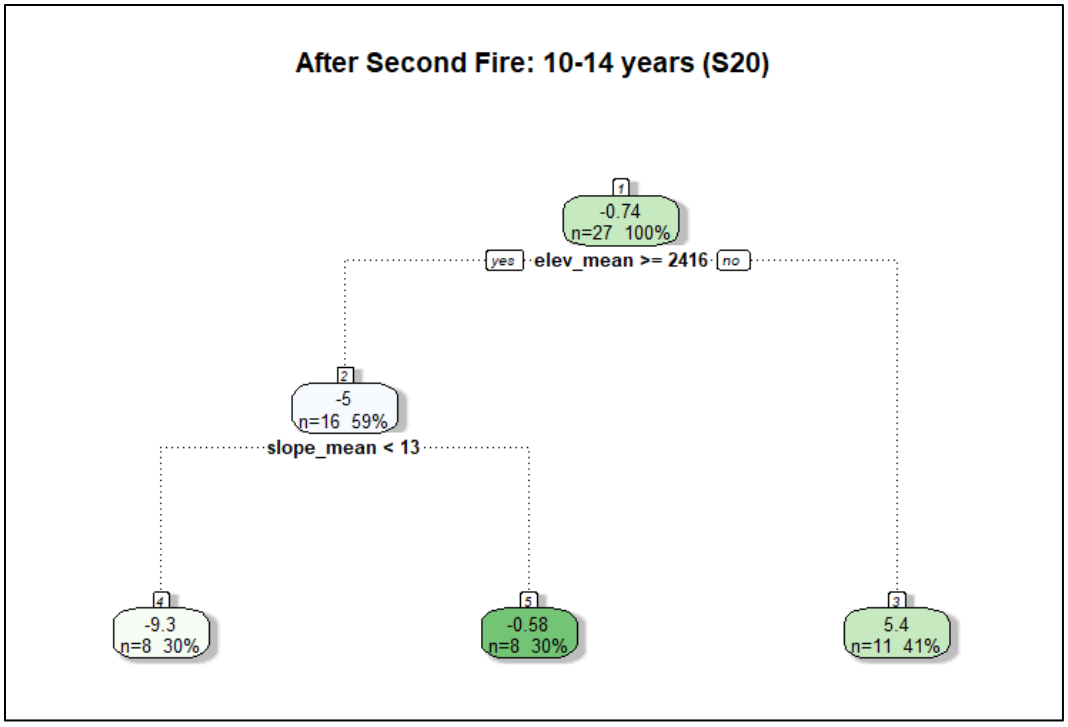

Figure 15. Regression tree diagram for median CN change in 19 analyzed watersheds that recorded runoff events 15+ years following the second wildfire in the watershed. The storage value was assumed to be 5% (S05).

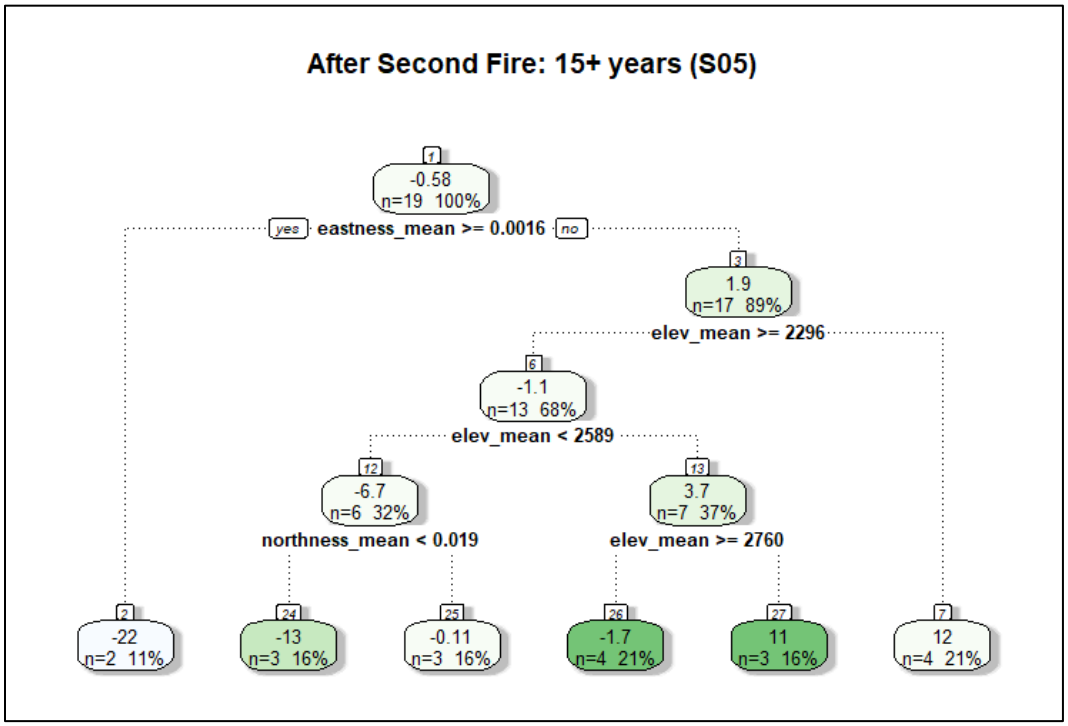

Figure 16. Regression tree diagram for median CN change in 19 analyzed watersheds that recorded runoff events all years following the second wildfire in the watershed. The storage value was assumed to be 20% (S20).

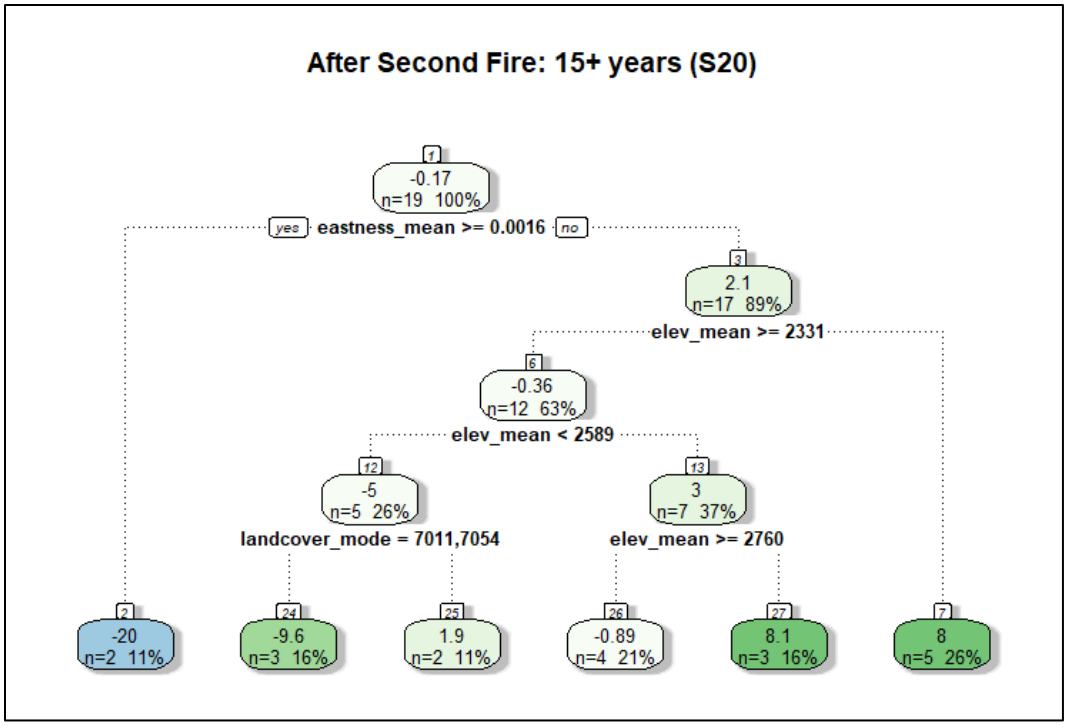

Figure 17. Regression tree diagram for median CN change in 19 analyzed watersheds that recorded runoff events all years following the first wildfire in the 24 “best subset” watersheds. The storage value was assumed to be 5% (S05).

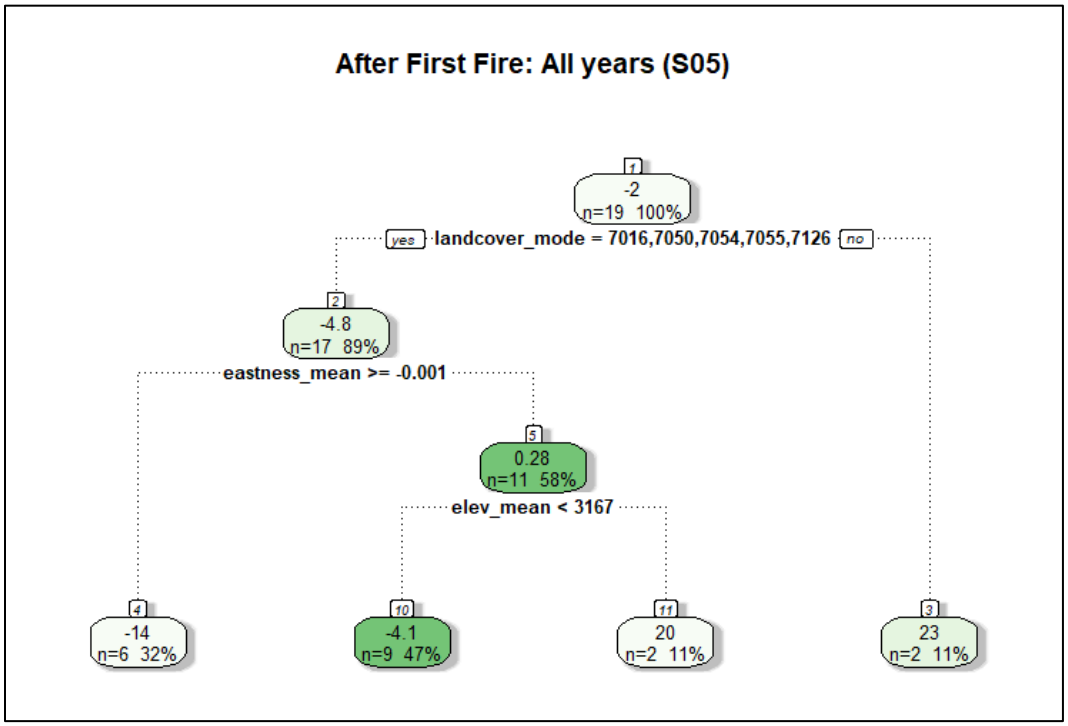

Figure 18. Regression tree diagram for median CN change in 19 analyzed watersheds that recorded runoff events all years following the first wildfire in the 24 "best subset" watersheds. The storage value was assumed to be 20% (S20).

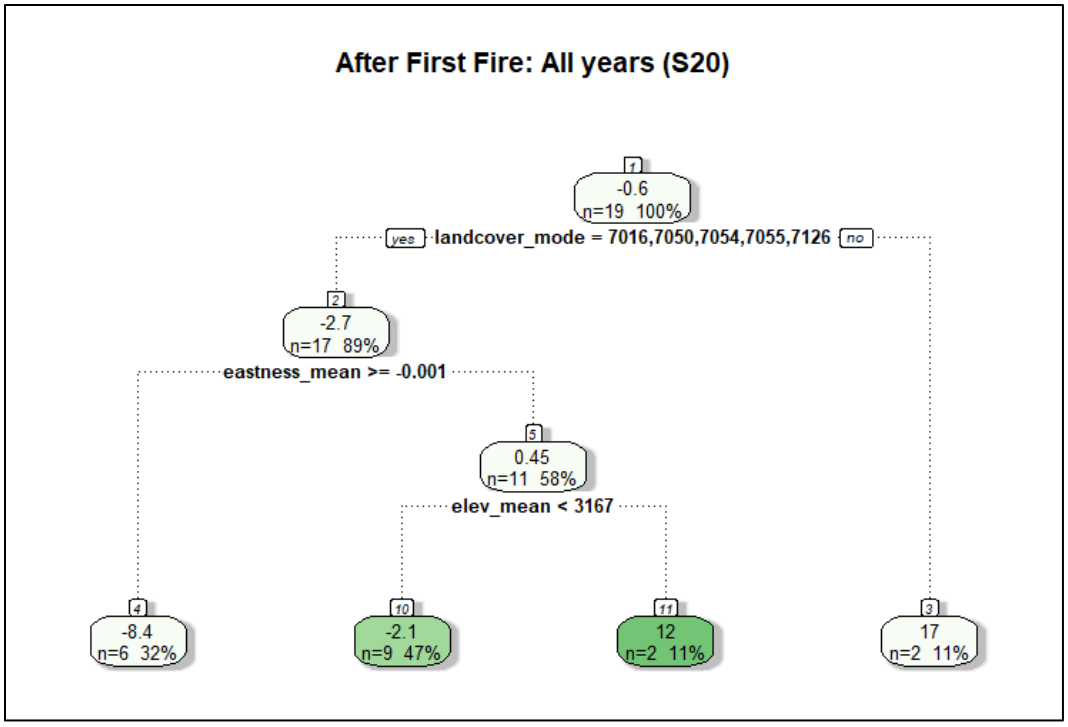

Figure 19. Regression tree diagram for median CN change in 14 analyzed watersheds that recorded runoff events 5–9 years following the first wildfire in the 24 "best subset" watersheds. The storage value was assumed to be 5% (S05).

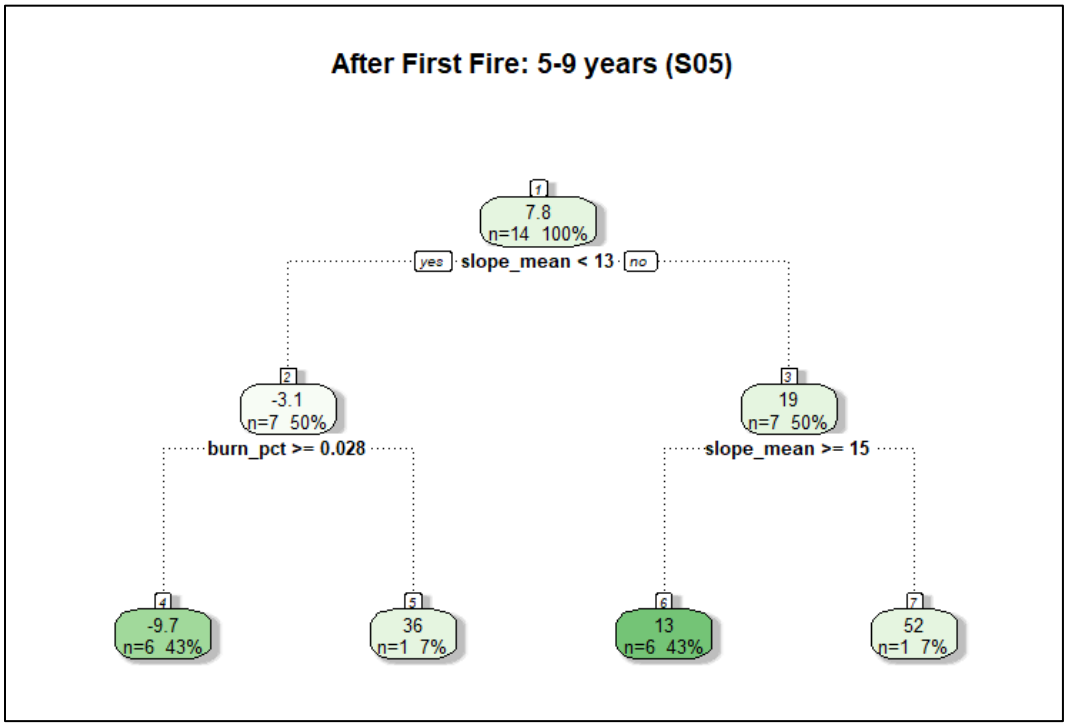

Figure 20. Regression tree diagram for median CN change in 14 analyzed watersheds that recorded runoff events 5–9 years following the first wildfire in the 24 "best subset" watersheds. The storage value was assumed to be 20% (S20).

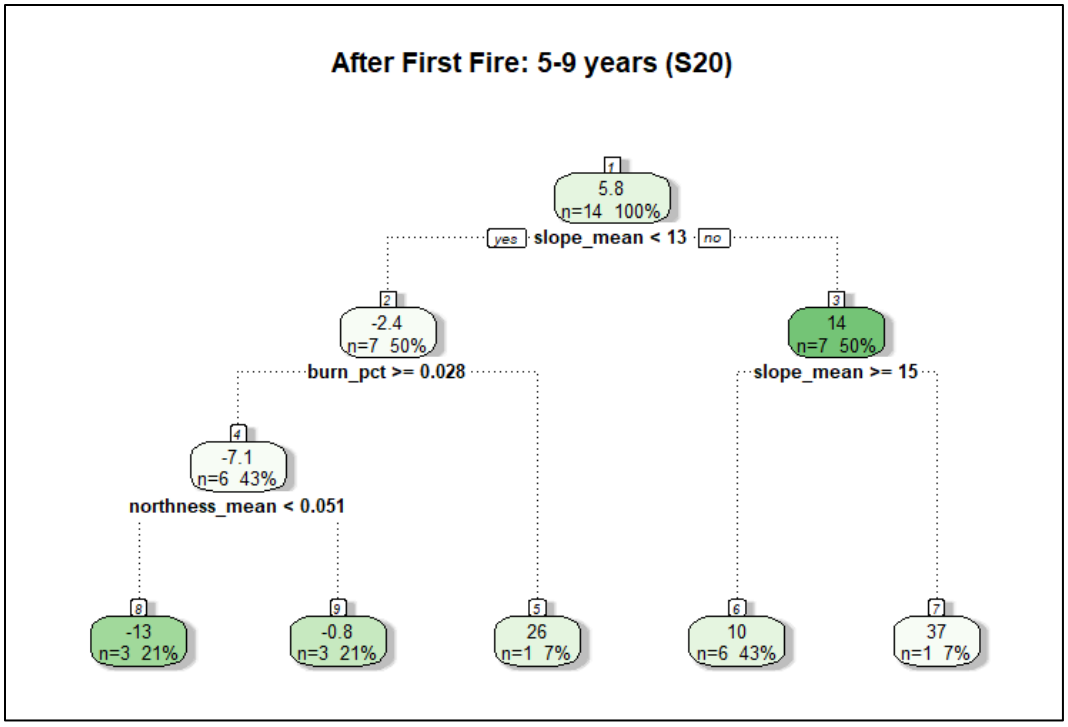

Figure 21. Regression tree diagram for median CN change in 11 analyzed watersheds that recorded runoff events 10–14 years following the first wildfire in the 24 "best subset" watersheds. The storage value was assumed to be 5% (S05).

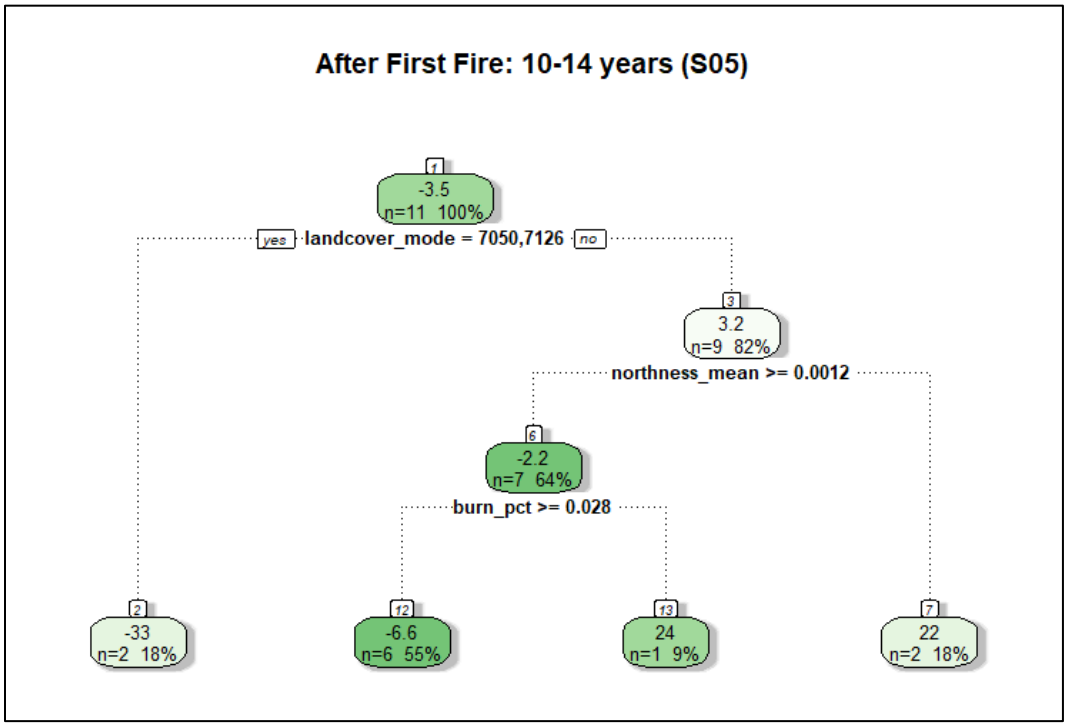

Figure 22. Regression tree diagram for median CN change in 11 analyzed watersheds that recorded runoff events 10–14 years following the first wildfire in the 24 "best subset" watersheds. The storage value was assumed to be 20% (S20).

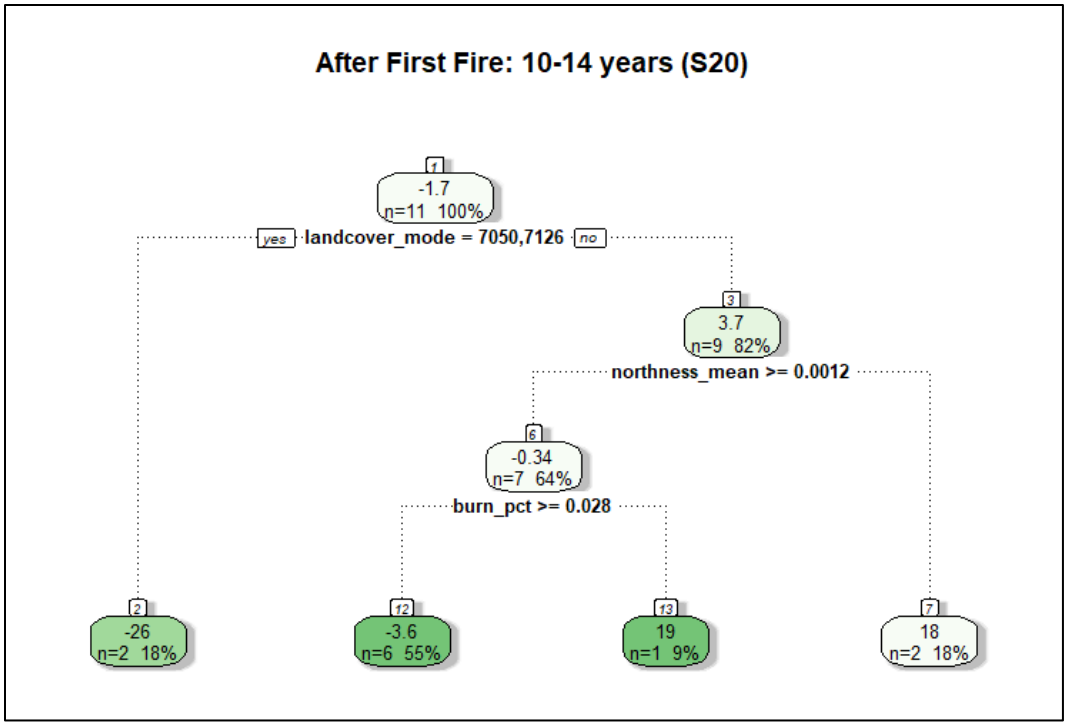

Figure 23. Regression tree diagram for median CN change in 11 analyzed watersheds that recorded runoff events 15+ years following the first wildfire in the 24 "best subset" watersheds. The storage value was assumed to be 5% (S05).

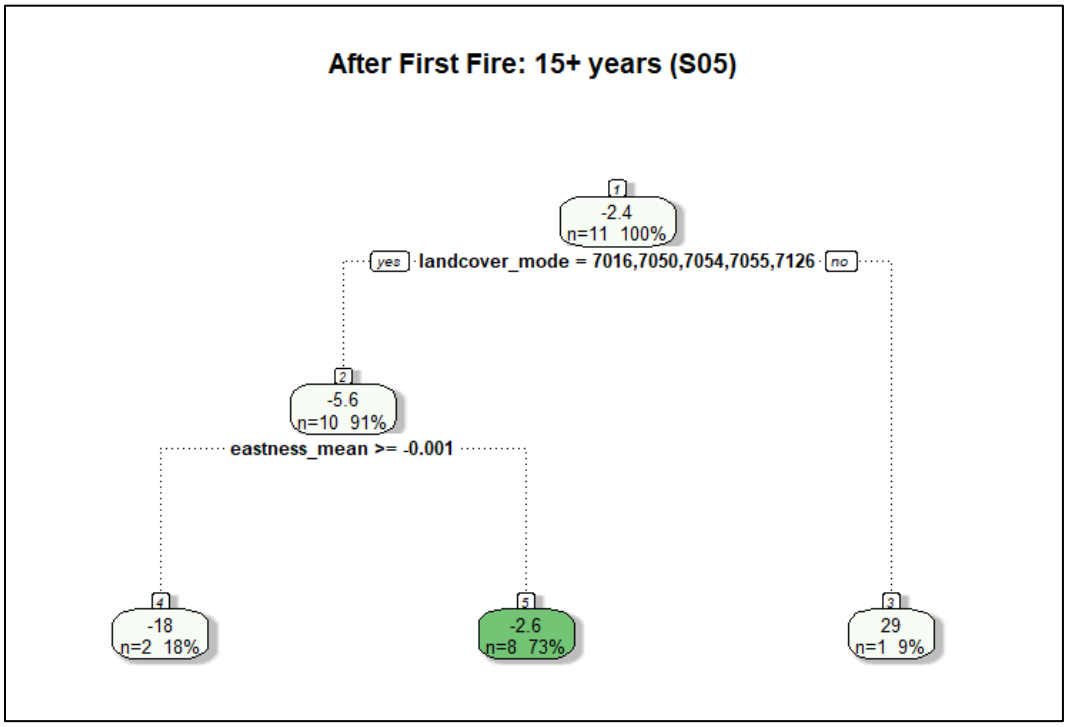

Figure 24. Regression tree diagram for median CN change in 11 analyzed watersheds that recorded runoff events 15+ years following the first wildfire in the 24 "best subset" watersheds. The storage value was assumed to be 20% (S20).

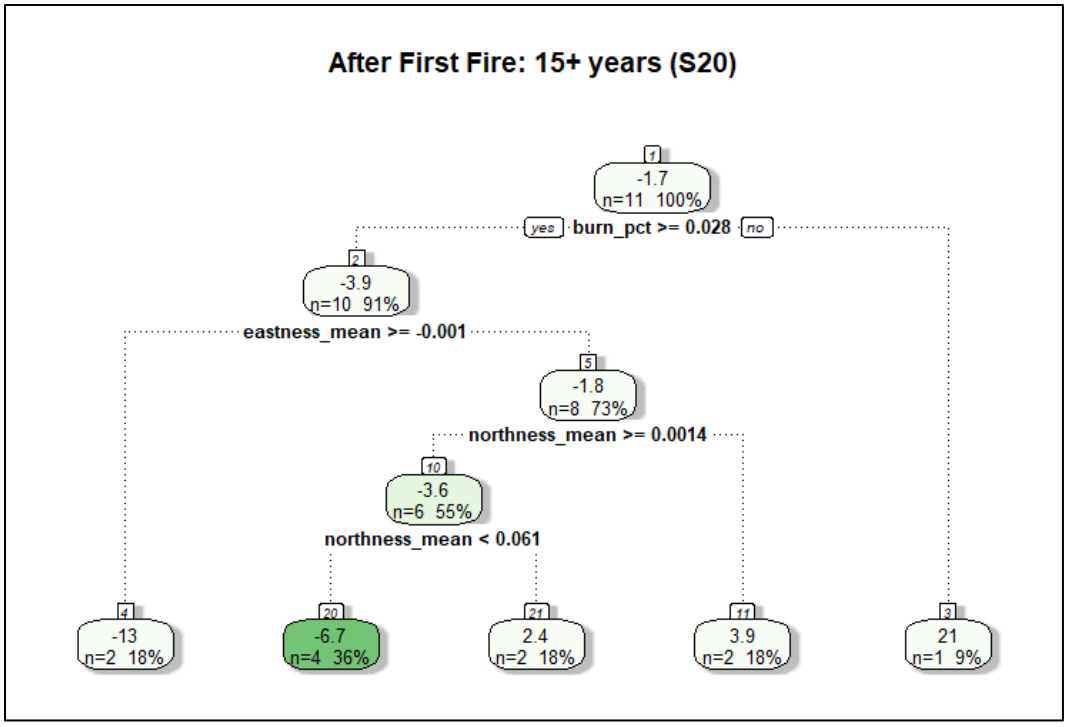

Abbreviations

AORC	Analysis of Record for Calibration
BAER	Burned Area Emergency Response
CN	Curve number
CODWR	Colorado Division of Water Resources
CONUS	Continental United States
DEM	Digital elevation map
GLM	General Linear Model
HEC-HMS	Hydrologic Engineering Center–Hydrologic Modelling System
HUC4	Hydrologic Unit Code (4-digit)
KGE	Kling-Gupta efficiency
LISEM	Limburg Soil Erosion Model
MAE	Mean absolute error
NAD 83	North American Datum of 1983
NAVD 88	North American Vertical Datum of 1983
NRCS	Natural Resource Conservation Service
NSE	Nash-Sutcliffe model efficiency
PFHydro	Post-wildfire hydrology modeling tool
RSME	Root-mean-square error
S	Storage
SCS	Soil Conservation Service
SWE	Snow water equivalent
US	United States

USACE	United States Army Corps of Engineers
USGS	United States Geological Survey

REPORT DOCUMENTATION PAGE

1. REPORT DATE	2. REPORT TYPE	3. DATES COVERED	
June 2024	Final Report	START DATE FY23	END DATE FY24

4. TITLE AND SUBTITLE

Post-wildfire Curve Number Estimates for the Southern Rocky Mountains in Colorado, USA

5a. CONTRACT NUMBER	5b. GRANT NUMBER	5c. PROGRAM ELEMENT
5d. PROJECT NUMBER	**5e. TASK NUMBER**	**5f. WORK UNIT NUMBER**

6. AUTHOR(S)

Jeremy Giovando, Wyatt Reis, Rose Shillito, Elizabeth Shaloka, Christina Chow, Michael S. Kohn, and Natalie Memarsadeghi

7. PERFORMING ORGANIZATION NAME(S) AND ADDRESS(ES)

See reverse.

8. PERFORMING ORGANIZATION REPORT NUMBER

ERDC TR-24-12

9. SPONSORING/MONITORING AGENCY NAME(S) AND ADDRESS(ES)	10. SPONSOR/MONITOR'S ACRONYM(S)	11. SPONSOR/MONITOR'S REPORT NUMBER(S)
US Army Corps of Engineers (USACE) Washington, DC 20314-1000	USACE	

12. DISTRIBUTION/AVAILABILITY STATEMENT

Distribution Statement A. Approved for public release: distribution is unlimited.

13. SUPPLEMENTARY NOTES

AMSCO 504507

14. ABSTRACT

The curve number method first developed by the USDA Soil Conservation Service (now the Natural Resources Conservation Service) is often used for post-wildfire runoff assessments. These assessments are critical for land and emergency managers making decisions on life and property risks following a wildfire event. Three approaches (i.e., historical event observations, linear regression model, and regression tree model) were used to help estimate a post-wildfire curve number from watershed and wildfire parameters. For the first method, we used runoff events from 102 burned watersheds in Colorado, southern Wyoming, northern New Mexico, and eastern Utah to quantify changes in curve number values from pre- to post-wildfire conditions. The curve number changes from the measured runoff events vary substantially between positive and negative values. The measured curve number changes were then associated with watershed characteristics (e.g., slope, elevation, northness, and eastness) and land cover type to develop prediction models that provide estimates of post-wildfire curve number changes. Finally, we used a regression tree method to demonstrate that accurate predications can be developed using the measured curve number changes from our study domain. These models can be used for future post-wildfire assessments within the region.

15. SUBJECT TERMS

Curve number, Colorado, Flood risk, Hydrologic modeling, Hydrology, Post-Wildfire, Runoff, Wildfires

16. SECURITY CLASSIFICATION OF:			17. LIMITATION OF ABSTRACT	18. NUMBER OF PAGES
a. REPORT	b. ABSTRACT	C. THIS PAGE		
Unclassified	Unclassified	Unclassified	SAR	97

19a. NAME OF RESPONSIBLE PERSON	19b. TELEPHONE NUMBER (include area code)
Jeremy Giovando	(509) 540-6498

7. PERFORMING ORGANIZATION NAME(S) AND ADDRESS(ES) (concluded)

US Army Engineer Research and Development Center (ERDC)
Cold Regions Research and Engineering Laboratory (CRREL)
72 Lyme Road
Hanover, NH 03755-1290

US Army Engineer Research and Development Center
Coastal and Hydraulics Laboratory (CHL)
3909 Halls Ferry Road
Vicksburg, MS 39180-6199

US Army Corps of Engineers
Philadelphia District
1650 Arch Street
Philadelphia, PA 19103

US Geological Survey
Colorado Water Science Center
Denver Federal Center, MS-415 Building 53
Denver, CO 80225